Republic of Iraq
Ministry of Higher Education
and Scientific Research
Al-Nahrain University
College of Science
Department of Physics

The Effects of Electrodes Separation and Target Material by DC Discharge Magnetron Sputtering

A Thesis

Submitted to the College of Science/Al-Nahrain University as a partial fulfillment of the requirements for the Degree of Master of Science in Physics.

By

Ban Faisal Rasheed

B.Sc. Physics / College Science / Al-Nahrain University

1996

Supervised by

Asst. Prof. Dr. Khalid A. Yahya

May
2016 AC

Shaaban
1437 AH

اقْرَأْ بِاسْمِ رَبِّكَ الَّذِي خَلَقَ ﴿1﴾ خَلَقَ الْإِنسَانَ مِنْ عَلَقٍ ﴿2﴾
اقْرَأْ وَرَبُّكَ الْأَكْرَمُ ﴿3﴾ الَّذِي عَلَّمَ بِالْقَلَمِ ﴿4﴾ عَلَّمَ الْإِنسَانَ مَا
لَمْ يَعْلَمْ ﴿5﴾

صدق الله العظيم

سورة العلق الآية (١-٥)

Supervisor Certification

I, certify that this thesis entitled **" The Effects of Electrodes Separation and Target Material by DC Discharge Magnetron Sputtering"** was prepared by " **Ban Faisal Rasheed** " under my supervision at the College of Science / Al-Nahrain University as a partial fulfillment of the requirements for the Degree of Master of Science in Physics.

Signature:

Name: **Dr. Khalid A. Yahya**

Scientific Degree: Assistant Professor

Date: 29 / 2 / 2016

In view of the available recommendation, I forward this **thesis** for debate by the examining committee.

Signature:

Name: **Dr. Alaa Jabbar Ghazai**

Scientific Degree: Assistant Professor

Title: Head of Department of Physics

Date: 29 / 2 / 2016

Examination Committee Certification

We, the examining committee certify that we have read this thesis entitle **"The Effects of Electrodes Separation and Target Material by DC Discharge Magnetron Sputtering"** and examined the student **"Ban Faisal Rasheed"** in its content and that in our opinion, it is accepted for Degree of Master of Science in Physics.

Signature:
Name: **Dr. Saad N. Abood**
Title: **Professor**
Address: College of Science, Al-Nahrain University
Date: / / 2016
(The head of committee)

Signature:
Name: **Dr. Kadhim A. Aadim**
Title: **Asst. Professor**
Address: College of Science, University of Baghdad
Date: / / 2016
(Member)

Signature:
Name: **Dr. Sabah N. Mazhir**
Title: **Asst. Professor**
Address: College of Science for woman, University of Baghdad
Date: / / 2016
(Member)

Signature:
Name: **Dr. Khalid A. Yahya**
Title: **Asst. Professor**
Address: College of Science, Al-Nahrain University
Date: / / 2016
(Member/Supervisor)

I, hereby certify upon the decision of the examining committee.

Signature:
Name: **Dr. Hadi M. A. Abood**
Title: **Assistant Professor**
Address: Dean of College of Science, Al-Nahrain University
Date: / / 2016

Acknowledgement

Praise is to **Allah** Lord of the word, and best prayers and peace on his best messenger **Mohammed**, and his descendant, and his noble companions.

I would like to express my deep thanks and appreciation to my supervisors **Dr. Khalid A. Yahya** for his suggestion of this project and gave me advice and guidance help me to output this work in this way, ask **God** grant him the best reward.

Thanks to the head and staff of the physics department, college of science, Al-Nahrain University.

I want to thanks **Dr. Thamir Abdul-Jabbar** for his a available assistance during my study.

I would like to express my gratitude to **Dr. Hassan N. Hashim** who help me in my work.

I thanks **Miss. Alaa Adnan** in department of chemistry, college of science/Al- Nahrain university for help me in testing samples.

I would like to give my deepest thanks to my mother and father for their love and support all the time.

Finally, I not forget to express my gratitude to my family and to my friends who encouraged me.

Abstract

In this work, a DC planner magnetron sputtering system used. Which consists of a cylindrical chamber, made from (Borosilicate). It contains two circular electrodes made from stainless steel. The cathode electrode is carried the target material and permanent magnet while a glass sample, which must coat, is placed on the anode electrode. In this works, gold and silver used as a target materials.

The objective of this study is to examine the effects of operating parameters such as, electrodes separation, sputtering current, and type of target materials on the properties of glass surface coated under the influence of magnetic field. The surface morphology for the coated samples are studied by atomic force microscopy (AFM). Furthermore, electron temperature, ion and electron densities and other plasma parameters are determined by a cylindrical single Langmuir probe where the pressure up to(0.2 mbar).

It is found that a linear increase in electron and ion densities and an exponential decrease in electron temperature with five values of electrodes separation (3,4,4.5,5 and 6) cm. That was observed for gold and silver target materials. Also, the discharge voltage using gold target is greater than that for silver target. Electron temperature decreased for gold and silver targets as the electrodes separation increased. The ion density increased which caused increasing in average grain diameter, height at sputtering current, I_d=30 mA , when the target is gold.

However, the average grain diameter is decreased and the height of grain increased at I_d=40 mA using silver target. On the other

hand, the values of electron temperature using silver target is greater than that for gold target. Also, the relation of average grain diameter, height and roughness surface as a function of electrodes separation are nonlinear.

The minimum average values of grain diameter, height are (90 nm) and (6 nm) respectively for using gold at I_d =30 mA and d=4 cm. For using silver at I_d =40 mA the minimum average grain diameter is also (90 nm) at d=5 cm and height is (5.5 nm) at d=4 cm.

For all discharge currents (20,30,40,50 3and 60)mA , the minimum average grain height at the same electrodes separation d=4 cm for using silver and gold target except the value of I_d=50 mA, whom a maximum average grain height is obtained.

Finally, the sputtering yield for silver target is greater than that for gold target.

List of Contents

List of Figures

List of Tables

Table	Page

List of Alphabetic Symbols

Symbols	Meaning	Unites
A_p	Probe surface area.	m^2
B	Magnetic flux	Gauss
d	Electrodes separation	cm
e	Charge of electron	C
E	Energy of ion particle	eV
F_L	Central Larmur force	N
G_d	Grain diameter	nm
G_h	Grain height	nm
I_{es}	Electron saturation current	mA
I_e	Electron current	mA
I_p	Probe current	mA
I_i	Ion current	μA
I_d	Discharge (sputtering) current	mA
I_a	Anode current	μA
k_B	Boltzmann's constant	J / °K
L	Plasma length	Cm
m_e	Mass of electron	Kg
m_i	Mass of ion	Kg
M	Mass of charged particles	Kg
M_1	Mass of argon	Kg
M_2	Mass of target	Kg
n_e	Electron density	m^{-3}
N_D	Number of particles in Deby sphere	dimensionless
n_g	Density of gas atoms	m^{-3}
n_i	Density of ion	m^{-3}
P	Gas pressure	mbar
q	Charge of particle	C
r	Radius of argon atom	cm
r_L	Larmur radius	cm
r_p	Langmuir probe radius	cm
T_e	Electron temperature	eV
T_i	Ion temperature	eV
T_g	Gas temperature	eV

U_b	Surface binding energy	eV
V_b	Breakdown voltage	volt
V_s	Sheath potential	volt
v	Velocity of particles	m/s
$v_\perp$	Velocity of particles perpendicular to B	m/s
$V_{cathode}$	Cathode potential	volt
V_f	Floting potential	volt
V_p	Probe potential	volt
V_{pp}	Plasma potential	volt
X	x- axis	cm
y	y- axis	cm
Y(E)	Sputtering yield	dimensionless
$R_{av.}$	Roughness average	nm

List of Greek Symbols

Symbol	Meaning	Unites
α	Constant in Sigmund formula	
γ	Secondary electron emission coefficient	
$\epsilon_\circ$	Permittivity of free space	F/m
λ_D	Deby length	cm
λ_m	Mean free path	cm
σ	Cross section for electron-neutral atoms collisions.	cm^2
τ	The mean time between collisions of charges.	Sec
ω	Frequency of collisions for plasma with atoms .	Hz
ω_{pe}	Plasma frequency of electron	Hz
ω_c	Cyclotron frequency	Hz

List of Abbreviations

Abbreviation	Definition
AFM	Atomic Force Microscopy
LIF	Laser Induced Fluoresce
OES	Optical Emission Spectroscopy
OML	Orbital Motion Limit
PMS	Pules Magnetron Sputtering
PVD	Physical Vapor Deposition
SFM	Scanning Force Microscopy

Chapter One

Introduction and Literature Review

1-1 Introduction

The glow discharge is a kind of plasma, which consists of an ionized gas with equal concentrations of positive and negative charges, and neutral species (quasi-neutral). Furthermore, the particles are exhibited collective behavior. The glow discharge is achieved by applying a potential difference between two electrodes inserted into chamber filled with inert or molecular gas at a low pressure. Here, electrically charged particles are moved under the influence of an electric field between electrodes [1].

Cold plasma technologies have found extensive applications for material processing, 30 years, and they now widely field used in different applications such as, medicine and industrial process [2].

Physical vapor deposition (PVD) technologies using different methods such us, thermal evaporation and sputtering are the major processing in surface coating, thin films, and nanotechnologies [3].

Plasma sputtering process, is one of the most common way which becomes widely accepted manufacturing method for the production thin films of various materials. The use of plasma sputtering for material deposition is widely used such as, in magnetron sputtering plasma source using noble gas to generate the plasma. Generally, a DC magnetron sputtering source is usually used to sputter conducting target, as in present work, while RF magnetron source is used for sputtering insulating or semiconductor target [4,5]. In present work, the gold and silver thin films have been prepared using DC magnetron sputtering source.

1-2 Plasma Classification

Plasma is commonly defined as the fourth state of mater, that consists of a randomly moving charged atomic particles of a certain condition to remain the electrically neutral and collective behavior for plasma. More than 99% of all visible matter in the universe is in plasma state [6].

According to thermodynamic equilibrium, plasma can be classified into two categories, non–equilibrium (non-thermal)plasma and equilibrium (thermal) plasma. In non-thermal or cold plasma which is low-pressure, plasma characterized by high electron temperature T_e and low ion temperature T_i. In thermal plasma or hot, plasma are characterized by the electron temperature being equal to the gas temperature T_g.

Plasma with the temperature range of 2000-3000K and with charge particle density of 10^{19}-10^{21} m^{-3} are termed thermal plasma and the temperature range of 300-600K with charge particle density approximately 10^{13}- 10^{16} m^{-3} are called non-thermal plasma[7].

Plasma application covers an extremely wide range of plasma ion density and electron temperature as shown in figure(1-1) [8].

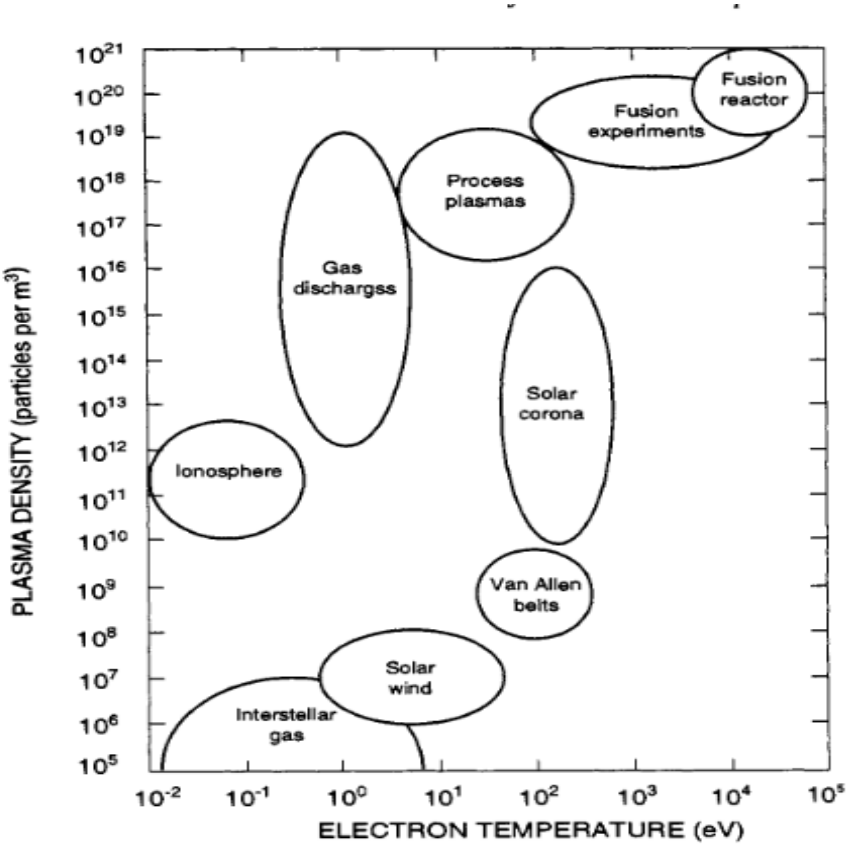

Figure (1-1) Some Plasma applications at different values of plasma densities and electron temperatures [8]

1-3 Sputtering process

Sputtering process was first reported by Grove in 1853 [9]. The removal of surface atoms (target) by bombarded with energetic ions is called sputtering process. The ejected atoms are traveled a distance until reached the substrate and start to condense into a film. In addition, there are number of the processes occur when a fast ions hits the target such as, secondary electron emission, sputtering target atom in an excited or ionized state, surface diffusion, surface reaction, incident particle implantation ,heating and photon emission as shown in figure(1-2) [10].

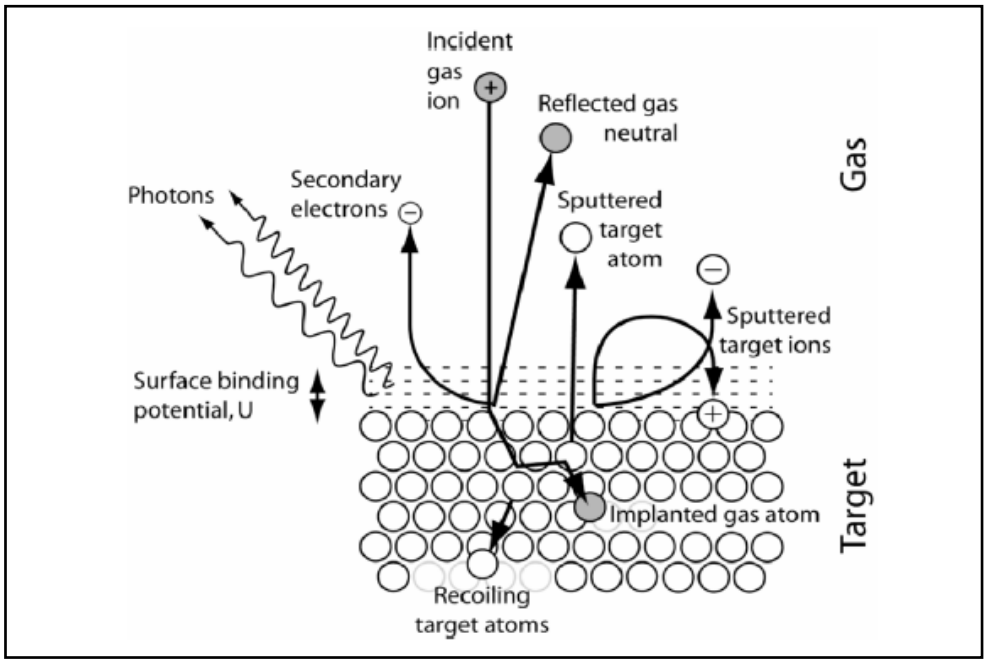

Figure (1-2) A schematic of the sputtering process[10].

The sputtering process is widely used for surface cleaning and deposition of thin films[11].The target material (cathode electrode) is placed in a chamber filled with gas at a low pressure and set on a negative potential. This negative potential is accelerated electron towards the grounded chamber wall and ionized gas atoms by the collision process. The ions of gas are accelerated towards the target and can be ejected atoms and collected on the substrate. In diode sputtering the degree of ionization gas is low. So to increase the ionization and the deposition rate ,a magnetic field is used to confine electrons near the cathode (target) and caused of increasing the ionization rate. Furthermore, the effect of magnetic field are clear to sustain a discharge in low gas pressure [12]. This method known as magnetron sputtering as in present work.

1-4 Structure of DC glow discharge

Another name for the glow discharge is a Plasma, which is an electrical current flowing through a gas that glows by light emission from the excited gas atoms. Various luminous and dark characteristics for glow discharge observed by early researchers, which is explain in figure(1-3)[13].

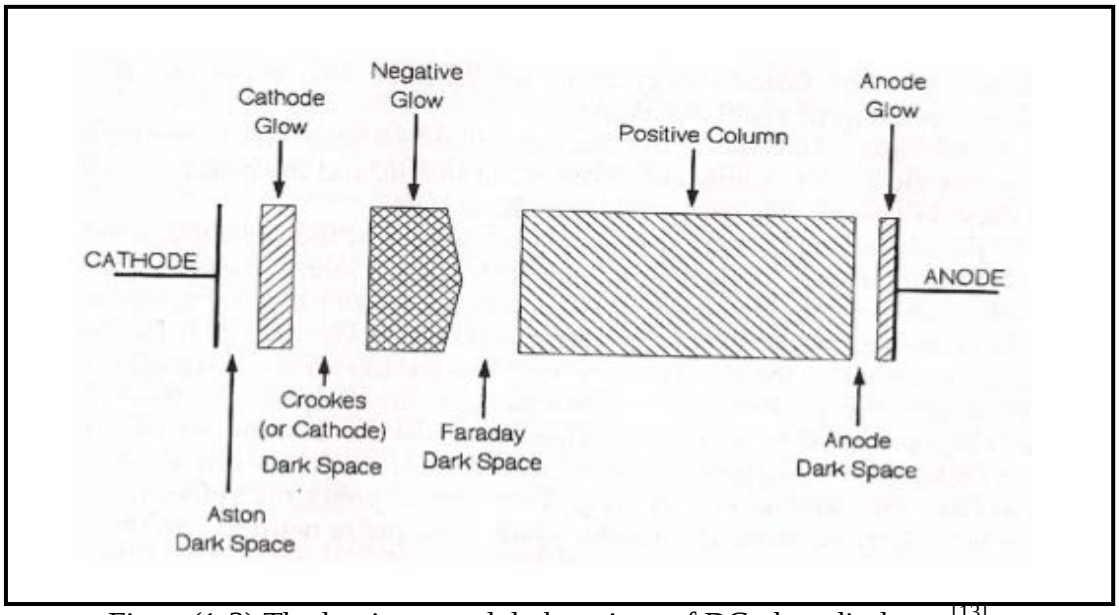

Figure(1-3) The luminous and dark regions of DC glow discharge[13].

Aston dark space is the region where the electrons emitted from the cathode has very low energy and ions are rapidly accelerated towards the cathode. The electrons cannot excite or ionize any gas particles due to their low energy[14]. The next region is also known as the "cathode sheath" of processing plasmas, but it is usually several times thicker than the actual sheath. This region, the Crookes (or cathode) dark space, is a region of primary interest, its thickness is approximately the mean distance traveled by an electron from the cathode before it makes an

ionizing collision. High velocity electrons that have accelerated across the cathode fall and low velocity electrons from impact ionization of neutral gas atoms are both present in this region. In the negative glow region, enhanced visible emission is due to the larger cross section of secondary electrons for excitation of neutrals. Electrons lose their energy in the negative glow region, so that when they arrive in the Faraday dark space, they are not able to neither excite or ionize any neutral gas atoms nor gain any more kinetic energy. The rest of the luminous region is called the positive column. Here electrons can gain enough kinetic energy from the small electric field in order to excite neutral gas atoms again as they move towards the anode. Ions with sufficient kinetic energy can also bombard the anode and emit secondary electrons, which then excite neutrals, producing the anode glow[15].

1-5 DC Glow discharge phenomena

The discharges between two electrodes is depending on different parameters such as, type of electrode material, geometry of electrodes, the pressure and the type of gas used. In general, the main formation regions of a DC discharges in low pressure gas are illustrated in figure(1-4)[16,17].

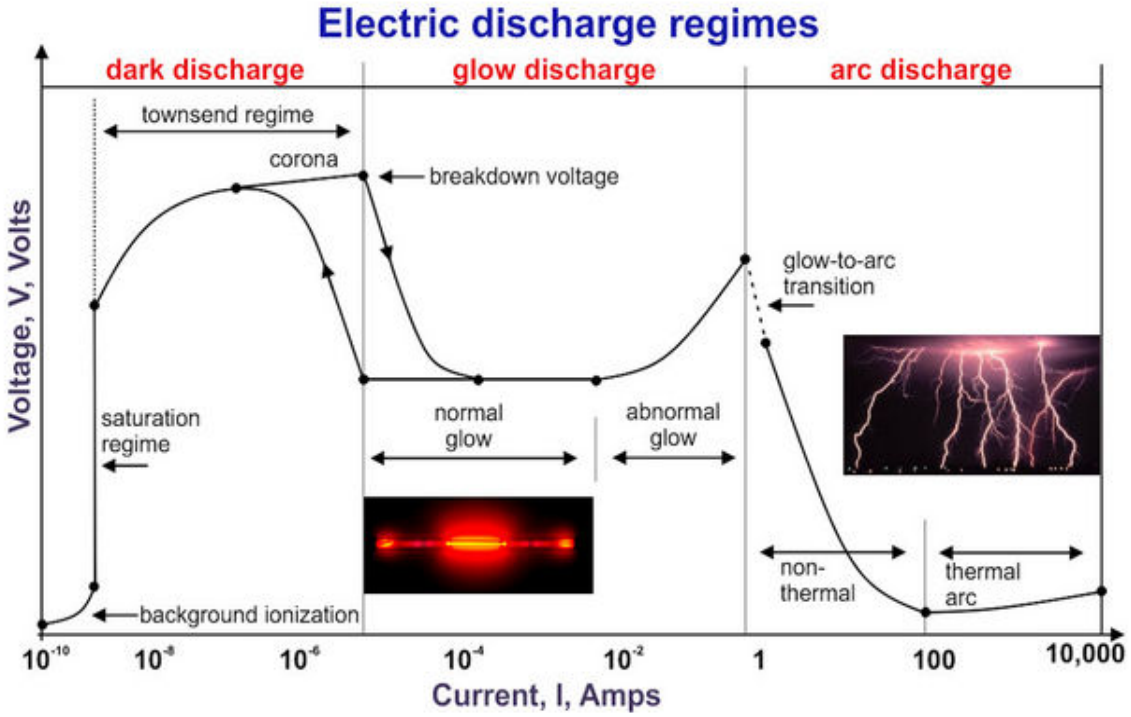

Figure (1-4) I-V characteristics of DC electrical discharge regions[16].

1-5-1 Dark discharge region

Dark discharge region is also known as Townsend's discharge is no appreciable light emission from such a discharge. Firstly, a very small current flow when a voltage is applied. The current is nearly constant and then the current increased as the voltage increased, and this is due to increase charged particles by collisions of gas atoms and electrodes.

1-5-2 Glow discharge region

This region is divided into two sub regions normal and abnormal glow discharge. In the normal glow, the voltage needed to sustain the discharge is at its minimum . Furthermore, the increasing in a current do not lead to a decrease of voltage. This sub region is ended when the whole of electrodes surfaces is covered by discharging of gas. On the other hand, in abnormal sub region, the discharges are fully covered the electrodes and any further increased current leads to increase of the cathode fall, and the voltage are increased .

1-5-3 Arc discharge region

In this region, the electrons are emitted from the cathode by thermionic or field emission. The arc discharge current is much greater than the current in a glow discharge region with low voltage.

1-6 Previous works

Theoretical and experimental studies in the field of DC plasma discharge to sputter material has been attempted by many researchers.

In 1980, Maniv and Westwood[18] have been operated and characterized a planar magnetron for Ar/H_2 mixtures gas to determine the effect of H_2 gas on the sputtering characteristics. An Al target was sputtered in DC and RF discharge at power up to 2.3kW. It has been shown experimentally that the addition of H_2 gas to Ar gases does not reduce the deposition rate of Al but causes a stable operation for the system.

In 1987, Spencer et al.[19] carried out an experimental investigation to study the influence of the magnetic field strength and distribution on the operating characteristic of a planar magnetron. Also, the configuration of the magnetic field has been studied. This study showed that suitable magnetic fields parallel to the target surface can give uniform target corrosion at low operating pressure with high efficient coating.

In 1991, Czekaj et al.[20] a theoretical study for the energy spectrum of ions striking the cathode of a DC planar magnetron has been studied. It was considered that, the ionization processes taking place in

the discharge cathode sheath. The results from this model are compared with experimental studies and it gives or shows a good agreement.

In 1997, Spatenka et al.[21] carried out an experimental study to diagnostic plasma near the target using Langmuir probe in a planar magnetron system. In the study, the electron density, electron temperature, plasma and floating potential and electron distribution function are measured in various positions between target and substrate under different conditions in the discharge. The research is proved that the additional magnetic confinement leads to two times higher electron density.

In 1998,Stokroos et al.[22] presented an experimental investigation to study the differences in conductive layers of Au/Pd, Pd and Cr, with a thickness of 1.5-3 nm ,deposited by planar magnetron sputtering device. This study showed that the particular construction of the sputtering devices, source –target distance, voltage employed, play an important role in the result.

In 2000, Kelly and Arnell [4]carried out a theoretical investigation to discuss the recent development made in the magnetron sputtering. These include closed field unbalanced, magnetron sputtering, pulsed magnetron sputtering and variable field strength magnetron. Also, several industrial applications are discussed.

In 2001, Szikora [23] has studied the characteristic parameter for DC planar magnetron discharge using Langmuir probe. He estimated the electron temperature and plasma potential using argon and argon-nitrogen discharge for titanium and copper as a target. The results showed that, the plasma potential and the floating potential varied between (-1.5 to -2.8 v) and (-20 to 0 v) respectively. Also, noticed that the electron temperature for Ti target is higher than that for Cu target.

In 2004, Kelly et al.[24] carried out an experimental investigation using pulsed magnetron sputtering (PMS) to deposit different dielectric materials. This study has shown that the PMS leads to hotter and more energetic plasma in comparison with DC discharge, and enhanced film properties.

In 2005, Costin et al.[25] analyzed the influence of the secondary electron emission induced by ion impact. In the study, a metallic cathode was used in a DC planar magnetron discharge. The effect of magnetic field, gas pressure upon the coefficient of secondary emission is discussed. The result showed that the inhomogeneity of magnetic field determines the spatial variation of the net secondary emission coefficient, and the minimum value of it are controlled by the reflection probability of the electron surface.

In 2007, Sum et al.[26] carried out an experimental investigation to study the influence of the gap spacing, d , on the breakdown voltage at constant argon gas pressure. They have been shown that the breakdown voltage increases with increasing of the gap spacing between electrodes. Furthermore, they found that the best spacing between electrodes is 2.5 mm for his conditions and system.

In 2010, Baranor et al.[27] studied the current–voltage characteristics of the planar magnetron experimentally and numerically. The model of the planar magnetron based on the measured current–voltage characteristics. The discharge pressure is varied in range (0.7-1.7 Pa). The magnetic field is of (0.033-0.12 T) near the cathode surface.

The dependence on the background gas density of the current is observed from the experiment results.

Also, **in 2010 Xin et al.**[28] studied the grain size and surface morphology of sputtered Au films which deposited by DC magnetron sputtering on Si substrates. The surface roughness as a function of film thickness with different temperature of substrate. It showed that the surface roughness increases with the increasing of grain size.

In 2012, by Asanithi et al. [29] experimental research to fabricate Ag nanoparticles was deposited on unheated substrates using dc magnetron sputtering. The depositions were carried out at two conditions the sputtering current and sputtering time. This study showed that the average size of Ag nanoparticles is 1.8 nm at a distance between the target –substrate 10 cm and depending on sputtering conditions.

In 2013, Rauch and Anders[30] carried out a theoretical investigation to estimate electron drift velocities in magnetron discharges using fluid approximation. In this study, single particle motion can be considered in a given electric and magnetic field to estimate drifts. In unbalanced magnetron, the magnetic and electric fields were measured. It showed that, the gradient of magnetic flux drifts and the curvature drift may reach values comparable to, or even greater than the cross product of electric and magnetic field drift velocities if the electrons are very energetic.

In 2015, Sahu et al.[31] have been investigated and measured the high –power dc magnetron sputtering discharge using Langmuir probe.

Also, an optical emission spectroscopy diagnostics method was used to compare the results. Furthermore, the analysis suggested that the warm electron in the plasma can be formed due to the collision less Landau damping.

1-7 Aim of the work

1-Study the effects of electrodes separation and target materials for low voltage DC discharge magnetron sputtering on operation conditions for minimum grain size of the coated samples and plasma parameters.

2-Study the morphology of surface coated samples at a constant argon gas pressure .

Chapter Two

Theoretical Considerations

2-1 Introduction

In this chapter, will give a basic concepts in plasma discharges and background on, magnetically confined plasmas and Pashen law. Also, some methods of plasma diagnostics, specifically single Langmuir probe in diagnosing plasma properties.

2-2 Plasma Concepts

2-2-1 Deby Length

One of the important parameter of plasma is Deby length. Plasma can similarity in way with conductors, where the surface charges arrange themselves so the net electric field is zero inside the surface. So, if an electric field is created in the plasma, the charged particles will be redistributed in order to shield the potential up to a distance called the Deby length, λ_D , which is given by[32,33]

$$\lambda_D = [\epsilon_\circ k_B T_e / e^2 n_e]^{½} \quad \cdots\cdots\cdots\cdots\cdots\cdots\cdots\cdots\cdots\cdots\cdots\cdots\cdots\cdots\cdots\cdots(2\text{-}1)$$

Where n_e is the density of electrons (m^{-3}), e electron charge, $\epsilon_\circ$ is the permittivity of free space, k_B is the Boltzmann constant and T_e is the electron temperature in (eV).

There are three conditions that an ionized gas satisfy to be called plasma [32], the first condition is

$$\lambda_D \ll L \quad \cdots\cdots\cdots\cdots\cdots\cdots\cdots\cdots\cdots\cdots\cdots\cdots\cdots\cdots\cdots\cdots(2\text{-}2)$$

Where L is the system dimension (plasma length) . Also, the second condition is

$$N_D \gg 1 \quad \cdots\cdots\cdots\cdots\cdots\cdots\cdots\cdots\cdots\cdots\cdots\cdots\cdots\cdots\cdots\cdots(2\text{-}3)$$

N_D is the number of particles in Deby sphere has radius equal to λ_D.

$N_D = \frac{4\pi}{3} n_e \lambda_D^3$ ……………………………………………………(2-4)

Finally, the third condition if ω is the frequency of collisions of plasma particles with atom and τ the mean time between collisions of charged then

$\omega\tau > 1$ ……………………………………………………(2-5)

2-2-2 Plasma sheath

At the edge of plasma, a potential exists, and it allows the flow of ions and electrons, to the wall to be balanced.

The electrons are far more mobile than the ions, thus plasma is therefor always a positive potential relative to any surface in contact with it . The none - neutral potential region between the plasma and the wall is called a plasma sheath as shown in figure(2-1)[33].

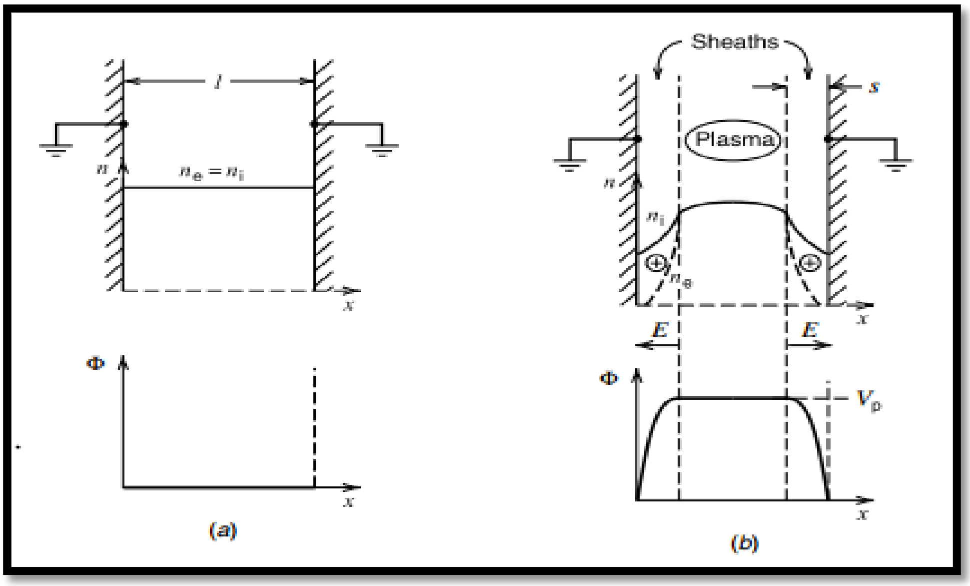

Figure (2-1) The formation of a plasma sheath:(a) initial ion and electron densities and potential; (b) densities, electric field, and potential after formation of the sheath[33].

The plasma sheath potential is given for a planar surface by

$$V_S = [(k_B T_e/2e) \ln (m_e/2.3m_i)] \quad \cdots\cdots\cdots\cdots\cdots\cdots\cdots\cdots\cdots\cdots\cdots\cdots(2\text{-}6)$$

where m_e , m_i are the mass of electron and ion respectively.

2-2-3 Plasma frequency

If a certain point in a plasma region, when the electron density become larger than the uniform background, the coulomb force will be pulled back to their original positions and keep plasma neutral . If electrons overshoot their equilibrium positions , then the electron are subjected to coulomb force in opposite direction . These oscillation occur at frequency of electron called plasma frequency of electron, ω_{pe} , given by[34]

$$\omega_{pe} = \sqrt{e^2 n_e/\in_\circ m_e} \quad \cdots\cdots\cdots\cdots\cdots\cdots\cdots\cdots\cdots\cdots\cdots\cdots\cdots\cdots(2\text{-}7)$$

2-2-4 Mean free path

Mean free path, λ_m , is defined as the average distance that atoms or molecule's moves without colliding with something else. And is given by [34]

$$\lambda_m = [1/(4\,\sigma\, n_g)] \quad \cdots\cdots\cdots\cdots\cdots\cdots\cdots\cdots\cdots\cdots\cdots\cdots\cdots\cdots(2\text{-}8)$$

Where σ is momentum transfer cross section for electron - neutral atom collisions $\sigma = \pi\, r^2$

$$n_g = (P / k_B T_g) \quad \cdots\cdots\cdots\cdots\cdots\cdots\cdots\cdots\cdots\cdots\cdots\cdots\cdots\cdots(2\text{-}9)$$

n_g is the density of gas atoms, P gas pressure, T_g is the temperature of gas, r is the radius of gas atom.

2-2-5 Larmor radius and Cyclotron frequency

If an external magnetic flux, B, was applied on the charged particle of mass m, charge q and velocity v, the equation of motion is given by [35]

$$m\frac{d\vec{v}}{dt} = q\,\vec{v}\,x\,\vec{B} \quad \cdots\cdots\cdots\cdots\cdots\cdots\cdots\cdots\cdots\cdots\cdots\cdots\cdots\cdots\cdots\cdots(2\text{-}10)$$

Figure(2-2) shows the effect of magnetic field that leads the charged particle to move in helical or curved lines around the magnetic field direction in circular orbits of Larmor radius r_L

$$r_L = mv_\perp/qB \quad \cdots\cdots\cdots\cdots\cdots\cdots\cdots\cdots\cdots\cdots\cdots\cdots\cdots\cdots\cdots\cdots(2\text{-}11)$$

Where $v_\perp$ is velocity perpendicular to B.

Also, the cyclotron frequency, ω_c , is given by

$$\omega_c = v_\perp/r_L \quad \cdots\cdots\cdots\cdots\cdots\cdots\cdots\cdots\cdots\cdots\cdots\cdots\cdots\cdots\cdots\cdots(2\text{-}12)$$

$$\omega_c = |qB|/m \quad \cdots\cdots\cdots\cdots\cdots\cdots\cdots\cdots\cdots\cdots\cdots\cdots\cdots\cdots\cdots\cdots(2\text{-}13)$$

Where

F_L is the central Larmur Force.

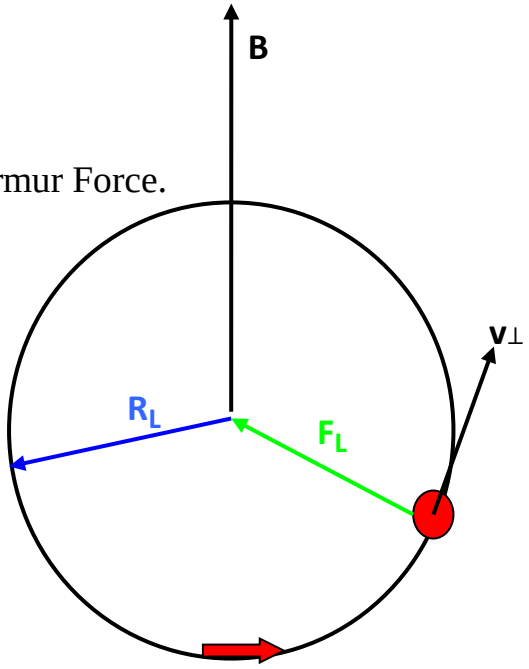

Figure(2-2) Cyclotron motion of a charged particle.

2-3 Magnetic Field in Magnetrons

The electric and magnetic fields are used to confine secondary electron which are generated near the cathode electrode.

This confinement of magnetic flux leads to increase the probability that an electron will have a collision with gas atom and increasing the ionization process. Also, lower operating pressure and lower operating voltage that generate a dense plasma near cathode region.

According to the shape and magnitude of magnetic flux, there are two type of magnetron as shown in figure(2-3)[4]

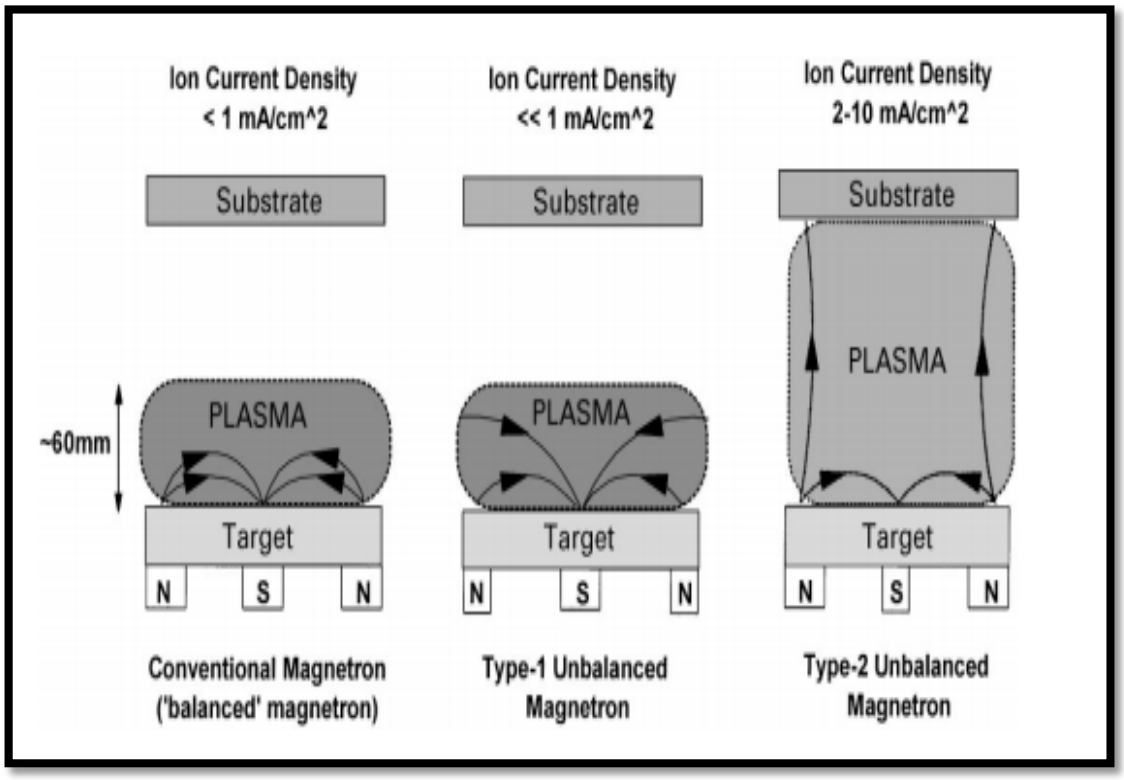

Figure (2-3) Schematic representation of the plasma confinement observed in conventional and unbalance magnetrons[4].

The plasma in the conventional balanced magnetrons is strongly confined to the region of the target and produced a dense plasma, not more than few centimeters from the target. Therefore, the film grown on substrate placed within this region will be affected by

strong ion bombardment which affects the structure and film growing. Substrate is placed out of this region and the density of plasma will be low and the ion substrate current insufficient to modify the structure of the film. In the case of increasing the negative bias applied to the cathode this leads to increase the energy of bombarding ions which cause stresses and defects in the film.

In unbalanced magnetrons the outer ring of magnets is strengthened relative to the central pole. So, not all the field lines are closed between the central and outer poles in the magnetron, but some are directed towards the substrate, and some secondary electrons able to follow these field lines. The plasma allowed to flow out towards the substrate, thus high ion currents can be extracted from the plasma this can show in figure(2-3) type-2. While in type-1 for the same figure the central pole was strengthened relative to the outer pole. So, the field lines which do not close in on themselves are directed toward the chamber walls and the plasma density in the substrate region is low. Ion current densities in unbalance magnetrons approximately higher than for conventional balance magnetrons which can be routinely generated.

2-4 Electrical breakdown in gases

To produce and sustain the plasma certainly using electrical energy, so applied voltage must outrun the breakdown voltage for dielectric properties and convent a conductor. The breakdown voltage ,V_b , in gas discharge plasma is given as[36]

$$V_b = (B\,Pd)/\{\ln(A\,Pd) - \ln[\ln(1+\frac{1}{\gamma})]\} \quad \cdots\cdots\cdots\cdots\cdots\cdots\cdots\cdots\cdots (2\text{-}14)$$

$V_b = F(Pd)$, which is Pashen Law.

Where A and B numerical parameters for different gases , P pressure of gas, d electrodes separation and γ is secondary electron emission coefficient.

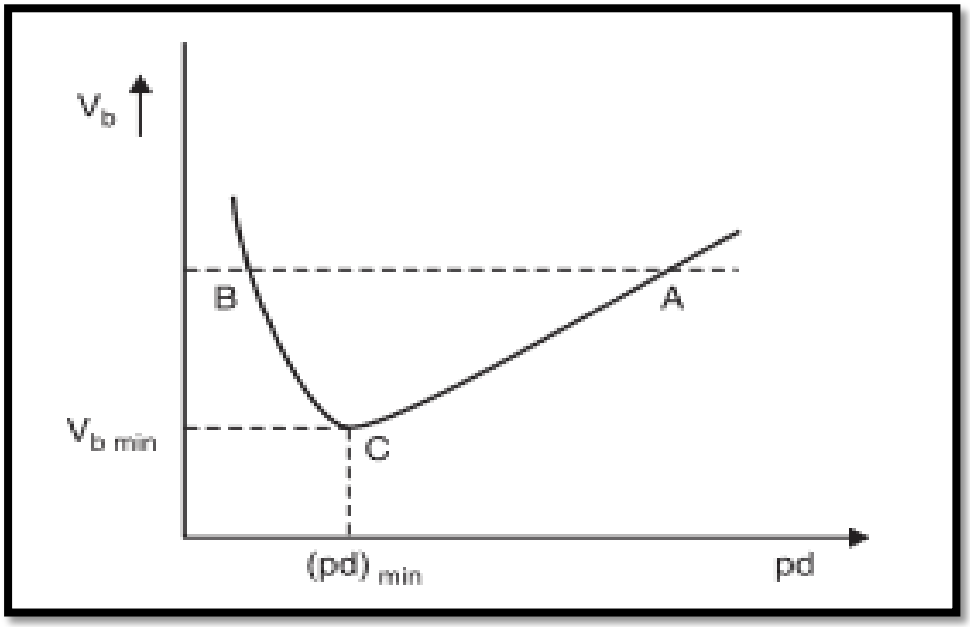

Figure(2-4) Pashen Law curve[36].

2-5 Plasma diagnostics

Plasma diagnostics are the using of some techniques to deduce information about the state of plasma and to determine plasma parameters such as electron temperature, electron and ion densities and other parameters. There are different methods for plasma diagnostics :

2-5-1 Optical emission spectroscopy

Optical emission spectroscopy (OES) is one of the types of remote diagnostics of plasma. In this method, a visible light is collected by lens and focused on to a photodiode detector. An interference filter are used to isolate a particular spectral line. By comparing the intensities of different spectral lines, the plasma parameters can be determined[37].

2-5-2 Microwave interferometry

In this remote diagnostic method, the radiation of microwave is launched by a horn antenna into plasma region through a window. The phase of microwave signal is changed inside plasma region and this change which increases with density of the plasma. By comparing between the phase of reference signal and propagated signal it can determine the plasma parameters[38].

2-5-3 Laser - induced florescence

Laser induced florescence (LIF) is both non-invasive and local because it uses intersecting beam paths. By using laser beam propagated in plasma region and lead to raise ions to an excited state. The excited ions fluoresce, giving a light which is collected by lens. The plasma parameter can be deduced from collected light using Doppler broadening of the line and ion velocity[37].

2-5-4 Langmuir probe

This plasma diagnostic technique was developed by Langmuir in 1923. Using a metal probe placed into plasma region to extract certain measurable parameters of plasma such as, electron temperature and electron density and energy distribution[39,40,41]. There are different types of Langmuir probes such as, single, double and triple probes.

The experimental measurements show that, the double and triple probe are good tools for the characterization of radio frequency (RF) generated discharge plasma[42].

2-6 Single Langmuir probe

This diagnostic technique is used in present work to determine plasma parameters. Single Langmuir probe is just a small metallic electrode using a wire of tungsten inserted into plasma region. A variable biasing voltage applied on this electrode, which may be positive and negative with respect to the plasma. The collecting current by the probe provides information's help us to determine the plasma parameters.

The probe is used to collect ion or electron current that flow into it in response to different known voltages. The I-V characteristic curve is shown in figure(2-5) [43,44].

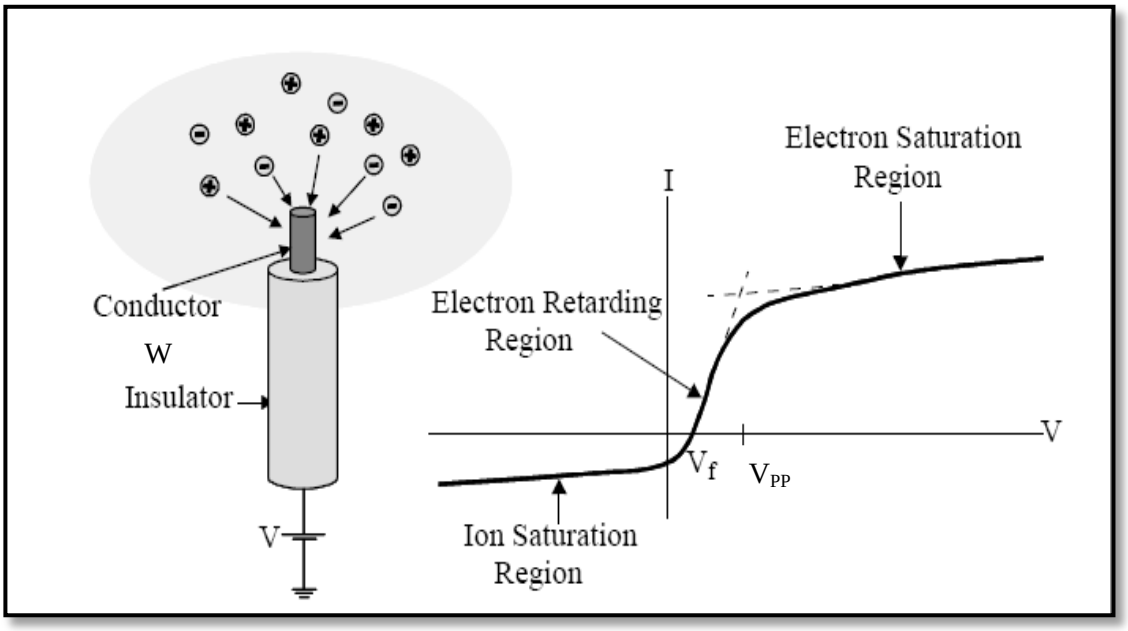

Figure(2-5) Schematic of a Langmuir probe and general appearance of the I –V characteristic curve in stationary plasma[45].

The qualitative behaviors of the figure can be shown as follows :

1-Region (c) :

At the point V_f which is called the floating potential, the probe is sufficiently negative to repulse all electrons and expect a flux of ions. This potential is assumed as insulated electrode inserted in to plasma. Almost all the electrons are repulsed at larger negative values of V_p and an ion sheath and saturation ion current[44].

$$I_i = A_p n_i e \frac{\sqrt{2}}{\pi} (-e V_p/m_i)^{½} \quad \cdots\cdots\cdots\cdots\cdots\cdots\cdots\cdots\cdots\cdots\cdots\cdots\cdots (2\text{-}15)$$

Where I_i , A_p ,n_i ,e ,V_p and m_i , are the ion current, probe surface area, ion density, electron charge, probe voltage and ion mass respectively.

The ion density is obtained from equation (2-15) :

$$n_i = (\pi/A_p e)\ (m_i/2e)^{½}(-\text{slope})^{½} \quad \cdots\cdots\cdots\cdots\cdots\cdots\cdots\cdots\cdots (2\text{-}16)$$

Where

$$\text{slope} = I_i^{2} / V_p \ .$$

2-Region (B) :

If the probe potential is made negative with respect to plasma potential, V_{pp}. The probe begin to repulse electrons and accelerate ions . Then electron current falls as V_p decreases into region of ion saturation current, this region is known the transition region (electron retarding regime). For Maxwellian distribution of electron , the electron current is given by[46]

$$I_e = I_{es}\ e^{[e(V_p - V_{pp})\ /\ k_B\ T_e]} \quad \cdots\cdots\cdots\cdots\cdots\cdots\cdots\cdots\cdots\cdots\cdots\cdots\cdots (2\text{-}17)$$

Where I_e , I_{es} , k_B and T_e , are the electron current, electron saturation current, Boltzmann's constant and electron temperature respectively.

The invers slope of the logarithmic plot of the electron retarding regime provides the electron temperature, using

$$d \ln I_p / dV_p = e / k_B T_e \quad \cdots\cdots\cdots (2\text{-}18)$$

3-Region (A) :

At voltage V_{PP} the potential of probe is the same as the plasma and there is no electric field at this point. The charged particles, because of their thermal velocities, emigrate to the probe. The current that collected by the probe is mostly an electron current because electrons move very faster than ions. If the voltage of probe is made positive with respect to the plasma, electron accelerated towards the probe, while ions are repulsed. Therefor near the probe surface there is an excess of negative charge which built up until the total charge is equal to the positive charge on the probe making very thin layer of charge (sheath). The area of the sheath is comparatively constant as the probe voltage is increased, this region know saturation electron current, I_{es} , can be determined referring to Orbital Motion Limit (OML) theory[44] and the selection of diameter of Langmuir probe is takes according to the collisionless condition for the same theory[4].

$r_L > r_p$ and $\lambda_m < r_p < \lambda_D$

$$I_{es} = (n_e e A_p/4)(8 k_B T_e / \pi m_e)^{1/2} \quad \cdots\cdots\cdots (2\text{-}19)$$

Where A_p is the area of probe, T_e is the temperature of electron and

n_e is the density of electron which can be calculated using equation

$$n_e = (4I_{es}\sqrt{\pi m_e})/(e A_p (8k_B T_e)^{½}) \quad \cdots\cdots\cdots\cdots\cdots\cdots\cdots\cdots\cdots\cdots(2\text{-}20)$$

4-Floting potential V_f :

It is defined by

$$I_i = I_e \quad \text{or} \quad I_i(V_f) + I_e(V_f) = 0$$

where I_e is given by eq. (2-17)

and I_i is given in eq. (2-15) [47]

$$V_f = V_{pp} - (k_B T_e/2e)\ln(2m_i/\pi m_e) \quad \cdots\cdots\cdots\cdots\cdots\cdots\cdots\cdots\cdots\cdots(2\text{-}21)$$

From this equation , floating potential depends only on the electron temperature and the species of ions involved .

5- Plasma potential V_{pp} :

Additionally, plasma potential called space potential. To obtain it, one must draw a straight lines through I-V curve in the transition region and the electron saturation region. And the voltage point is named V_{pp} , and the current is I_{es} .This does not act well it can be measured using eq.(2-21) after determined V_f .

2-7 Sputtering yield Y

Sputtering is quantified by the sputtering yield Y, which means the mean number of atoms removed per each incident particle. That is

Y = atoms removed / incident particles

The sputtering yield depends on the properties of both, the incident particle and target material .

Sputtering yield is the most basic measure of sputter efficiency Sigmund has presented a general theory of sputtering yield and driving the following equation : [17,48]

$$Y(E) = \frac{3}{\pi^2} \frac{\alpha}{U_b} \frac{M_1 \; M_2}{(M_1 + M_2)^2} \; E \quad \cdots\cdots\cdots\cdots\cdots\cdots\cdots\cdots\cdots\cdots\cdots\cdots\cdots\cdots (2\text{-}22)$$

with the boundary conditions

$$10 \; U_b < E < 1 \, \text{keV}$$

Where $\alpha = 0.15 + 0.13 \; M_2/M_1$

M_1 mass of gas atom, E energy of ion particle, M_2 mass of target atom and U_b surface binding energy(eV) its values for gold =4.13 eV and for silver =3.33 eV [49]

α is a function of the relative masses and the angle of incidence of the incoming ions, therefore sputtering yield depend on:

Firstly, the mass, the energy and angle of incidence of bombarding ions.

Secondly on the mass of the target atoms, the surface binding energies and the orientation of the crystallites of the solid[17,48].

2-8 Atomic Force Microscope (AFM)

The basic technique and inevitable for all nanoscopic research is Atomic Force Microscope (AFM). It is also known as Scanning Force Microscopy (SFM). To study the surface structure and quantifies surface topography. The first AFM was made in 1986. Two types of AFM modes, contact and Tapping or noncontact. AFM works by a tip very close to the sample surface. The standard of operation is measuring repulsive and attractive forces between the tip (probe) and the sample in constant height. The needful parts are the x/y and z pieso that are separately actuated by x/y drive and z-control with maximum precision , so atomic distance can be measured. A micro-fabricated cantilever with a sharp tip is deflected by particularity on a sample surface , much similar in a photograph but on very small scale. A laser beam reflects the backside of the cantilever into an image of the surface. Figure(2-6) schematic diagram for AFM.[50]

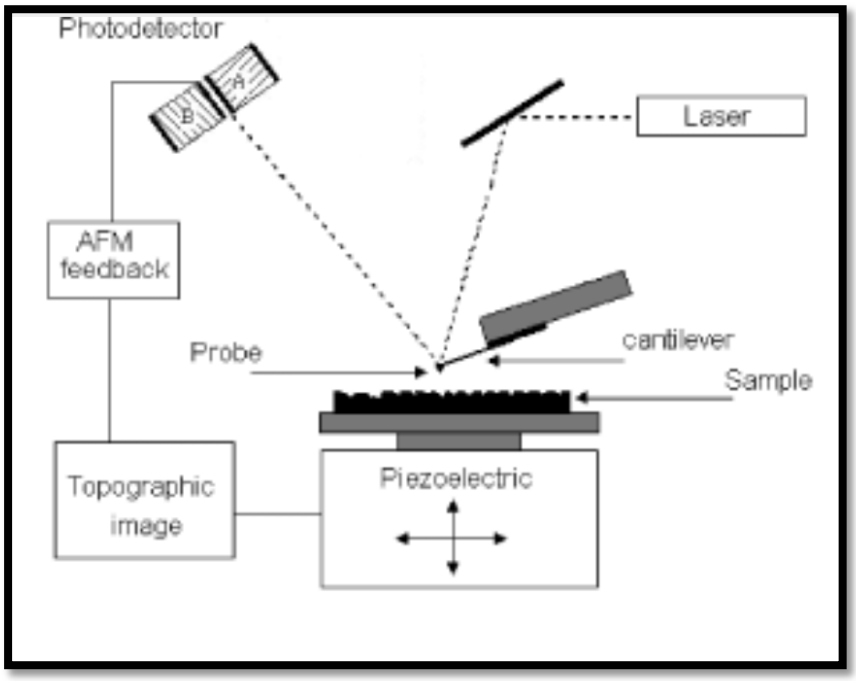

Figure(2-6) Schematic diagram of an AFM set up apparatus basic components[51].

2-9 Effect of target material on sputtering process

The type of target material for plasma sputtering source is an important parameters on sputtering process so, in a solid target material whose surface is bombarded by energetic particles several possible processes my occur as mentioned in figure(1-2). A surface atoms will be ejected from the surface, if it is resave an energy depending on the type of target material. Surface damage is accrue when lattice atom move to new lattice sites and it is losses amount of energy. Many common materials in sputtering such as gold and silver which are used in present works. Gold is a transition metal and it is densest than silver. The electrical conductivity is larger than other materials. Therefore, both gold and silver used in different applications such as electrical circuits and medicine. Table (2-1) shows the properties for the gold and silver targets which are in group (11) of the periodic table of elements [52,53].

Table (2-1) Gold and silver target materials properties.

Properties	Gold (Au)	Silver (Ag)
Atomic number	79	47
Atomic weight	197	107.66
Melting point ≈	1200	1000
Specific gravity≈	19.5	10.5
Specific heats	-0.324	-0.57
Density g/cm³	19.32	10.5
Thermal conductivity ($W. m^{-1}. K^{-1}$)	317	450

Chapter Three

Experimental Set up Description

3-1 Introduction

In this work, a DC planar magnetron sputtering system was manufactured by *Quorum Technologies*, used to study the effect of electrode separation, and target materials on the coated samples. Also, the plasma parameters are determined for this system by diagnostics of plasma discharge using a cylindrical single electrostatic Langmuir probe. Figure(3-1) shows photographic for the system.

Figure (3-1) Photograph of the sputtering system

A DC power supply is used to supply the system by range of voltages varied between (0, and 800) Volts and current between (0, and 100)mA.

3-2 Description of the system

The system consists of ;

1-Plasma chamber 2- Electrodes(cathode and anode) 3-Permanent magnets 4- Vacuum unit 5- Langmuir probe as shown in a schematic diagram in figure(3-2).

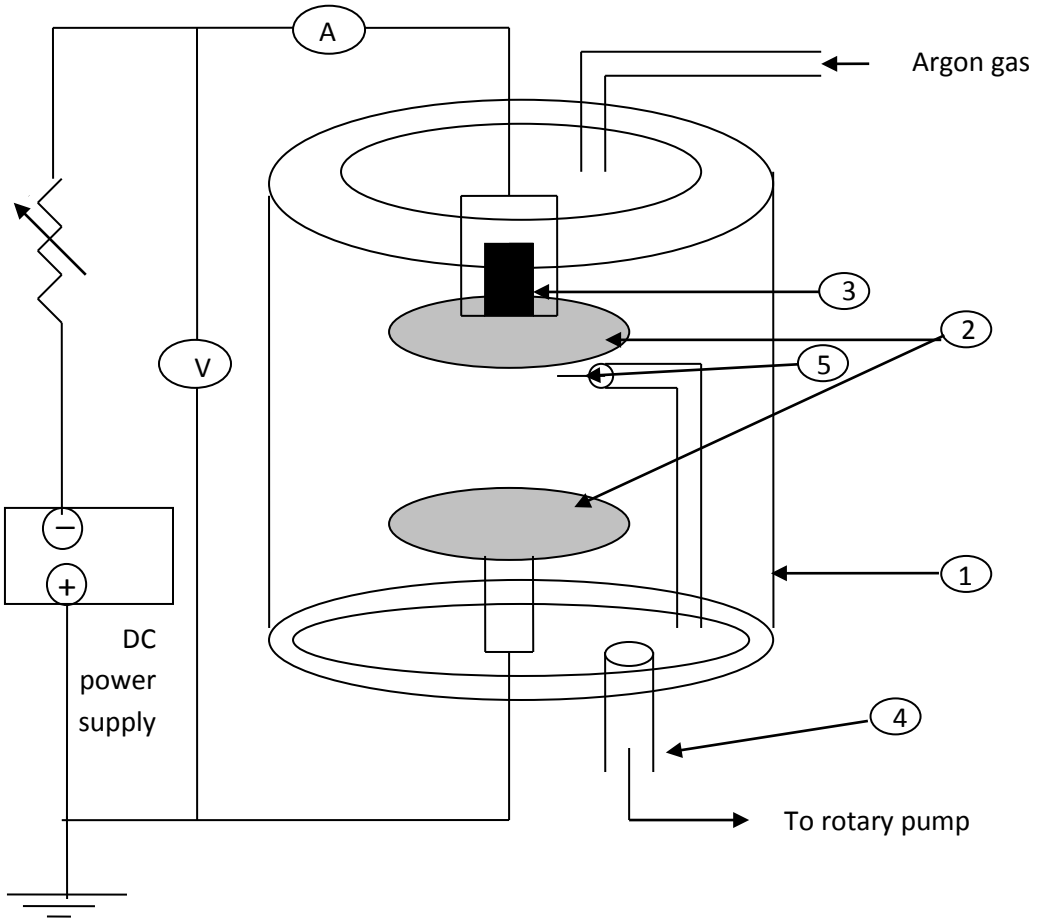

Figure(3-2) Schematic diagram of the experimental setup

3-2-1 Plasma chamber

A cylindrical discharge chamber for working system is a *Borosilicate* glass tube of (165 mm) diameter and (127 mm) high. A photograph of plasma chamber shown in figure(3-3) .

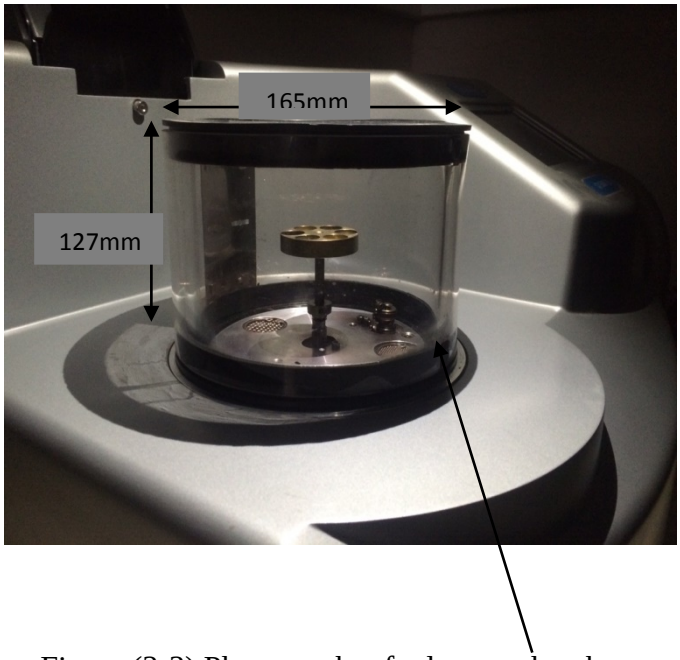

Figure (3-3) Photograph of plasma chamber .

3-2-2 Electrodes

Two parallel circular electrodes which are represented the cathode and anode poles are enclosed in the discharge chamber. The cathode is made of stainless steel with target material. In present work, gold and silver are used as a target of a diameter (57 mm) and thick (0.1 mm). A cylindrical permanent magnet is placed in the center of the cathode electrode to produce the magnetic field. Anode electrode is made of stainless steel with a diameter (50 mm) which represents a stage of substrate. Figure(3-4) shows a photograph of cathode and anode electrodes.

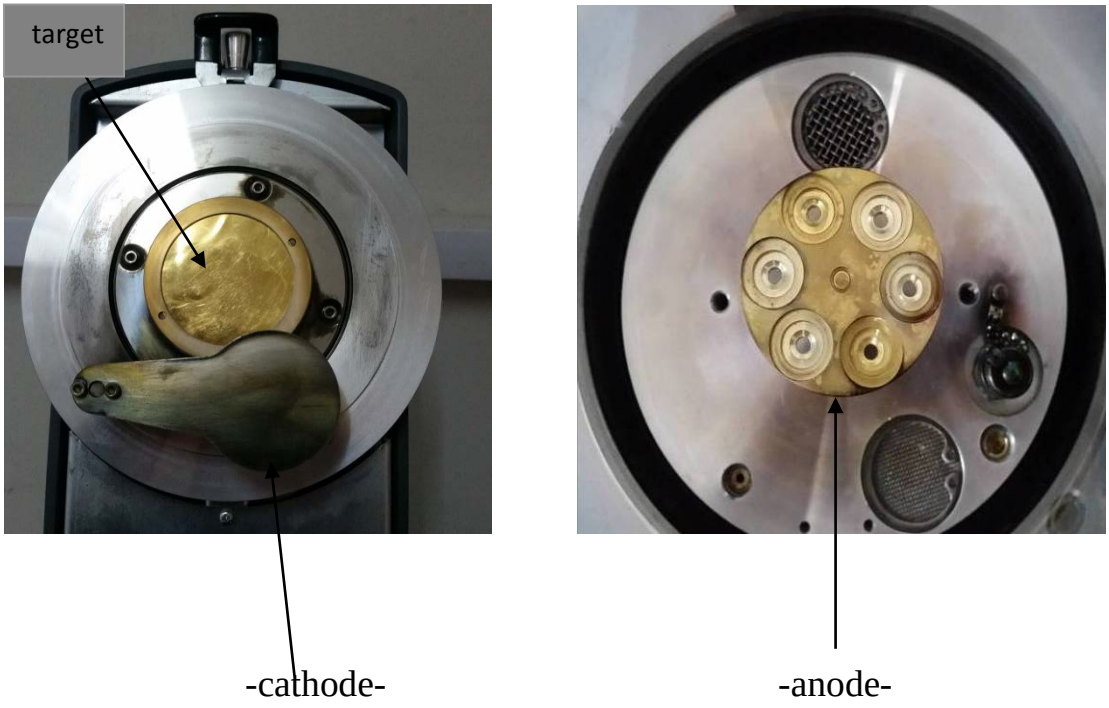

Figure (3-4) Photograph of cathode and anode electrodes.

3-2-3 Permanent magnet

Two cylindrical permanent magnets of diameter (12.5 mm) and thickness (6.3 mm) for each one are placed in the center of the cathode electrodes to produce a magnetic field using for confinement electrons near the target as shown in figure(3-5).

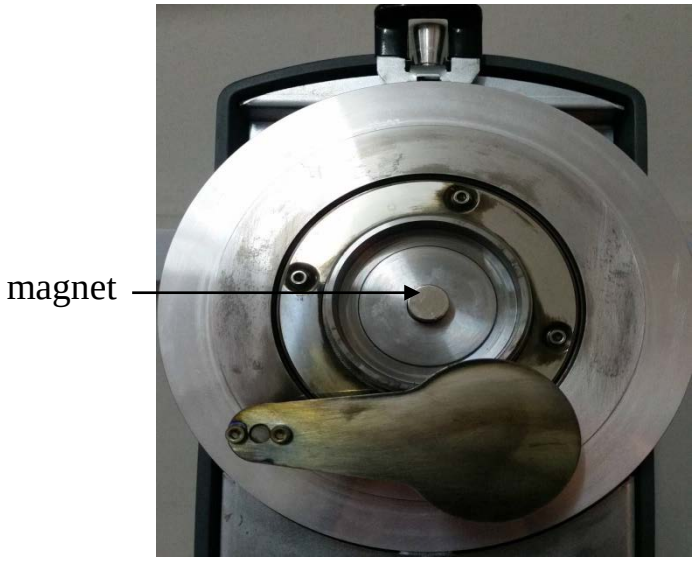

Figure (3-5) Photograph of a cylindrical permanent magnet.

3-2-4 Vacuum Unit

Vacuum in the discharge chamber is obtained using a two-stages rotary pump *VALUE VE280N*. The discharge chamber is evacuated to abase pressure of ($1x10^{-3}$) mbar. The pressure inside chamber is measured using *Edwards pirani gauge (1101).* The argon gas which used of purity is (99.999%) and fixed at pressure (0.2 mbar) inside chamber with a control of mass flowmeter.

3-3 Diagnostics of plasma discharge

A cylindrical single Langmuir probe made of tungsten wire of (0.5 mm) diameter and (8 mm) length used to characterize the plasma parameters with electrical circuit is used as shown in figure(3-6).

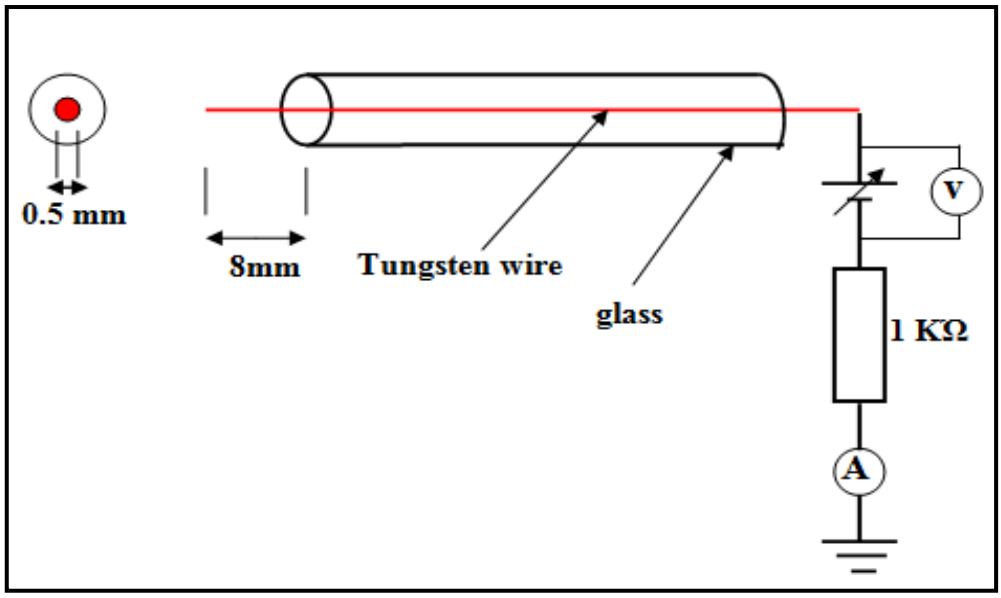

Figure (3-6) Schematic diagram for single Langmuir probe and electrical circuit.

The probe is threaded into a glass tube to insulate it from the plasma. The probe is positioned perpendicular to the electric field near the cathode (target) about (10 mm). The DC power supply **(***Stromversorgungsgerät* SV 59/52-4) is connected with probe varied between (-120 to +120) volt and (0-150) mA is used in the probe circuit as a positive and negative bias voltage for probe. Sputtering current measured by using *kitly* and a resistance (1 kΩ) connected with the electrical circuit.

3-4 Preparation for the sample

A glass substrate of dimensions (1cm x 1cm) deposited with Au and Ag at different electrodes separation and sputtering current. The substrates is cleaned with alcohol and dried in air before loading into the deposition chamber. Substrates are placed on anode electrode.

3-5 Operation of the system

1- Cleaning the plasma chamber and electrodes by alcohol.
2- Put the sample in a fixed place on the anode electrode after determined the separation between two electrodes.
3- Place the target material in the cathode electrode and then dropping off the gate at the chamber.
4- Switch on the system after preparing the operation conditions included the discharge current values, time of sputtering and flow of pressure.

5- Evacuated the chamber using a rotary vacuum pump to base pressure of about ($1x10^{-3}$ mbar). After that we inlet the argon gas to pressure (0.2 mbar). A voltage applied between the two electrodes inside the chamber to generate the plasma.
6- Record the cathode voltage for each discharge current at different electrodes separation.

3-6 Morphology of Coated Samples

In present work , the morphologies of coated samples are studied using AFM *(AA 2000) Angstrom Advanced Inc./ USA*. From this study, we determined the effects of electrode separation and target materials on morphology parameters such as average grain diameter, average grain height, roughness average , average grain size.

Chapter Four

Results and Discussions

4-1 Introduction

This chapter includes the results and analysis of the experimental measurements of plasma parameters using cylindrical single Langmuir probe. Also, the effects of separation between the cathode and anode , and the target materials. The morphology properties for gold and silver deposition was studied after preparing for different electrodes separation using Atomic Force Microscope (AFM). Furthermore, the sputtering yield was calculated for different electrodes separation and targets.

4-2 Distribution of magnetic flux

Figure(4-1-a) shows the radial distributions of magnetic flux for permanent magnet using the *Hall probe* (Alpha Lab Inc. / USA) across the cathode electrode diameter. This figure shows that the magnetic flux, B, is non-uniform . The magnetic flux has a maximum value (3350 Gauss) in the center of the cathode region, and then the flux decreases at the edge of cathode.

The axial distribution of the magnetic flux along the center of the discharge tube as a function of the distance between the electrodes is shown in figure(4-1-b). The magnetic flux has a maximum value (3350 Gauss) at the center of the cathode full region and then it decreased at the anode center.

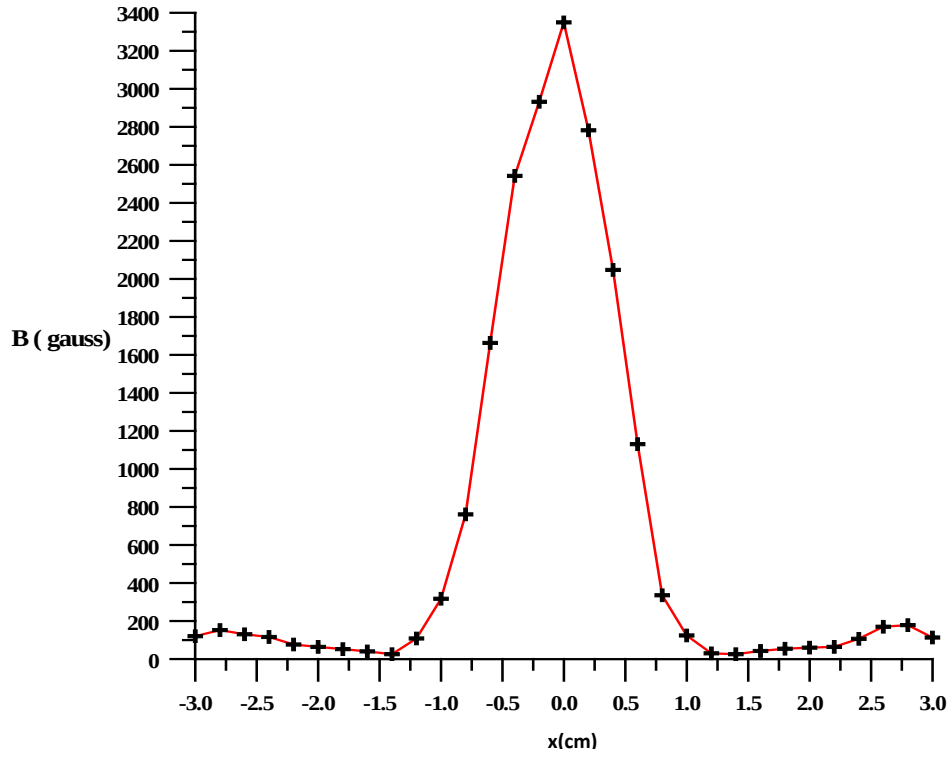

-a-

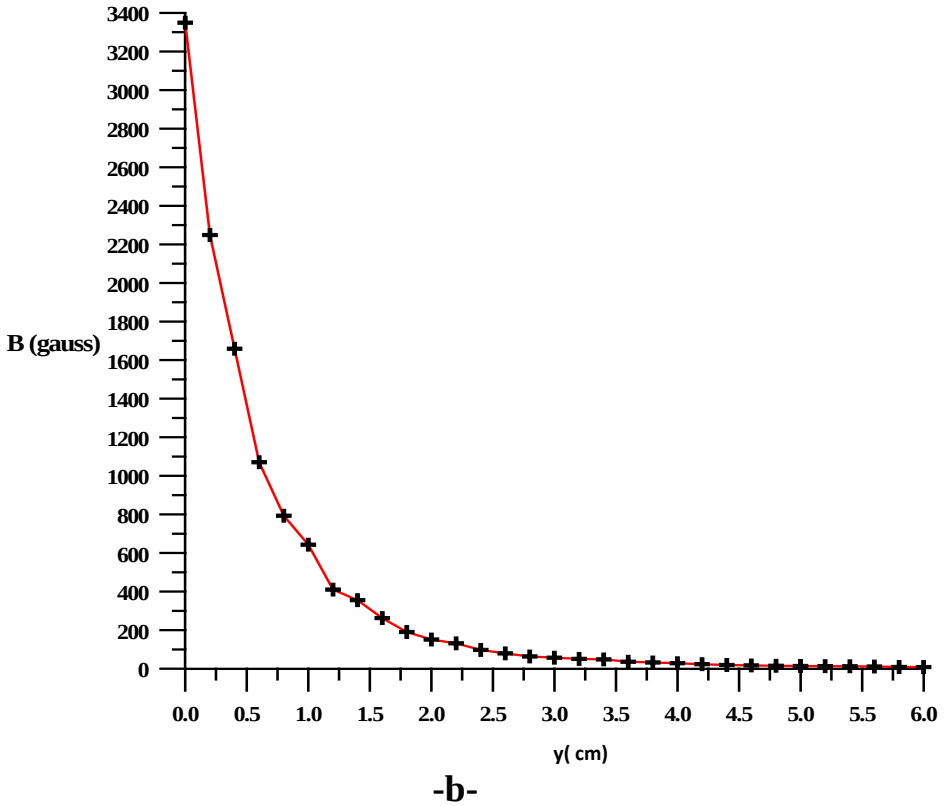

-b-

Figure (4-1) Magnetic flux distribution for **a-**radial distance from the edge to edge for cathode electrode passing through the center of the magnet. **b-**axial distance between cathode and anode electrodes.

4-3 Electrodes gap effect on I-V characteristic of DC discharge

4-3-1 I_d-$V_{cathode}$ characteristic

The variation of discharge current or sputtering current, I_d , (current measured at the cathode) with applied cathode DC voltage, $V_{cathode}$, for different electrodes separation(3,4,4.5,5 and 6)cm at fixed argon gas pressure P (0.2 mbar) for gold and silver target are shown in figure(4-2).

Figure(4-2-a) shows that as the discharge current increases the cathode voltage are increased with increasing the separation between electrodes for gold target. Also, in figure(4-2-b) the same behaviors have shown using silver target. It is shown that from figure(4-2) that the required voltage cathode for gold target is greater than the silver target. This behavior is agreement with results from A.R.Galaly [54], M.N.Stankov [55] and O.Barannor et al. [27].

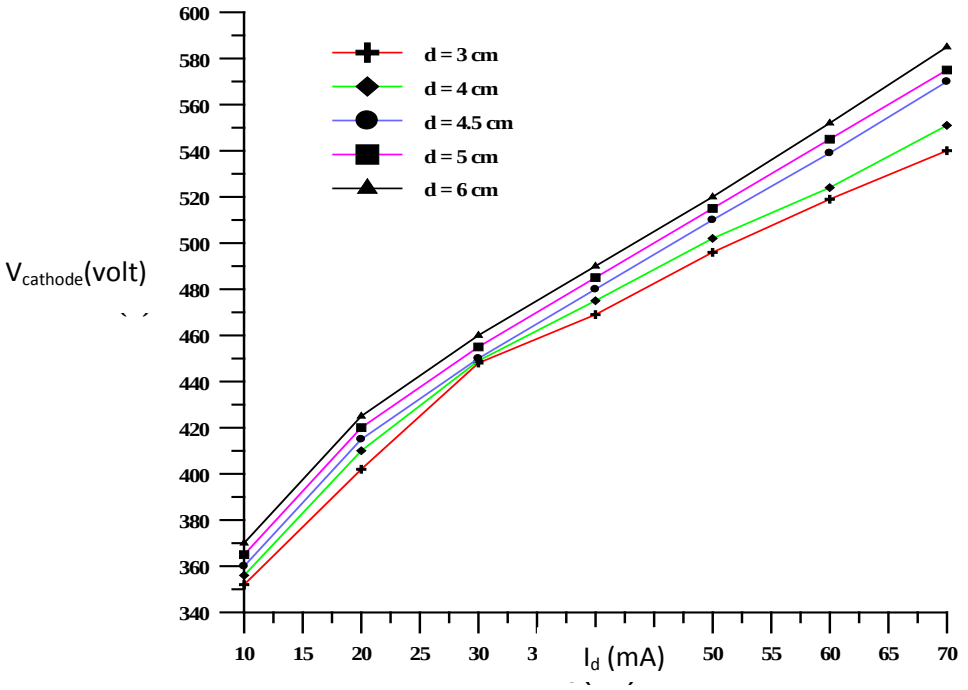

-a-

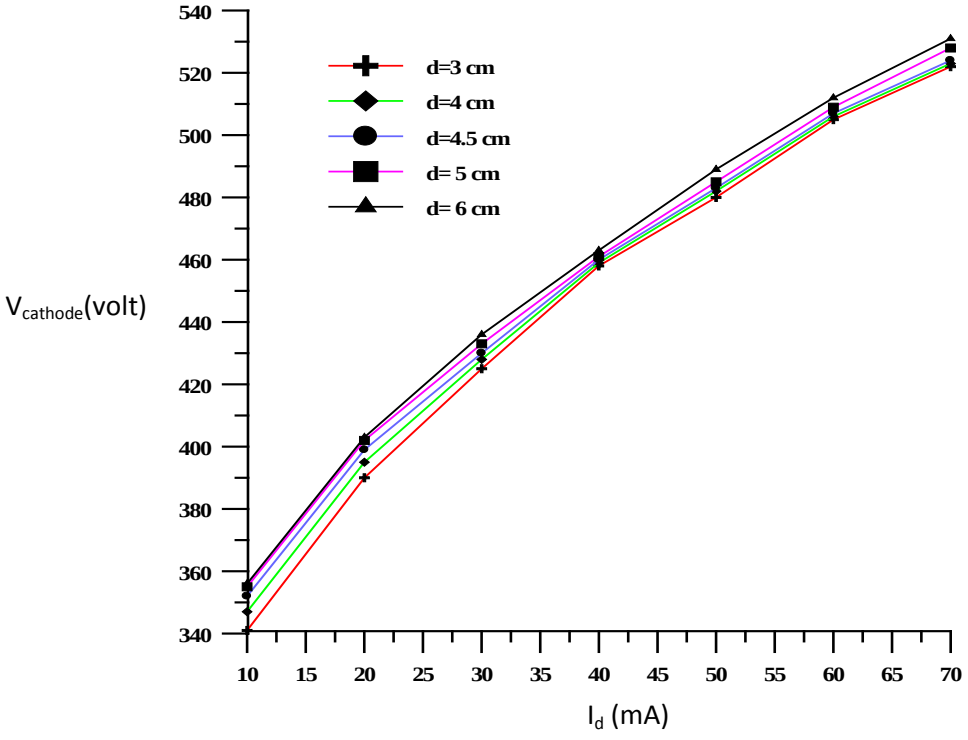

-b-

Figure(4-2) Voltage of cathode electrode as a function of sputtering current at P=0.2 mbar for different electrodes separation for **a**- gold target **b**-silver target.

4-3-2 $I_d - I_a$ characteristics

The anode current, I_a , which is measured at anode electrode are studied as a function of the discharge current I_d with different electrodes separation for gold and silver targets as shown in figure(4-3).

It was observed that, from figure(4-3-a) for gold target, the anode current increased as the discharge current increase with increasing electrodes separation. The same behaviors shown in figure (4-3-b) for silver target.

In general, it is clear from the figure(4-3) that, when a gold target was used, compare between the ratio of increasing anode current is about 3.7% from that for silver target.

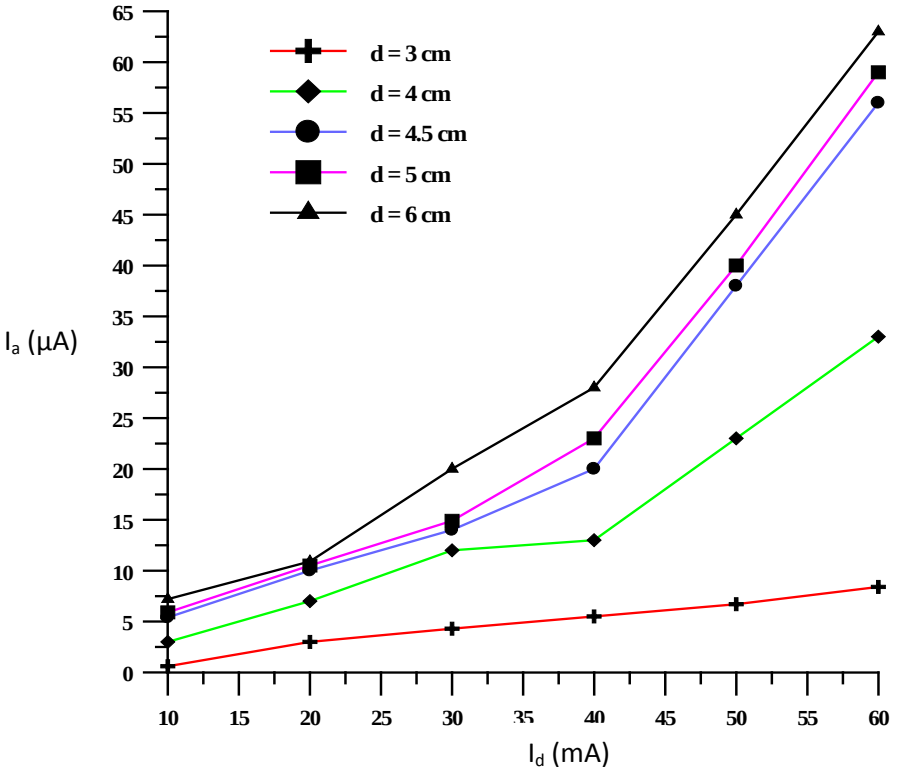

-a-

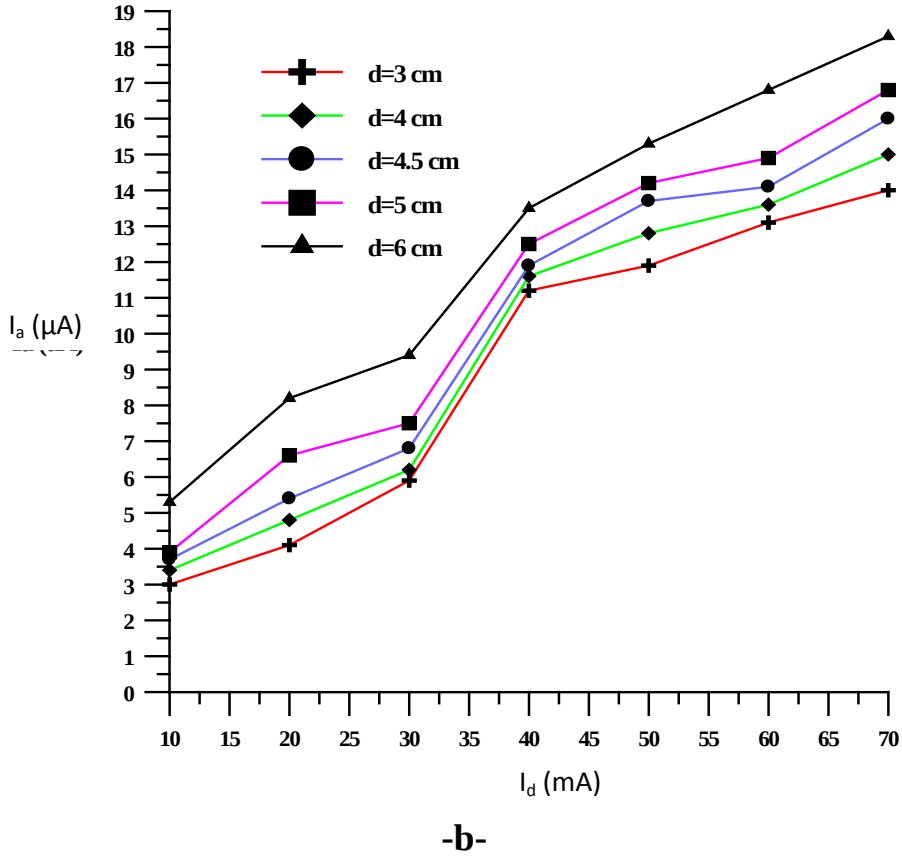

-b-

Figure (4-3) Anode current as a function of sputtering current at P=0.2 mbar for different electrodes separation for
a- gold target **b-** silver target.

4-4 Effects of electrodes separation on plasma parameters

The plasma parameters, (temperature of electron T_e, density of electron n_e and ion n_i) and other parameters was studied for different electrodes separation. A cylindrical single Langmuir probe was used to determine these parameters. The values of sputtering current has been selected according to the minimum grain size.

4-4-1 Temperature of electron T_e

The I-V characteristics for a cylindrical single Langmuir probe are measured at different electrodes separation(3.4.4.5,5 and 6) cm at fixed gas pressure (0.2 mbar) are shown in figures(4-4 to 4-8) for gold target and figures(4-9 to 4-13) for silver target.

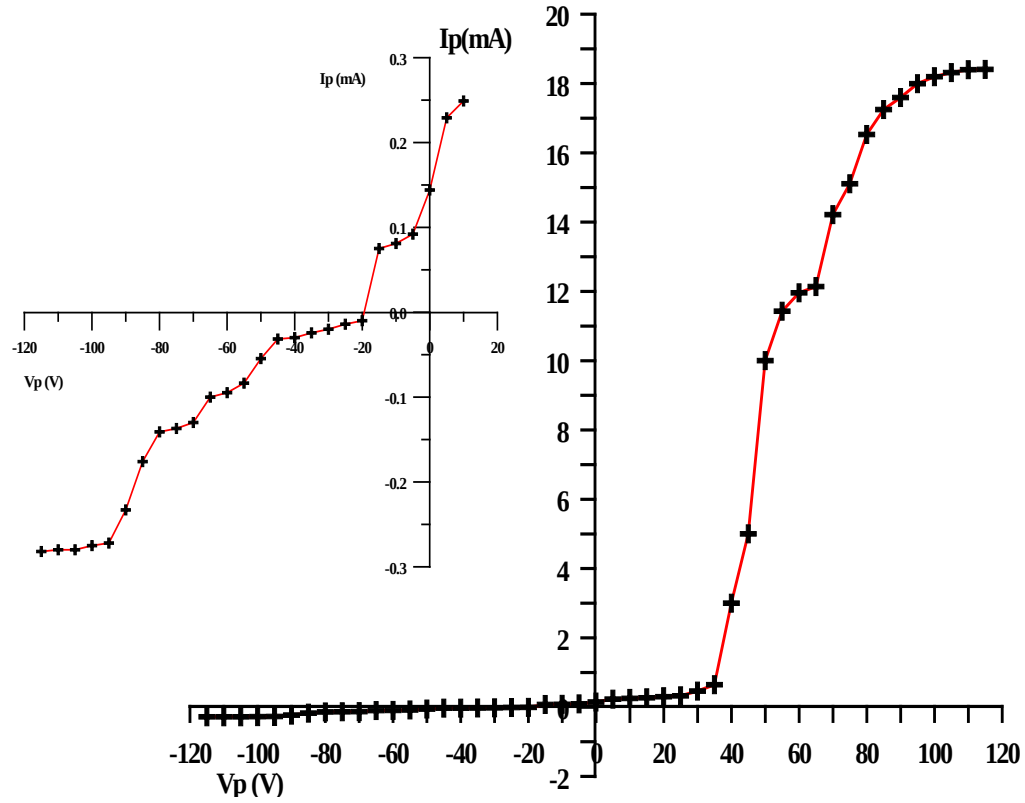

Figure (4-4) I-V characteristics curve of Langmuir probe for argon discharge at I_d=30 mA, P= 0.2 mbar and d=3cm using gold target.

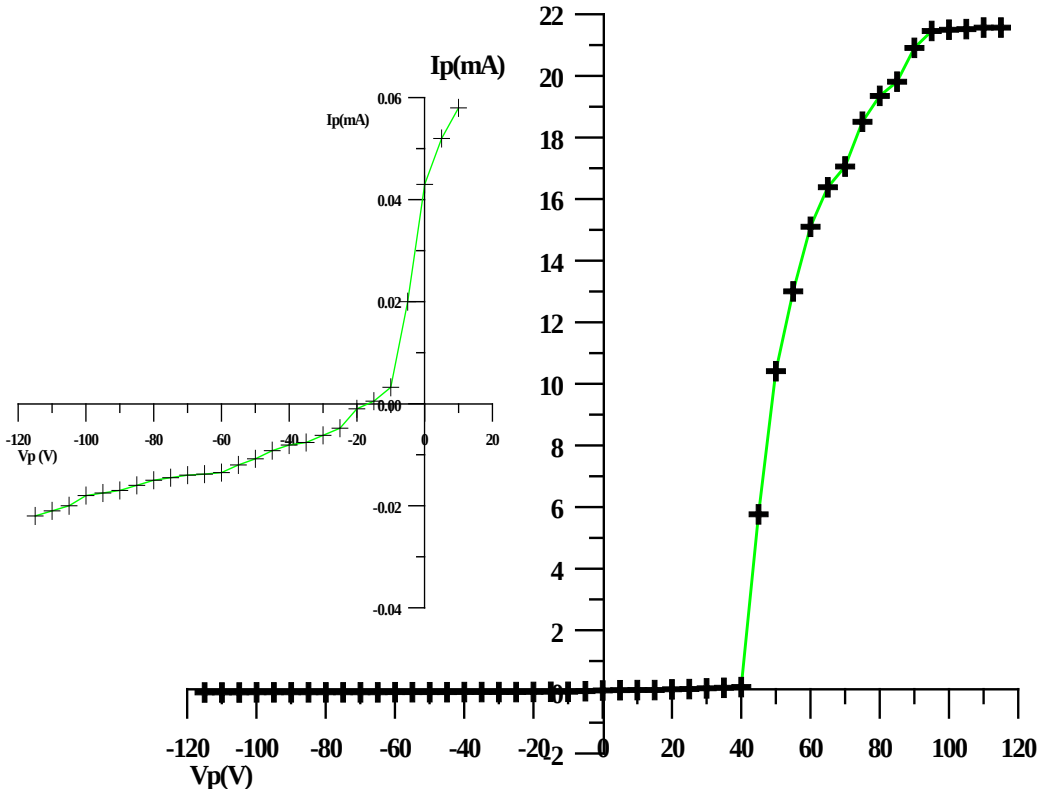

Figure (4-5) I-V characteristics curve of Langmuir probe for argon discharge at I_d=30 mA, P= 0.2 mbar and d=4cm using gold target.

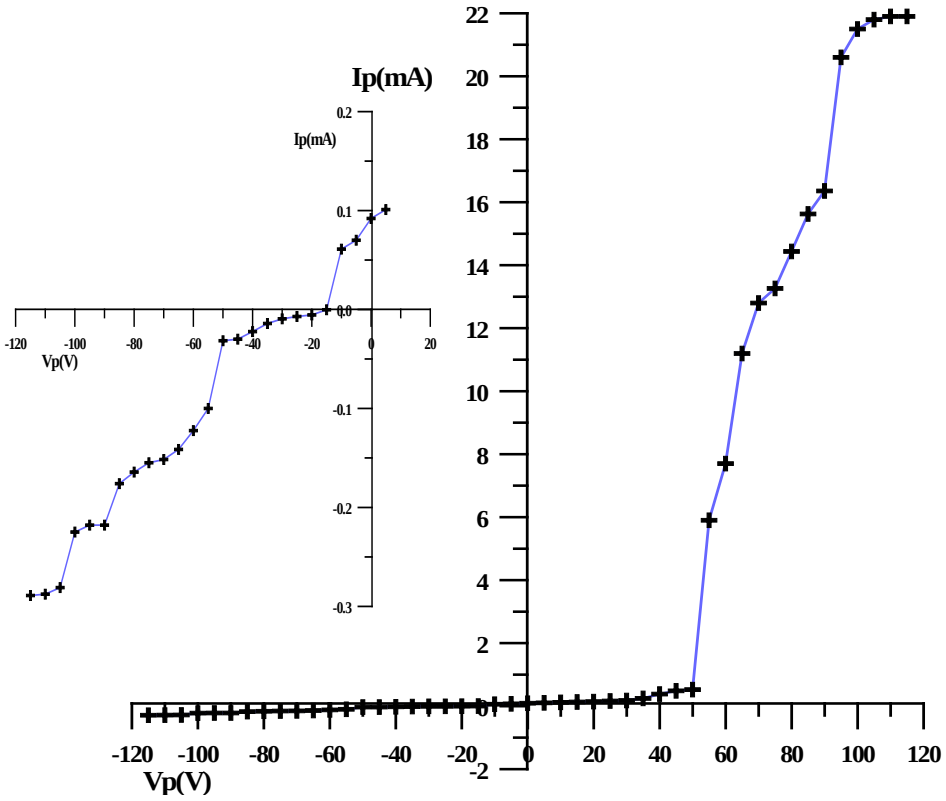

Figure(4-6) I-V characteristics curve of Langmuir probe for argon discharge at I_d=30 mA, P= 0.2 mbar and d=4.5cm using gold target.

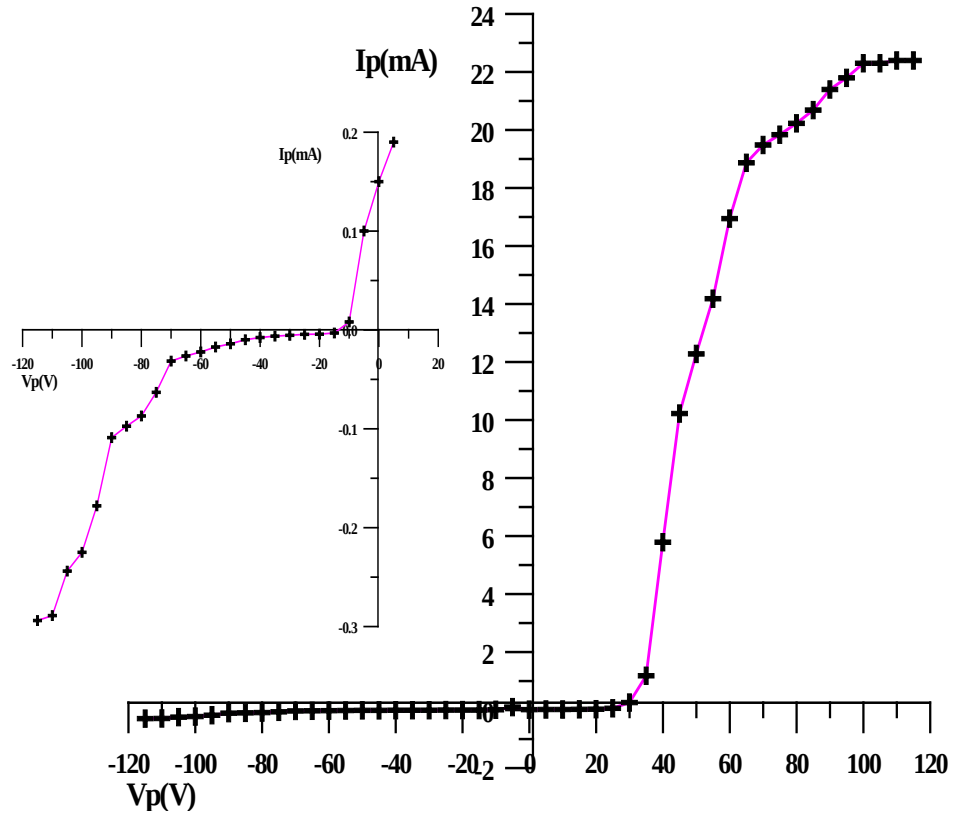

Figure (4-7) I-V characteristics curve of Langmuir probe for argondischarge at I_d=30 mA, P= 0.2 mbar and d=5cm using gold target .

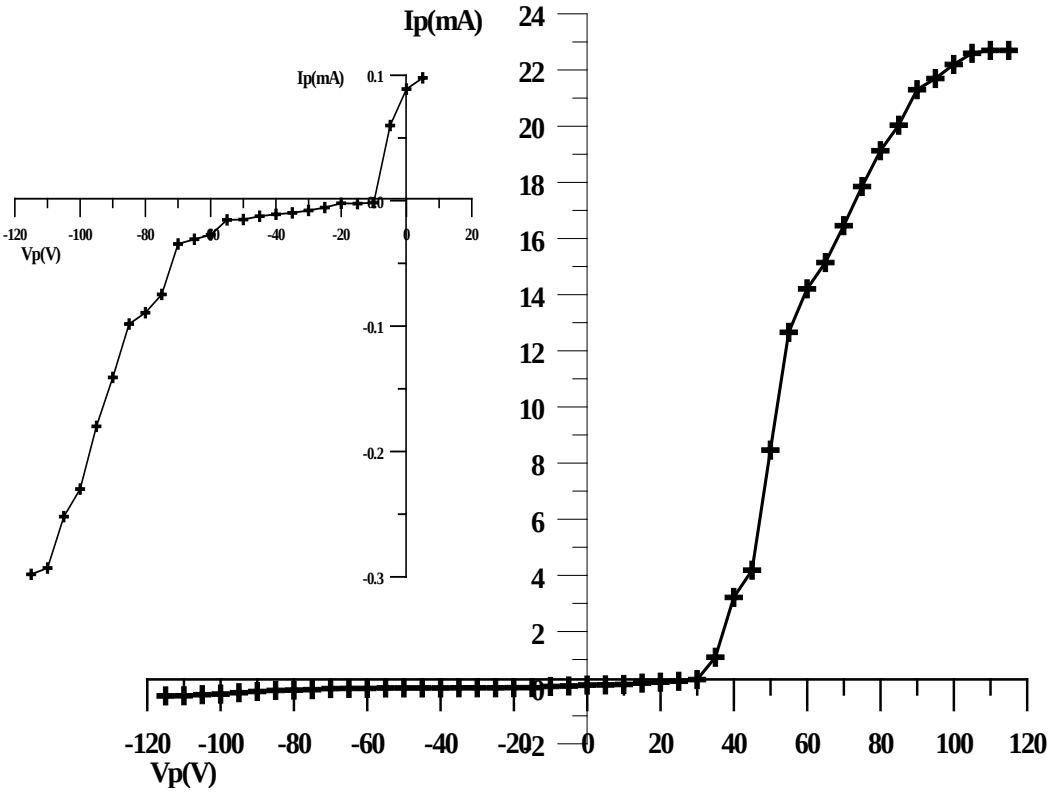

Figure(4-8) I-V characteristics curve of Langmuir probe for argon discharge at I_d =30 mA, P= 0.2 mbar and d=6cm using gold target.

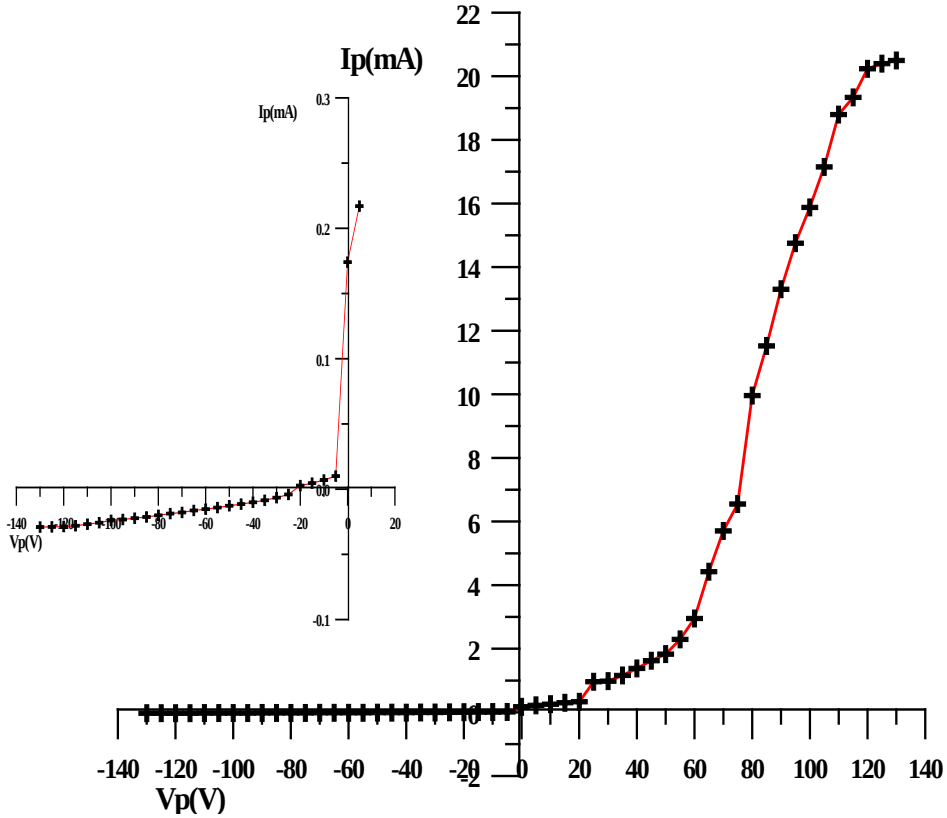

Figure(4-9) I-V characteristics curve of Langmuir probe for argon discharge at I_d=40 mA, P= 0.2 mbar and d=3cm using silver target.

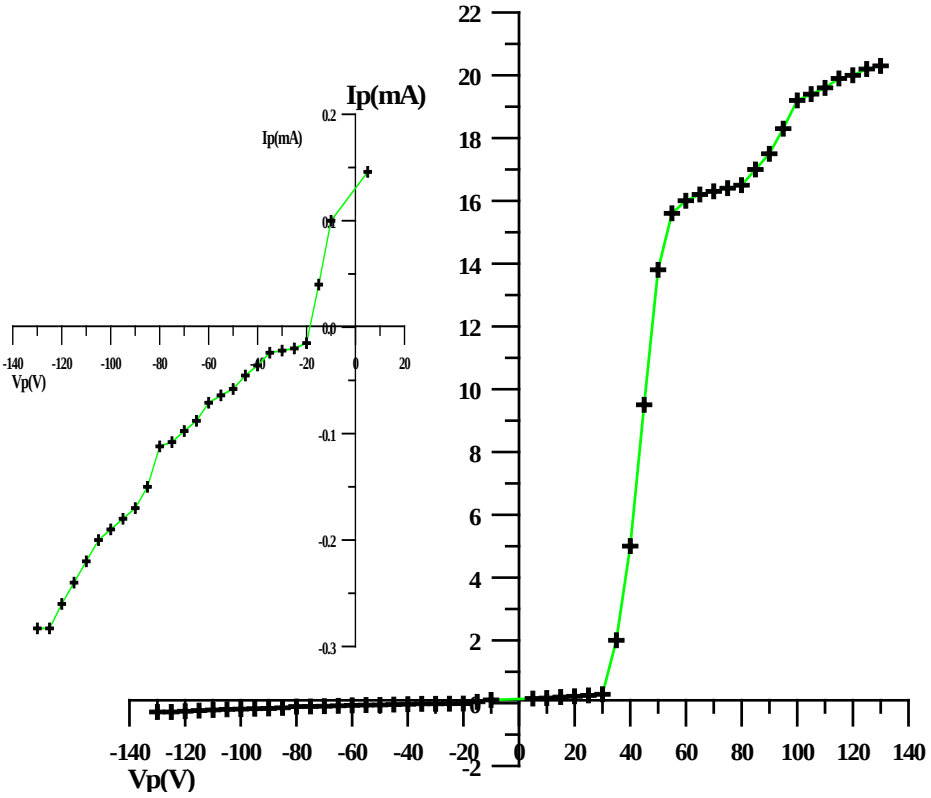

Figure(4-10) I-V characteristics curve of Langmuir probe for argon discharge at I_d =40 mA, P= 0.2 mbar and d=4cm using silver target.

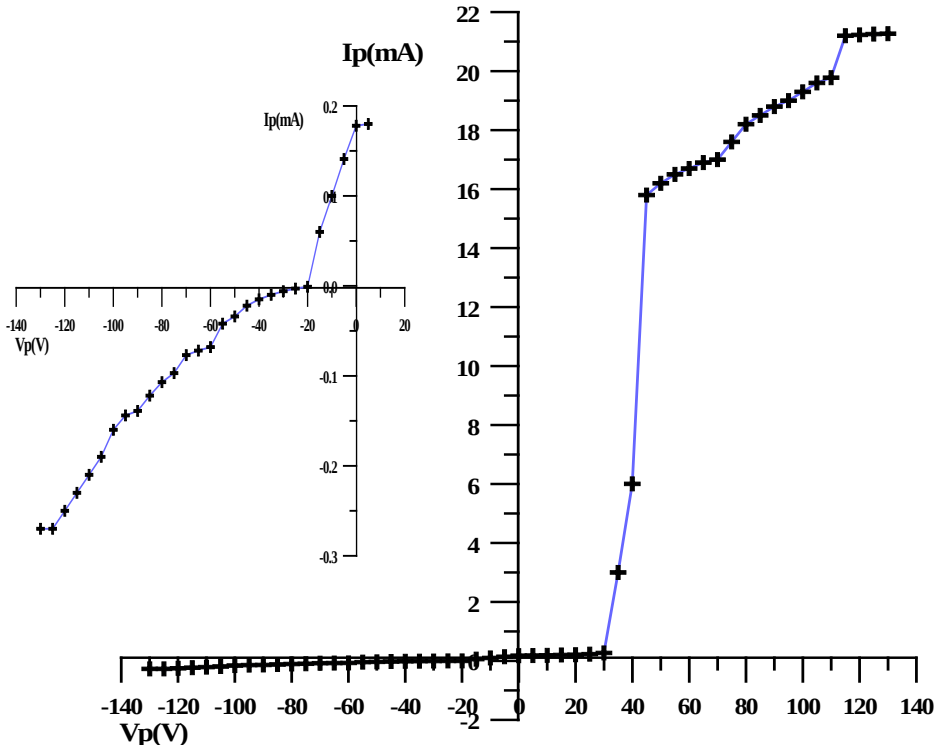

Figure (4-11) I-V characteristics curve of Langmuir probe for argon discharge at I_d=40 mA, P= 0.2 mbar and d=4.5cm using silver target.

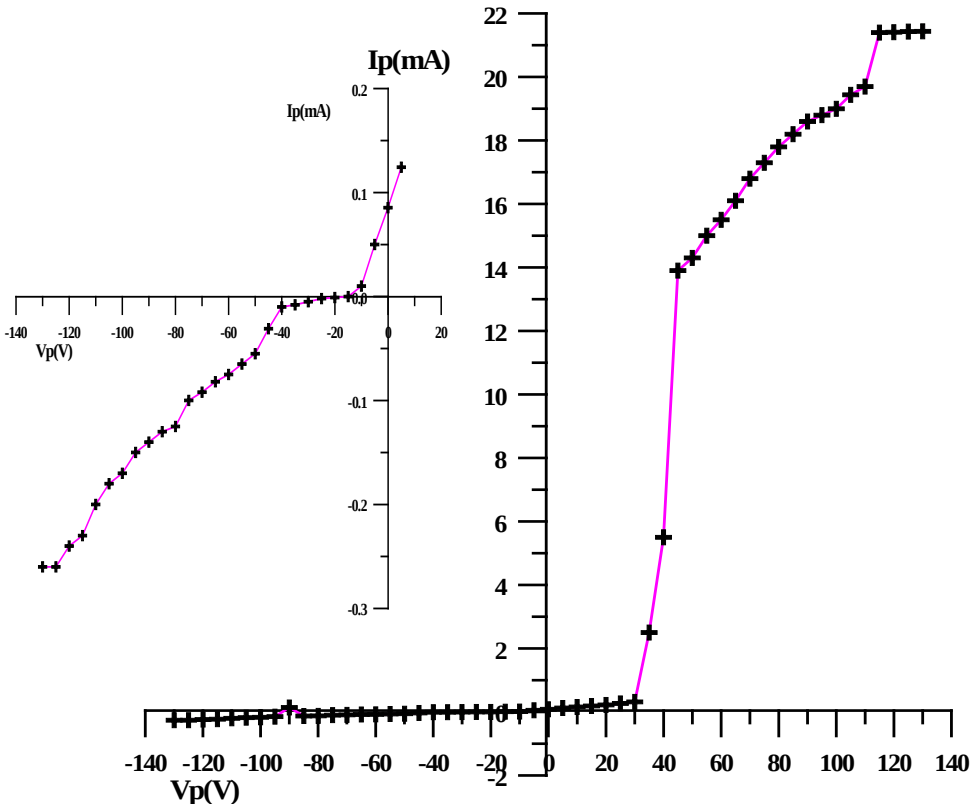

Figure(4-12) I-V characteristics curve of Langmuir probe for argon discharge at I_d=40 mA, P= 0.2 mbar and d=5cm using silver target.

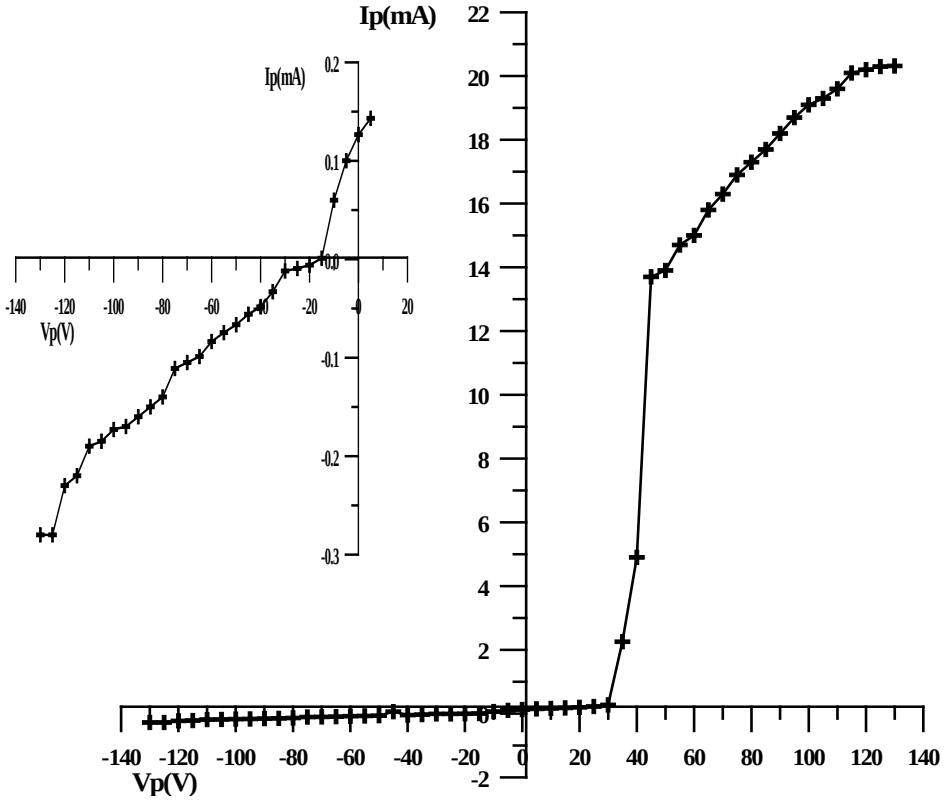

Figure(4-13) I-V characteristics curve of Langmuir probe for argon discharge at I_d=40 mA, P= 0.2 mbar and d=6cm using silver target.

The temperatures of electron for both targets are calculated using equation(2-18) from the inverse slope of logarithmic plot of the electron retarding region in figures(4-14 to 4-18) and figures(4-19 to 4-23) for gold and silver target respectively at different electrodes separation.

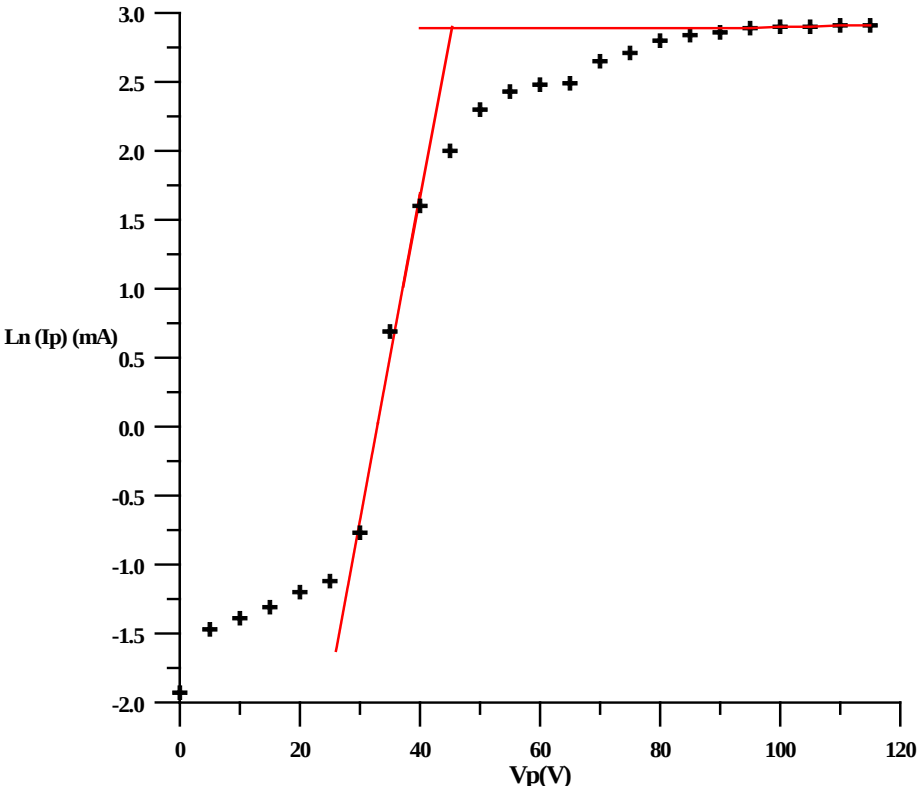

Figure (4-14) Variation of Ln(Ip) as a function of probe voltage at I_d= 30mA , P=0.2 mbar and d= 3cm using gold target.

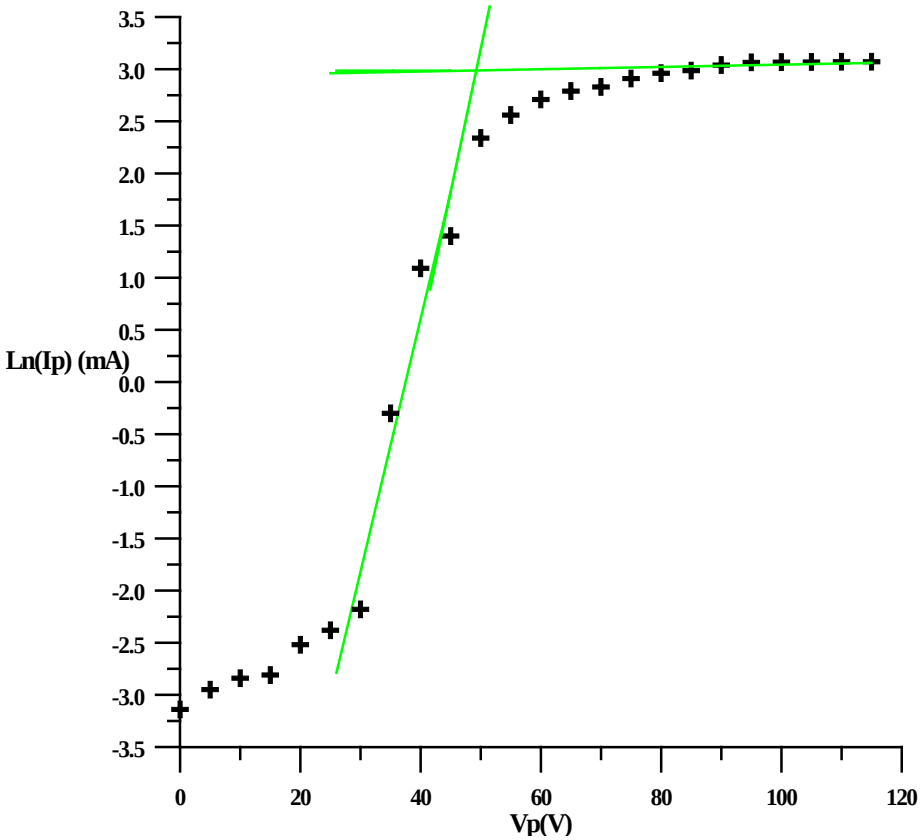

Figure(4-15) Variation of Ln(Ip) as a function of probe voltage at I_d= 30mA , P=0.2 mbar and d= 4cm using gold target.

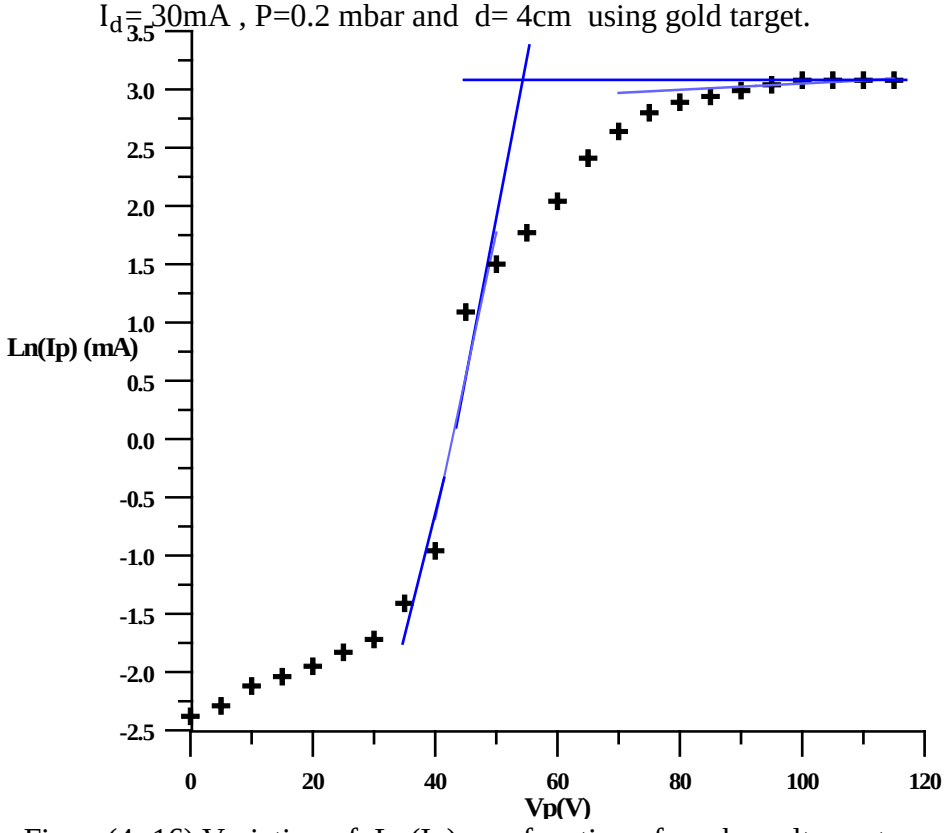

Figure(4=16) Variation of Ln(Ip) as a function of probe voltage at I_d= 30mA , P=0.2 mbar and d= 4.5cm using gold target.

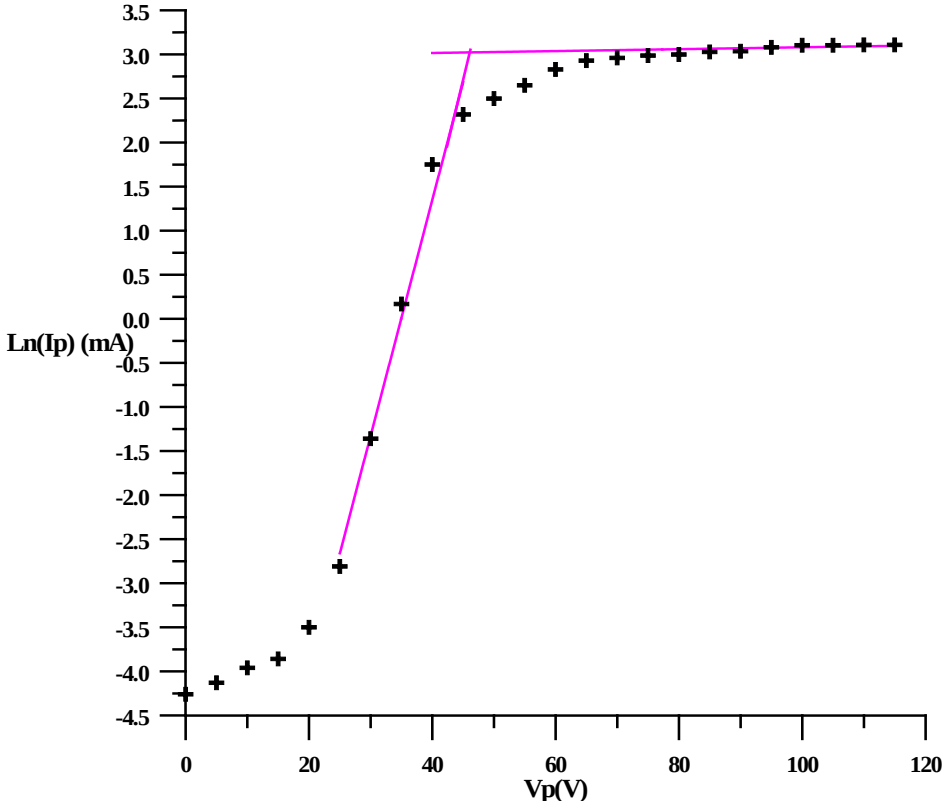

Figure(4-17) Variation of Ln(Ip) as a function of probe voltage at I_d= 30mA , P=0.2 mbar and d= 5cm using gold target.

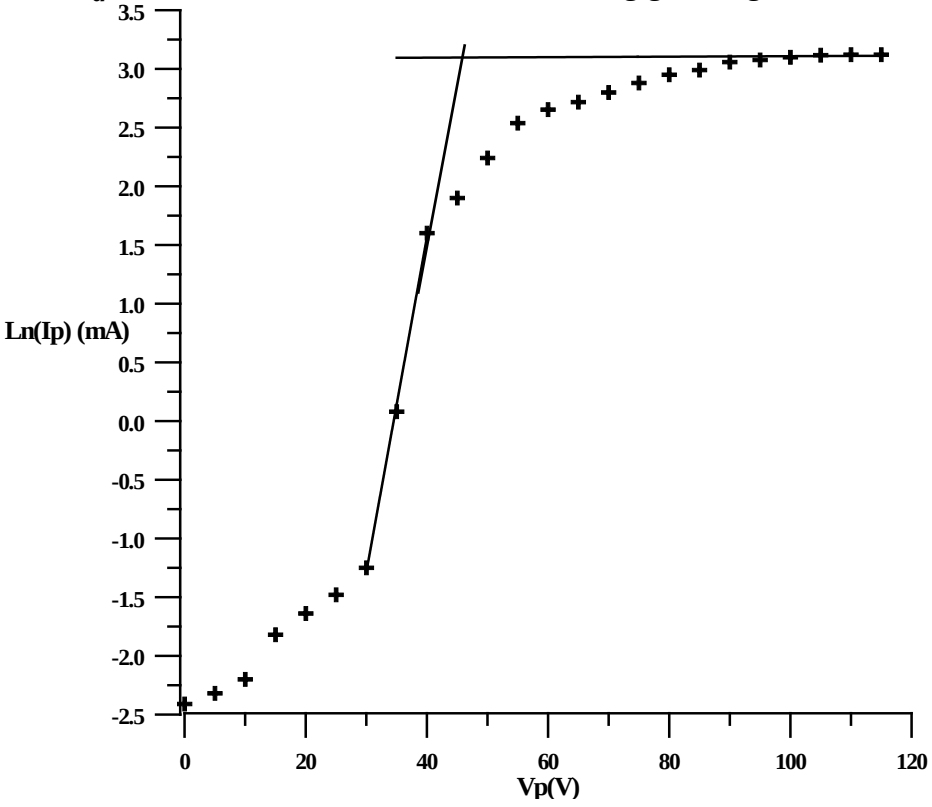

Figure(4-18) Variation of Ln(Ip) as a function of probe voltage at I_d= 30mA , P=0.2 mbar and d= 6cm using gold target.

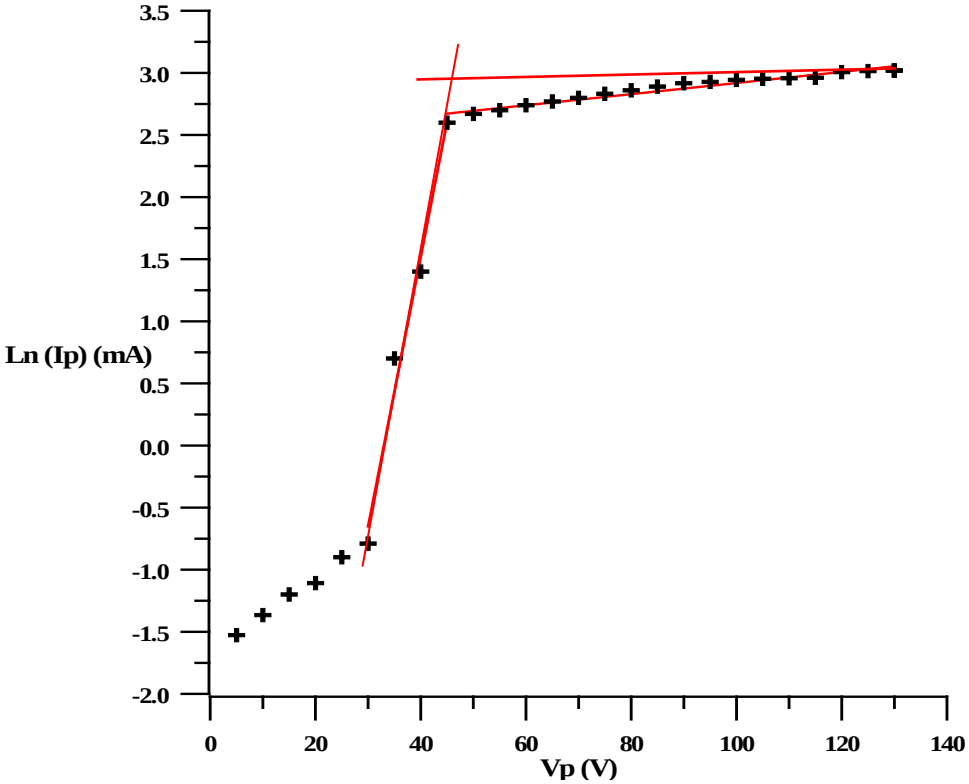

Figure(4-19)Variation of Ln(Ip) as a function of probe voltage at

I_d= 40mA , P=0.2 mbar and d= 3cm using silver target.

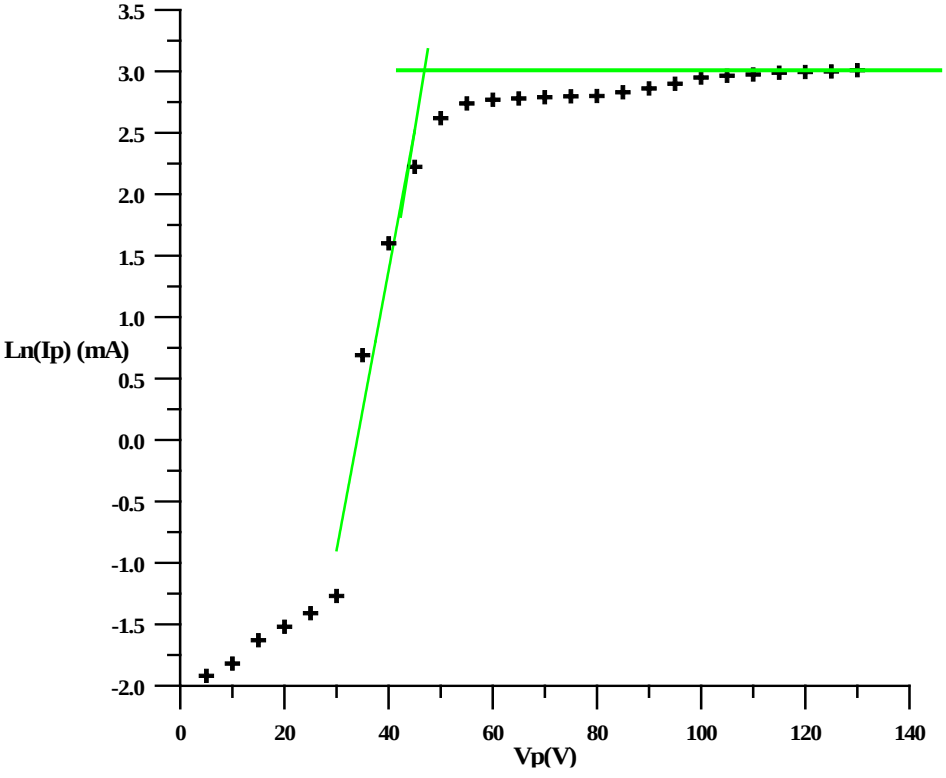

Figure(4-20) Variation of Ln(Ip) as a function of probe voltage at

I_d= 40mA , P=0.2 mbar and d= 4cm using silver target.

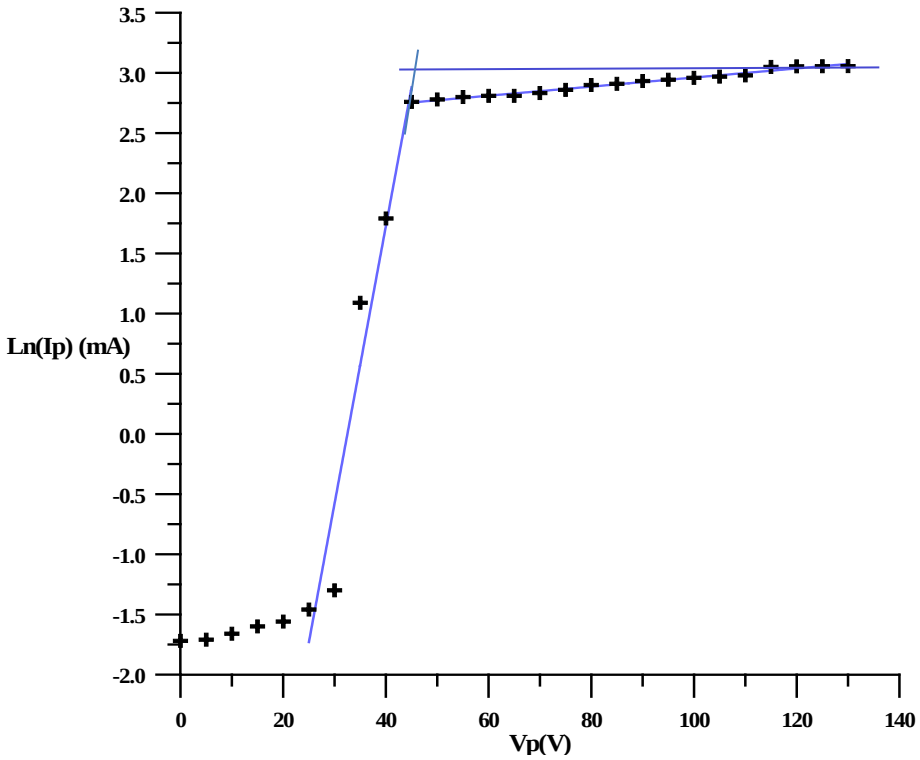

Figure(4-21) Variation of Ln(Ip) as a function of probe voltage at I_d= 40mA , P=0.2 mbar and d= 4.5cm using silver target.

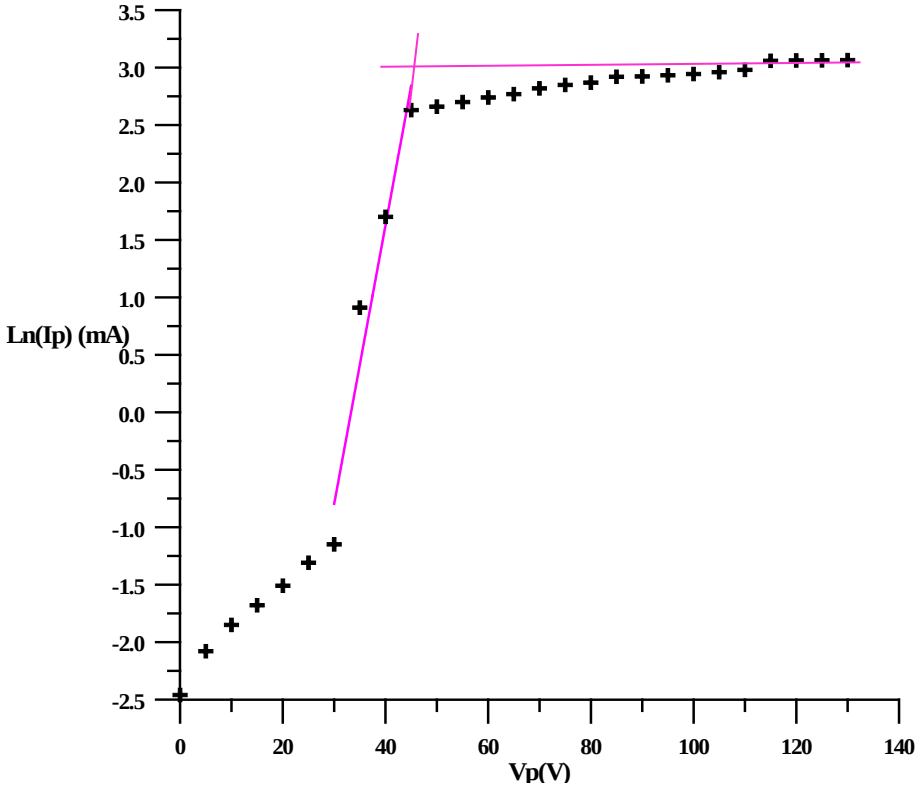

Figure(4-22) Variation of Ln(Ip) as a function of probe voltage at I_d= 40mA , P=0.2 mbar and d= 5cm using silver target.

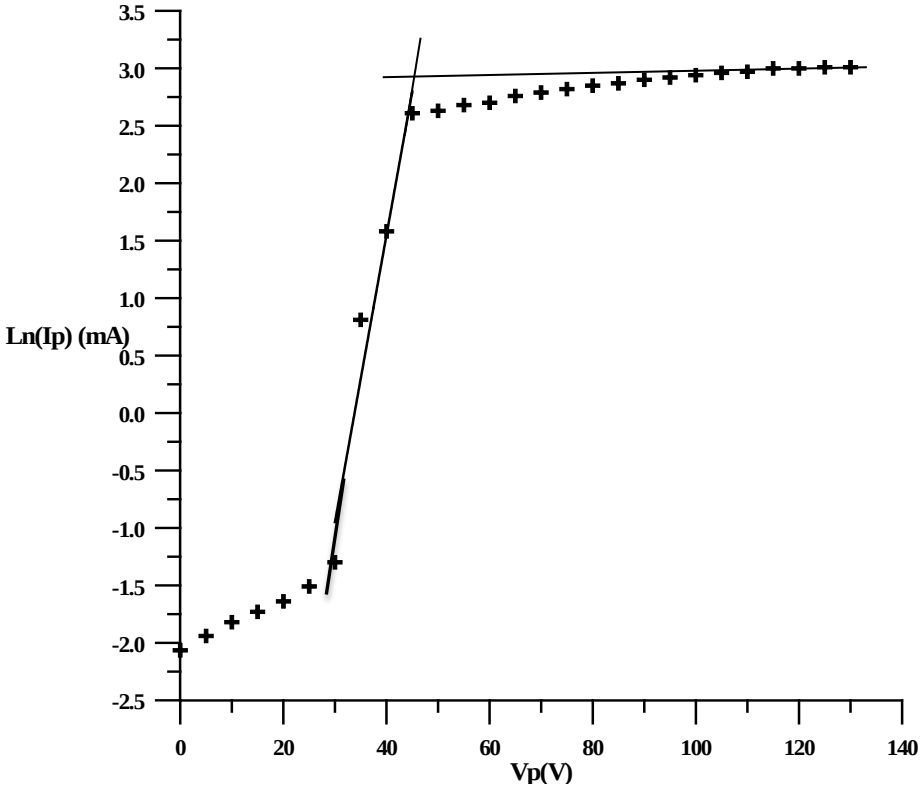

Figure(4-23) Variation of Ln(Ip) as a function of probe voltage at I_d= 40mA, P=0.2 mbar and d= 6cm using silver target.

Figures(4-24) shows the variations of temperature of electron as a function of electrodes separation for gold and silver target. It is notice that the temperature of electron is decreased with the separation of electrodes increasing. This is due to increase the collisions of electrons with atoms. The values of electron temperature for using silver target are greater than the temperature of electron for using gold target. This behavior agreement with results from E.F. Kotp and A.A.Al-Ojeery[56].

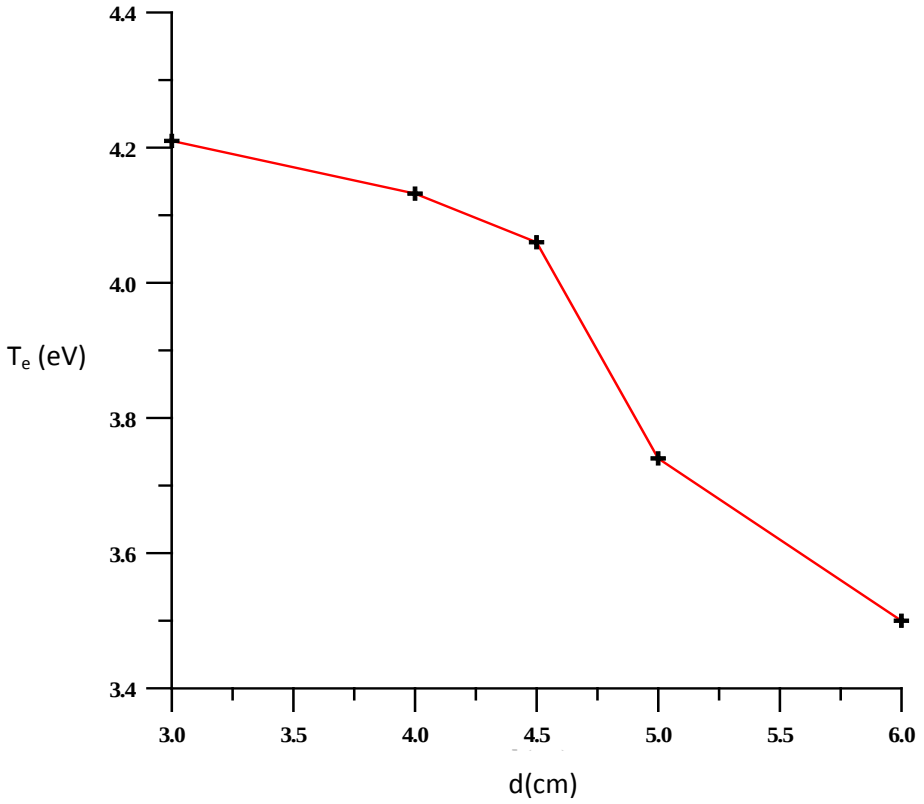

-a-

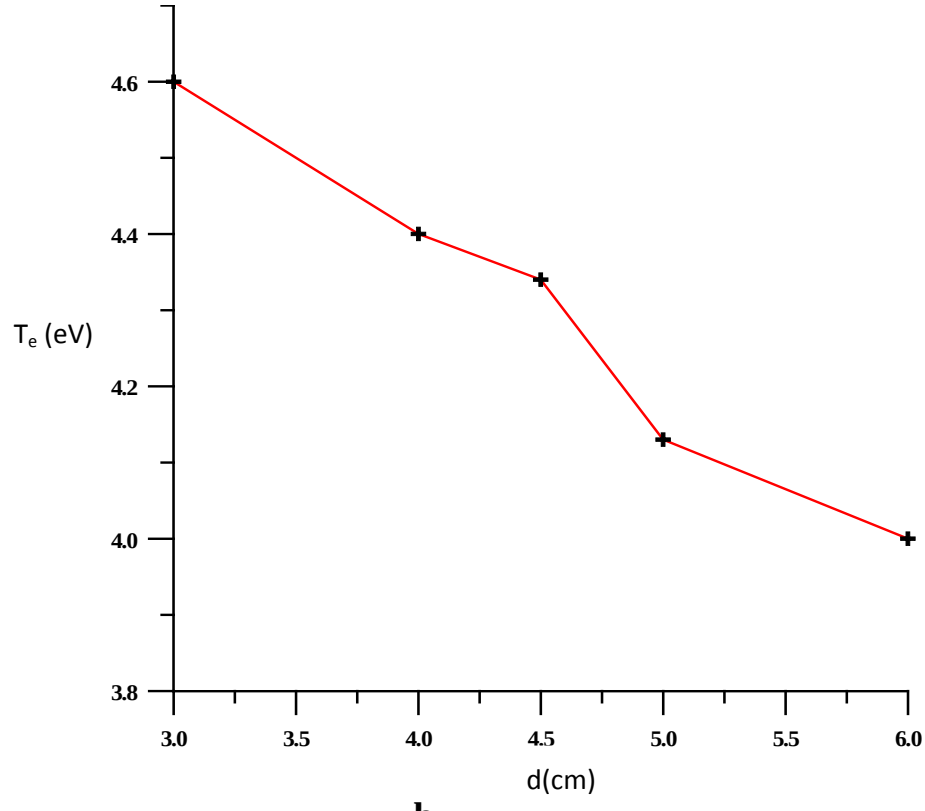

-b-

Figure(4-24)Variation of temperature of electron as a function of electrodes separation at **a**) I_d = 30 mA using gold target
b) I_d = 40 mA using silver target.

4-4-2 Electron density n_e

The electron density n_e are calculated using equation(2-20) for different electrodes separation. The saturation electron currents are determined using figures(4-14 to 4-18) for gold target and figures(4-19 to 4-23) for silver target.

The results of n_e at different electrodes separation are shown in figures(4-25) for using gold and silver targets.

The electron density is increased as electrodes separation increasing, this is due to increase secondary electrons.

The values of electron densities for using gold target are roughly greater than the values of electron densities for using silver target.

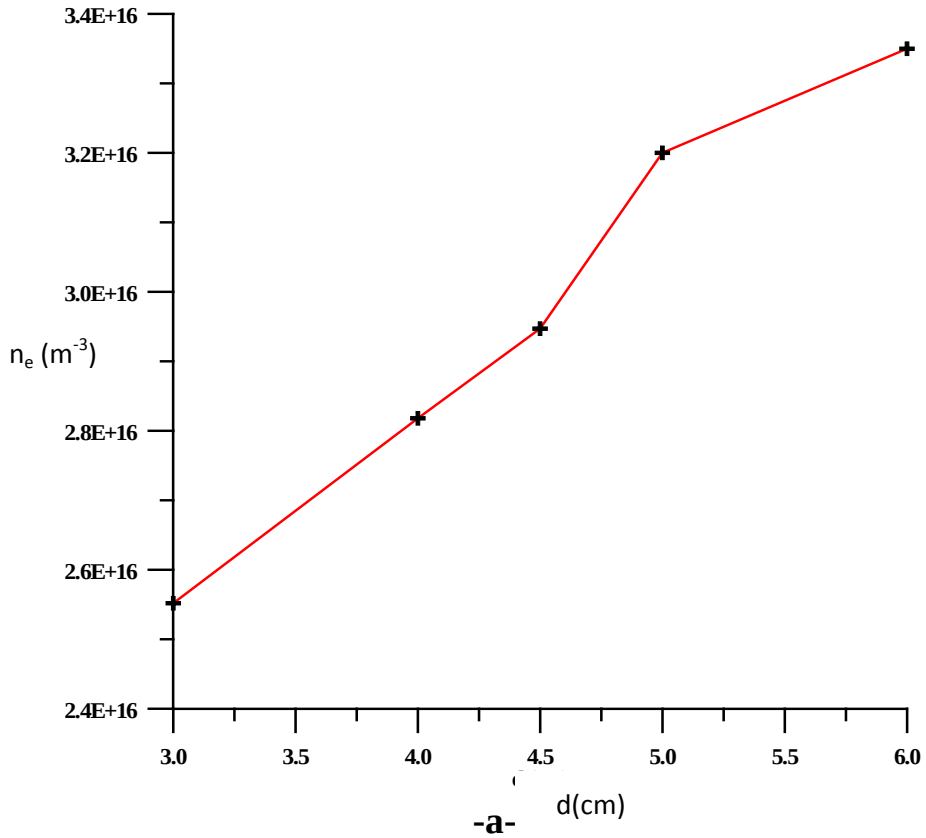

-a-

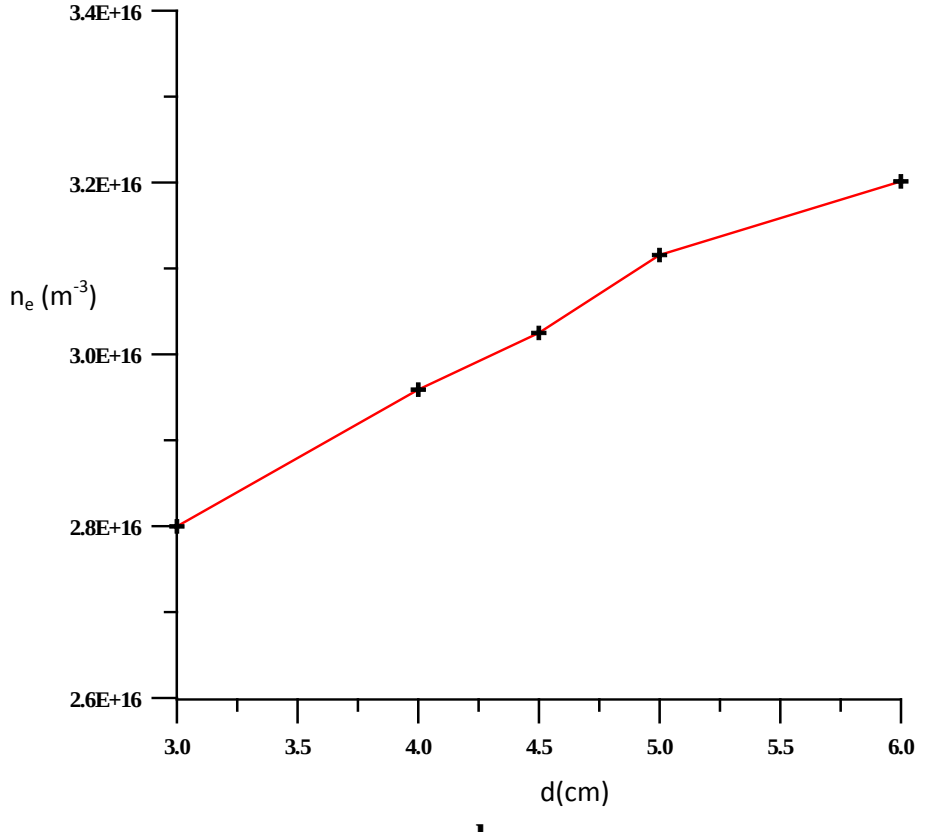

-b-

Figure(4-25) Variation of electron density as a function of electrodes separation at

a) I_d= 30 mA using gold target

b) I_d= 40 mA using silver target.

4-4-3 Ion density n_i

By using the ion saturation region in figures(4-4 to 4-8) for using gold target and figures(4-9 to 4-13) for silver target and the equation (2-16), the ion densities are estimated for different electrodes separation. The ion density can be calculated corresponding to orbital motion limit theory (OML).

Plotting a line fit for the square ion current as a function of probe voltage, the slope from this figure is used to calculate the ion density for different electrodes separation. The ion density is plotted as a function of different electrodes separation for both targets as shown in figure(4-26).

It is notice from this figure that the density of ion is increased as increasing the electrodes separation. Furthermore, it is observed that the ion density is slightly greater than the electron density for both targets. This is due to the effects of external magnetic field which increasing the probability of collisions. This behavior agreement with results from E.F.Kotop and A.A.Al-Ojeery [56].

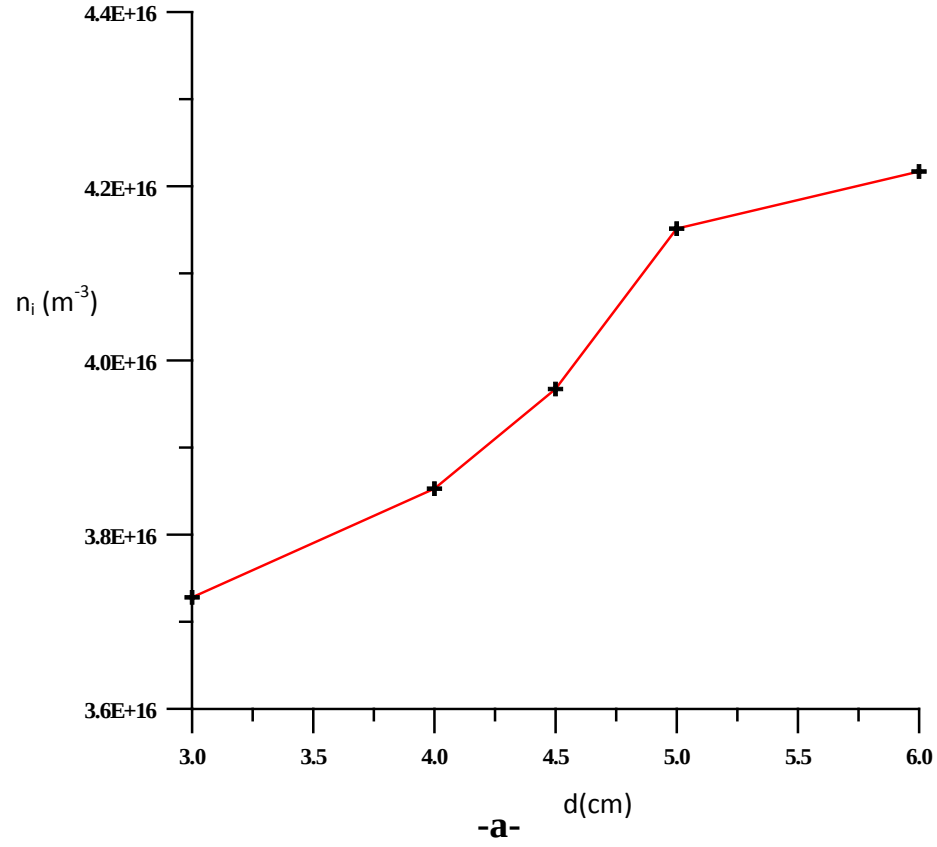

-a-

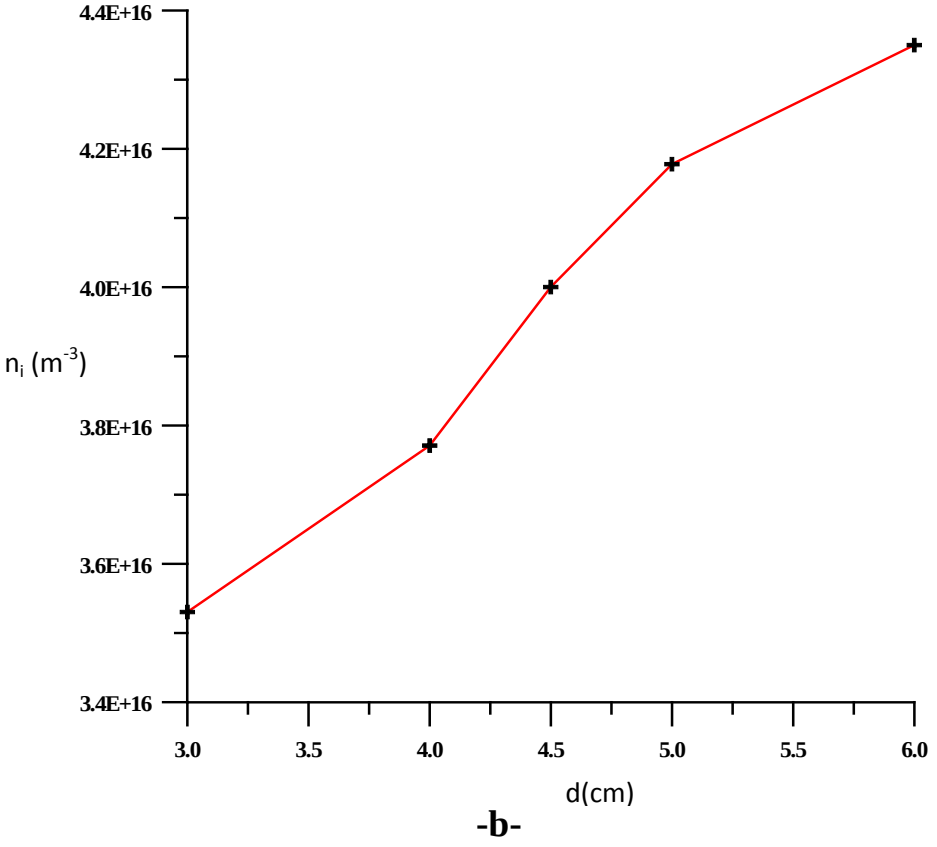

-b-

Figure(4-26) Variation of electron density as a function of electrodes separation for
a) I_d= 30 mA using gold target
b) I_d= 40 mA using silver target.

4-4-4 Other parameters of plasma

Table (4-1) shows the values of other plasma parameters, such as floating potential, plasma potential and Deby length at different electrodes separation for gold target at constant discharge (sputtering current I_d=30 mA).

Table (4-1) Other plasma parameters using gold at I_d=30 mA.

d(cm)	V_f (volt)	V_{pp}(volt)	λ_D(cm)
3	-19.5	43	0.00955
4	-17	47	0.00900
4.5	-15	49	0.00892
5	-13	50	0.00857
6	-12	51	0.00760

Table (4-2) shows the values of other plasma parameters, floating potential, plasma potential and Deby length at different electrodes separation for silver target at constant discharge (sputtering current I_d=40 mA).

Table (4-2) Others plasma parameters using silver at I_d=40 mA.

d(cm)	V_f (volt)	V_{pp}(volt)	λ_D(cm)
3	-22	46	0.00953
4	-18.7	47	0.00907
4.5	-17	48	0.00891
5	-16	49	0.00856
6	-15.8	50	0.00820

4-5 Effects of electrodes separation on morphology of coated samples

The dependence of morphology properties for gold and silver deposition was studied for different electrodes separation (3,4,4.5,5 and 6) cm between cathode and sample using Atomic Force Microscope (AFM). A series of Au and Ag sputtering particles on glass substrate were prepared at a constant gas pressure (0.2 mbar) and deposition time of (30 seconds) with different values of discharge sputtering currents (20,30,40,50 and 60) mA.

Figure(4-27) represent the effect of electrodes separation on gold surface morphologies at a constant discharge sputtering current (I_d=30 mA). Furthermore, the effects of the electrodes separation on silver surface morphology at a constant discharge sputtering current (I_d=40 mA) are shown in figure (4-28). The results from these figures are obtaining as below :

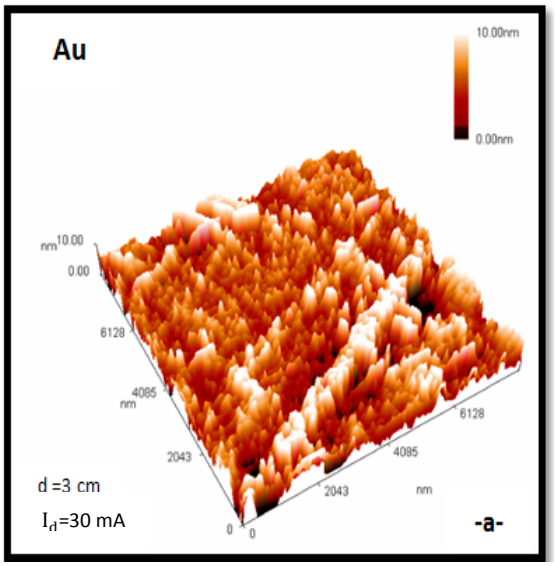
Au
10.00nm
0.00nm
nm10.00
0.00
6128
4085
nm
2043
0
0
2043
4085
6128
nm
d =3 cm
I_d=30 mA
-a-

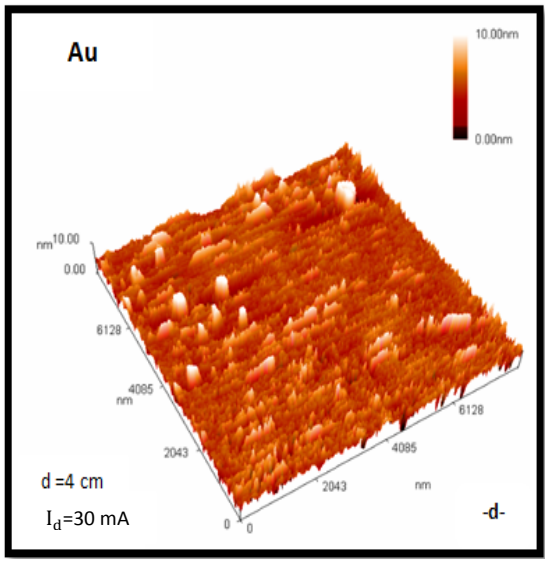
Au
10.00nm
0.00nm
nm10.00
0.00
6128
4085
nm
2043
0
0
2043
4085
6128
nm
d =4 cm
I_d=30 mA
-d-

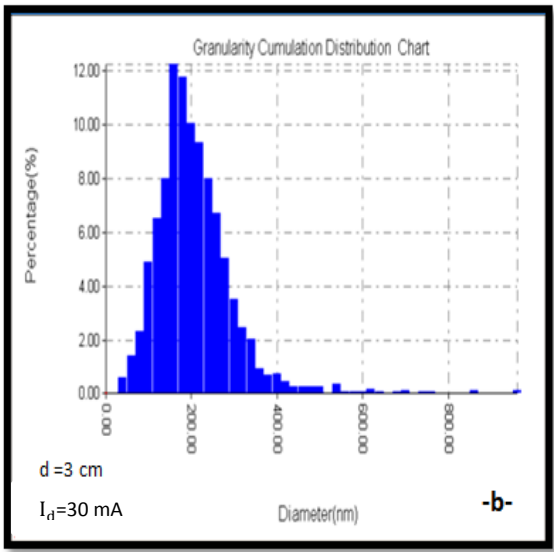
Granularity Cumulation Distribution Chart
Percentage(%)
12.00
10.00
8.00
6.00
4.00
2.00
0.00
0.00
200.00
400.00
600.00
800.00
Diameter(nm)
d =3 cm
I_d=30 mA
-b-

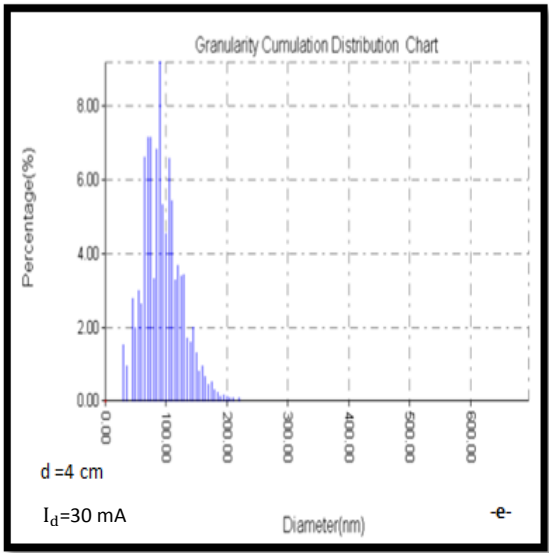
Granularity Cumulation Distribution Chart
Percentage(%)
8.00
6.00
4.00
2.00
0.00
0.00
100.00
200.00
300.00
400.00
500.00
600.00
Diameter(nm)
d =4 cm
I_d=30 mA
-e-

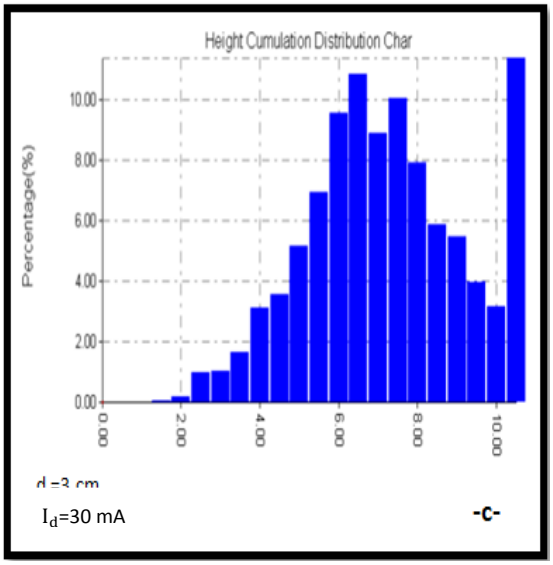
Height Cumulation Distribution Char
Percentage(%)
10.00
8.00
6.00
4.00
2.00
0.00
0.00
2.00
4.00
6.00
8.00
10.00
d =3 cm
I_d=30 mA
-c-

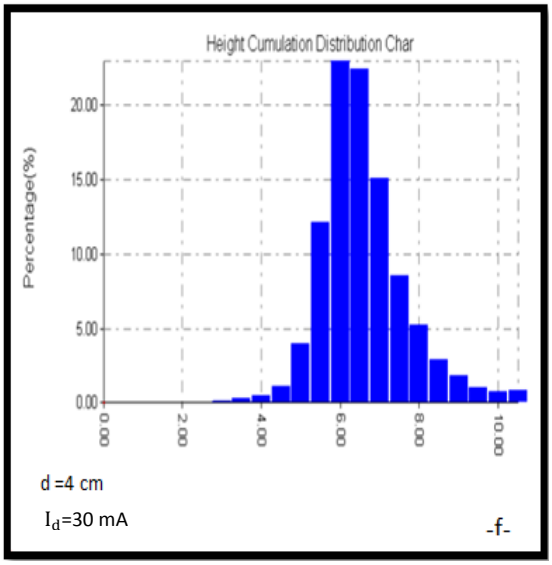
Height Cumulation Distribution Char
Percentage(%)
20.00
15.00
10.00
5.00
0.00
0.00
2.00
4.00
6.00
8.00
10.00
d =4 cm
I_d=30 mA
-f-

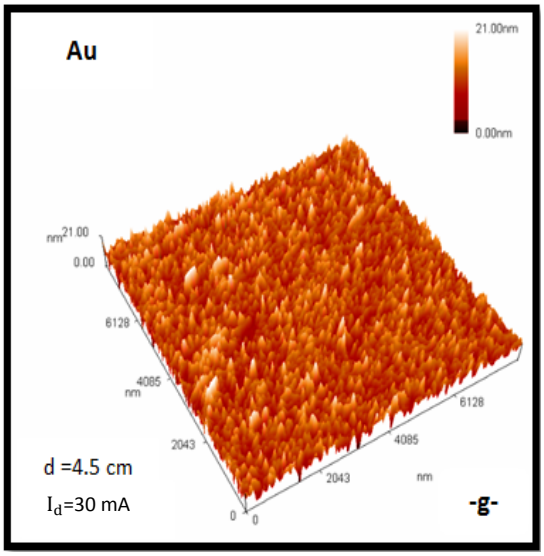
Au
21.00nm
0.00nm
d =4.5 cm
I_d=30 mA
-g-

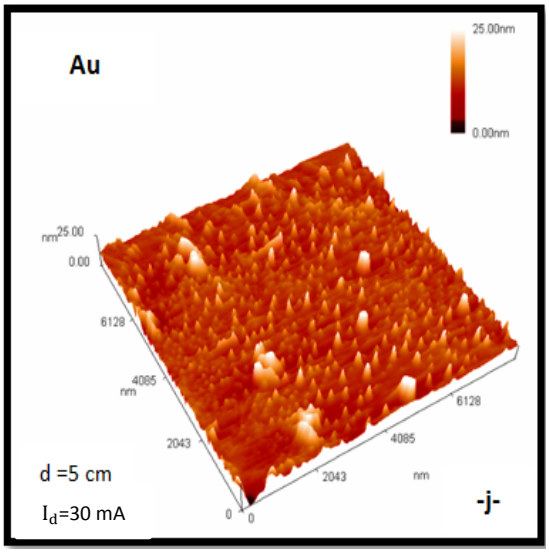
Au
25.00nm
0.00nm
d =5 cm
I_d=30 mA
-j-

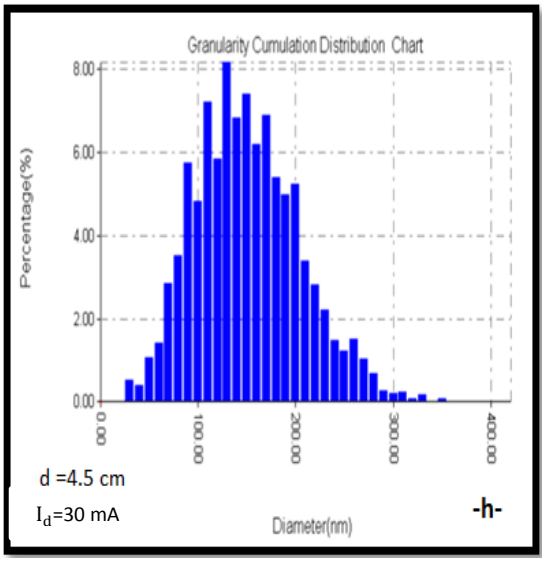
Granularity Cumulation Distribution Chart
Percentage(%)
Diameter(nm)
d =4.5 cm
I_d=30 mA
-h-

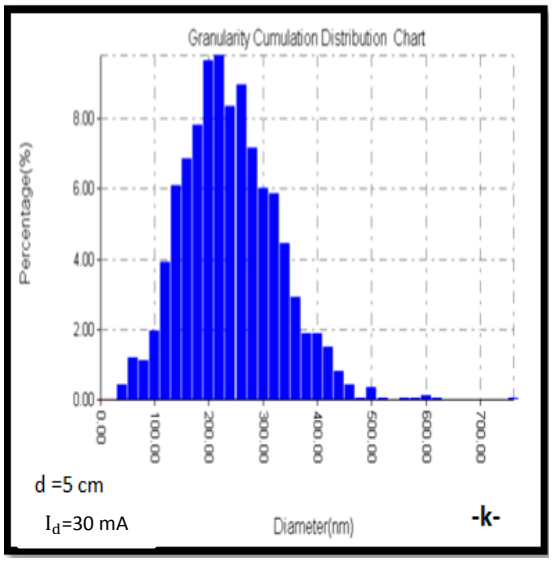
Granularity Cumulation Distribution Chart
Percentage(%)
Diameter(nm)
d =5 cm
I_d=30 mA
-k-

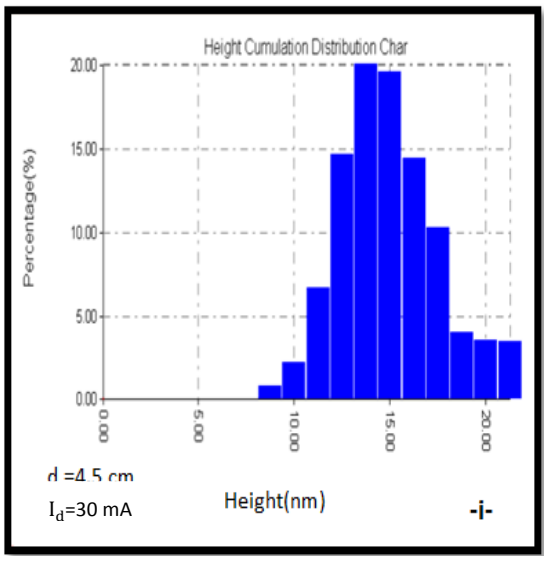
Height Cumulation Distribution Char
Percentage(%)
Height(nm)
I_d=30 mA
-i-

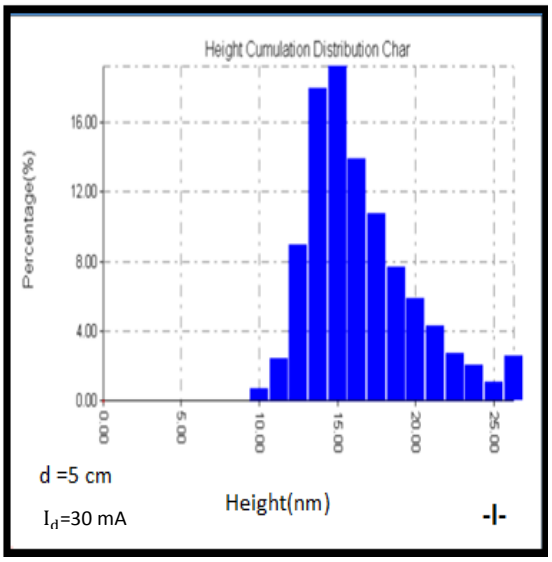
Height Cumulation Distribution Char
Percentage(%)
Height(nm)
d =5 cm
I_d=30 mA
-l-

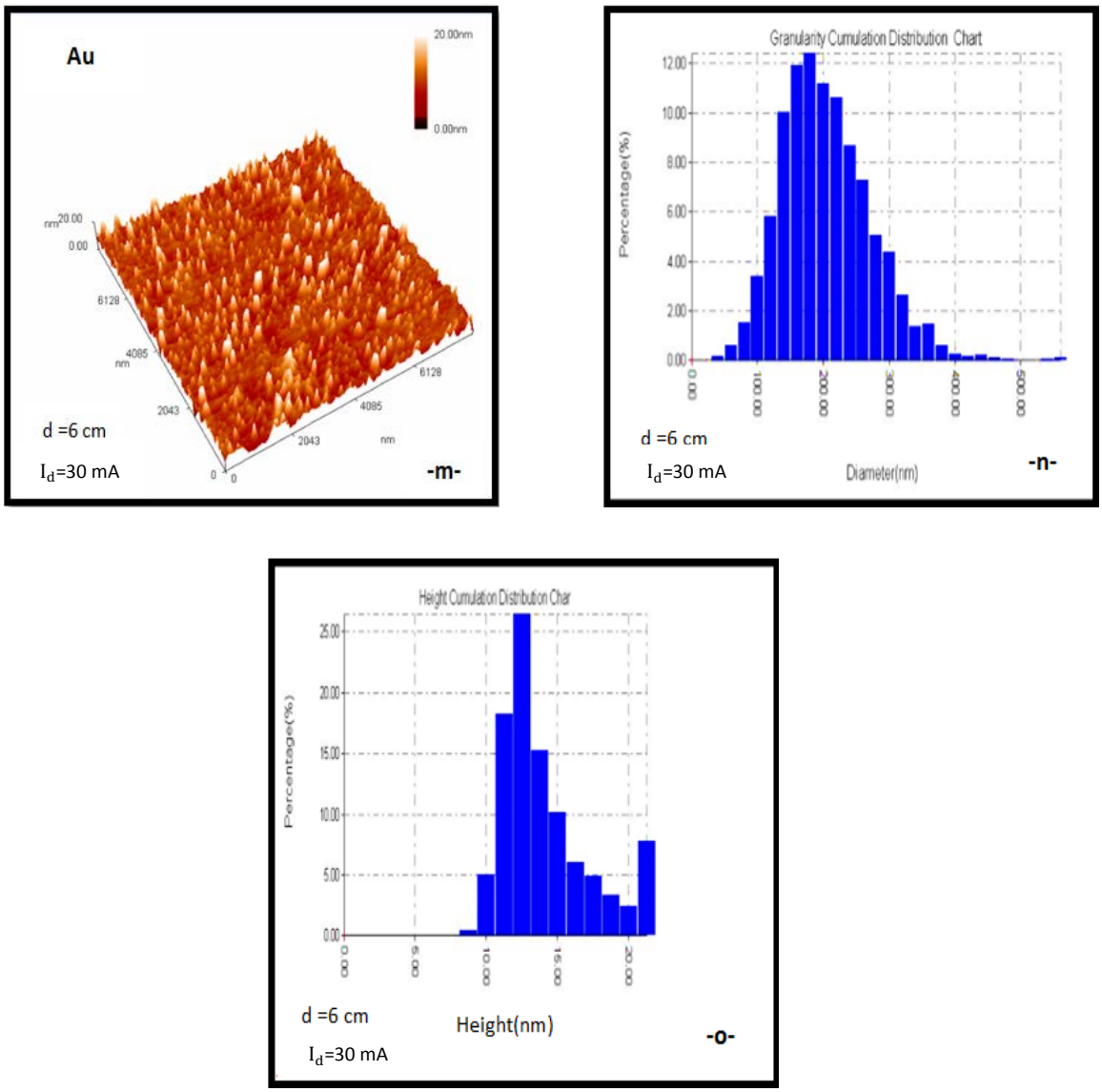

Figure (4 -27) Shows the results from AFM using Au target for different electrodes separation at I_d =30 mA. (a-d-g-j-m) 3D images, (b-e-h-k-n) Percentage of diameter size distribution and (c-f-i-l-o) Percentage of height distribution.

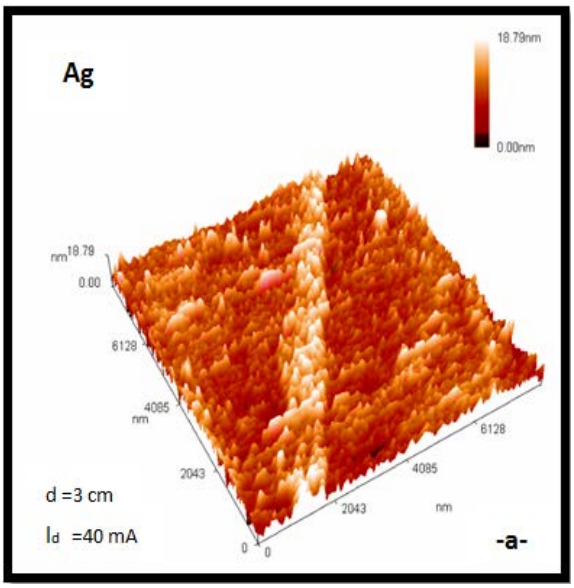
Ag
18.79nm
0.00nm
d =3 cm
Id =40 mA
-a-

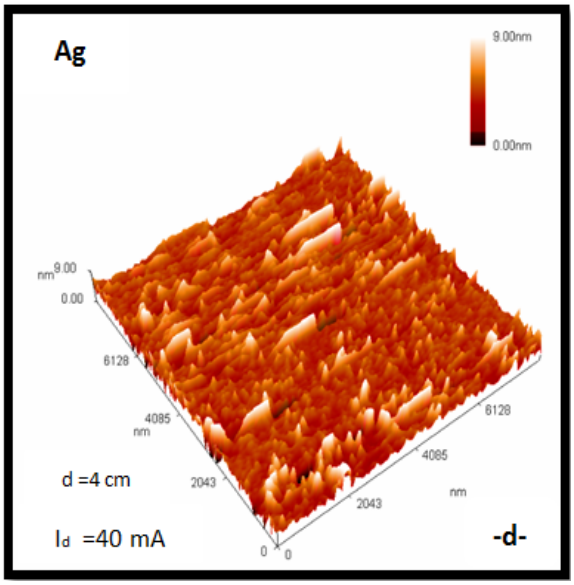
Ag
9.00nm
0.00nm
d =4 cm
Id =40 mA
-d-

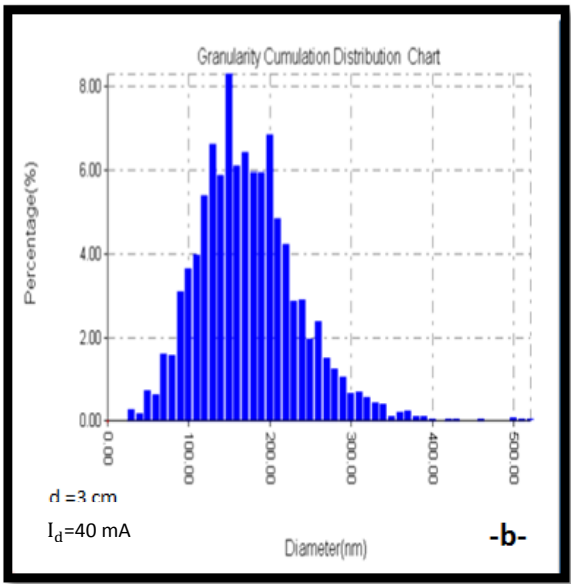
Granularity Cumulation Distribution Chart
Percentage(%)
Diameter(nm)
Id=40 mA
-b-

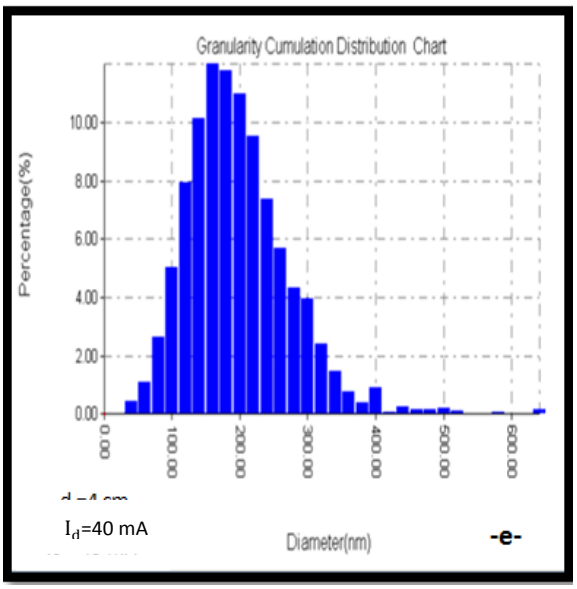
Granularity Cumulation Distribution Chart
Percentage(%)
Diameter(nm)
Id=40 mA
-e-

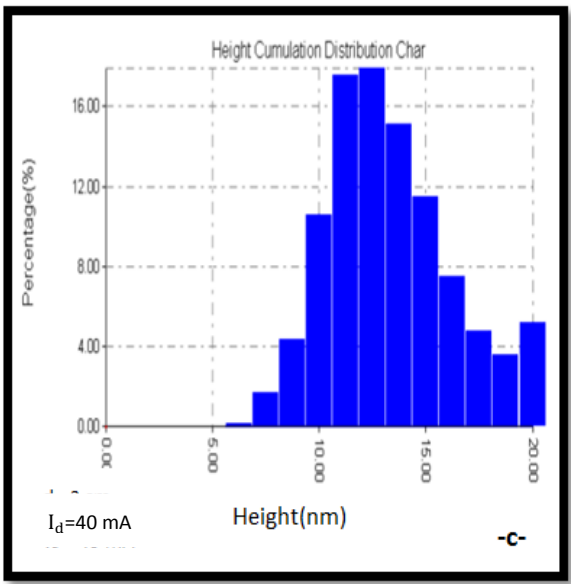
Height Cumulation Distribution Char
Percentage(%)
Height(nm)
Id=40 mA
-c-

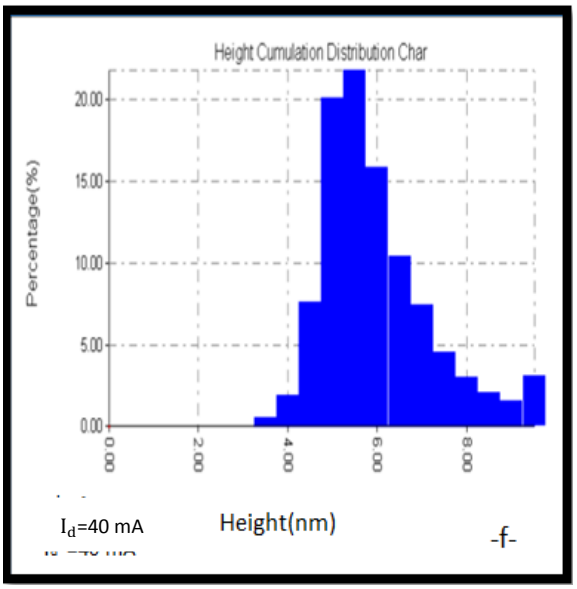
Height Cumulation Distribution Char
Percentage(%)
Height(nm)
Id=40 mA
-f-

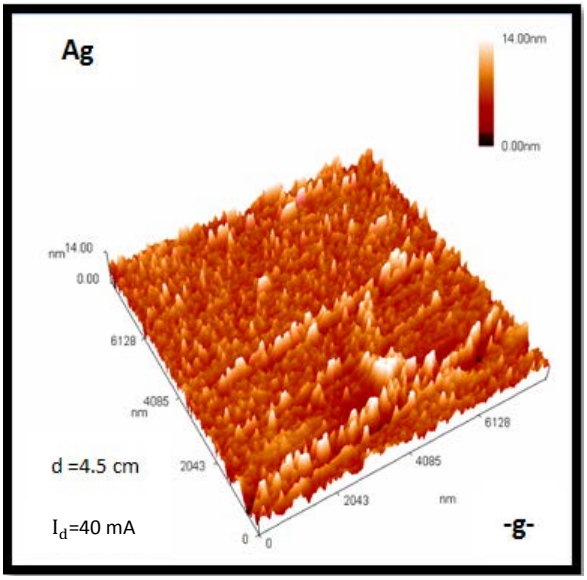
Ag
14.00nm
0.00nm
d =4.5 cm
I_d=40 mA
-g-

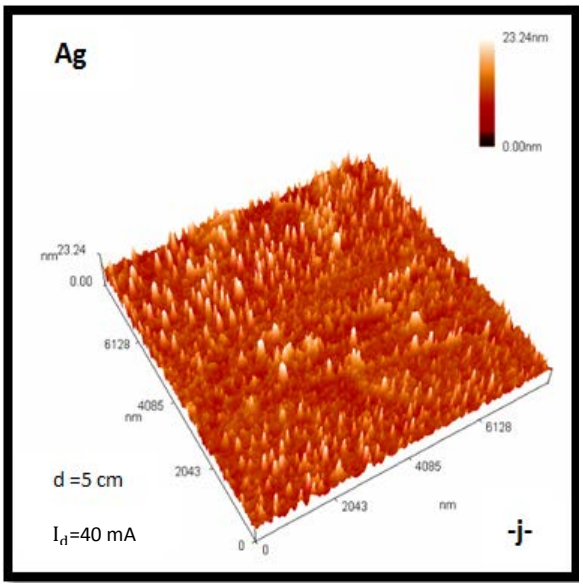
Ag
23.24nm
0.00nm
d =5 cm
I_d=40 mA
-j-

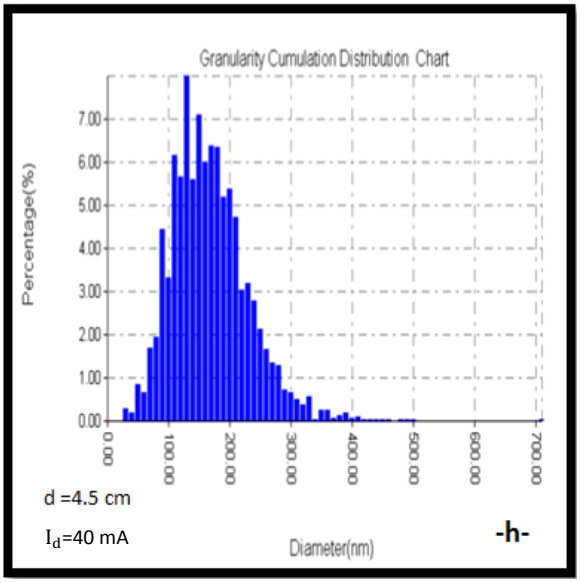
Granularity Cumulation Distribution Chart
Percentage(%)
Diameter(nm)
d =4.5 cm
I_d=40 mA
-h-

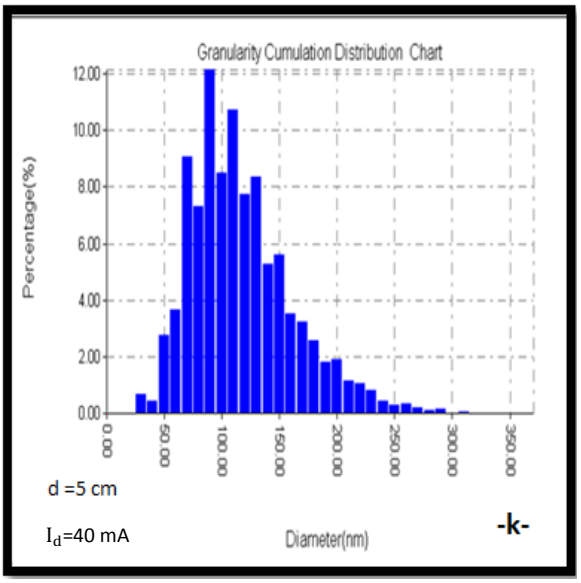
Granularity Cumulation Distribution Chart
Percentage(%)
Diameter(nm)
d =5 cm
I_d=40 mA
-k-

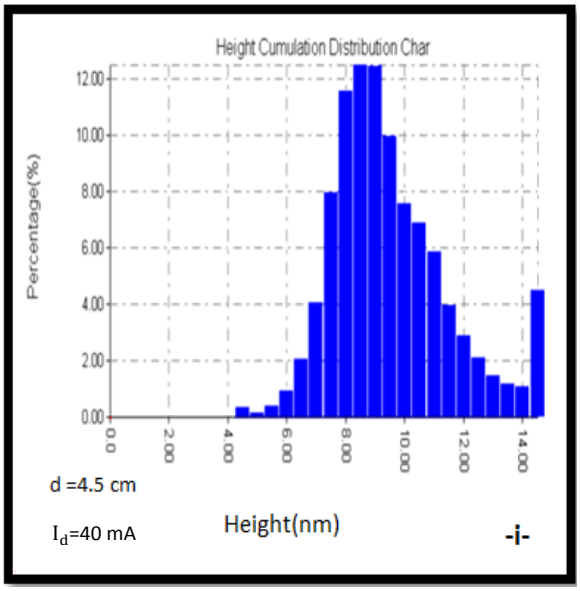
Height Cumulation Distribution Char
Percentage(%)
Height(nm)
d =4.5 cm
I_d=40 mA
-i-

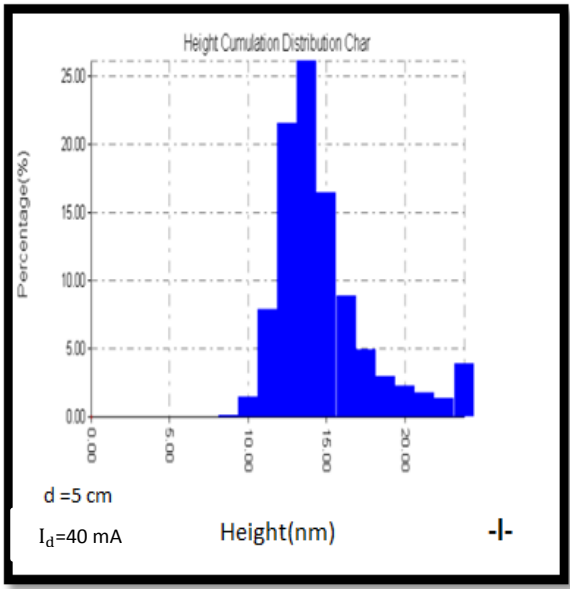
Height Cumulation Distribution Char
Percentage(%)
Height(nm)
d =5 cm
I_d=40 mA
-l-

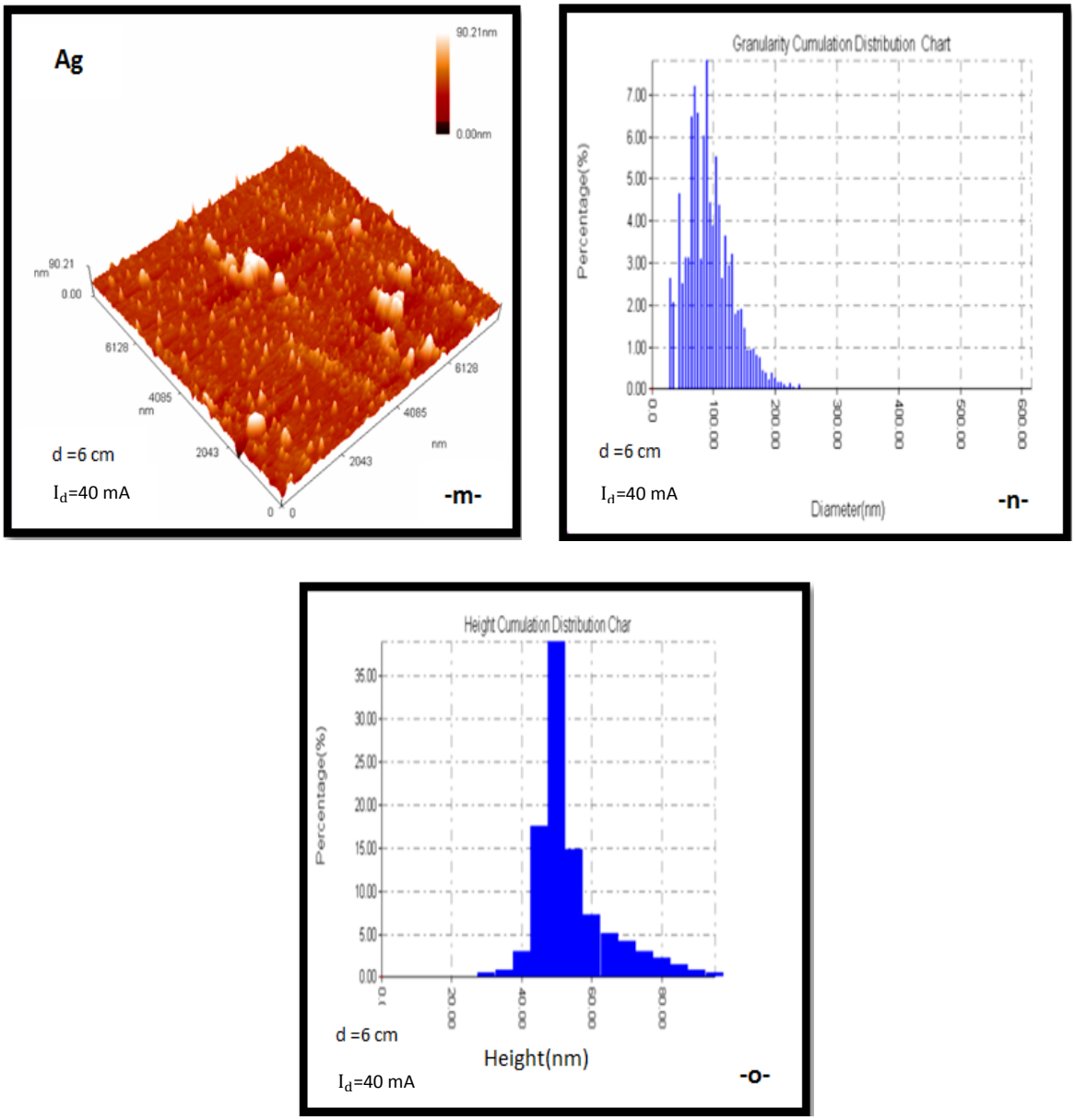

Figure (4-28) Shows the results from AFM using Ag target for different electrodes separation at I_d =40 mA. (a-d-g-j-m) 3D images, (b-e-h-k-n) Percentage of diameter size distribution and (c-f-i-l-o) Percentage of height distribution.

4-5-1 Grain diameter

In the figures(4-27-b-e-h-k-n) and 3D images of coated samples, the average grain diameter are studied at different electrodes separation using gold target, and obtained the following results in table (4-3) shows the maximum and minimum average values of grain diameter:

Table (4-3) Maximum and minimum grain diameter for gold target at I_d=30 mA.

G_d(nm)	percentage%	d(cm)	T_e(eV)	n_i(m^{-3})	n_e(m^{-3})
220	9.77	5	3.74	$4.1512x10^{16}$	$3.200x10^{16}$
90	9.14	4	4.132	$3.8527x10^{16}$	$2.947x10^{16}$

The reason for these different average values of grain diameter is due to the changes of plasma parameters. The temperature of electron at a minimum grain diameter is slightly greater than the temperature of electron at a maximum grain diameter.

In the same way, depending upon the data in figures (4-28-b-e-h-k-n) and 3D images for coater samples using silver target. The maximum and minimum average grain diameters are shown in table (4-4) :

Table(4-4)Maximum and minimum grain diameter for silver target at I_d=40 mA.

G_d(nm)	percentage%	d(cm)	T_e (eV)	n_i (m^{-3})	n_e (m^{-3})
160	11.99	4	4.4	$3.7709x10^{16}$	$2.9582x10^{16}$
90	12.11	5	4.13	$4.177x10^{16}$	$3.1155x10^{16}$
	7.8	6	4	$4.3435x10^{16}$	$3.2913x10^{16}$

The effect of changing electrodes separation was represented in table (4-4) by using silver target at discharge sputtering current I_d=40 mA. It is notice that there are two minimum grain diameter (90 nm) at electrodes separation (d=5 cm and d=6 cm).

The effect of target materials and electrodes separation on average grain diameter can show clearly from AFM results in figure(4-29).

In figure(4-29) electrodes separation effected leads to change the values of grain diameter. For using gold target, the minimum grain diameter (90 nm) at d=4 cm for I_d =20 mA and I_d =30 mA. The maximum grain diameter (260 nm) at d=3 cm for I_d =60 mA and at d=5 cm for I_d =40 mA.

For using silver target, at different electrodes separation for all sputtering current the minimum grain diameter (90 nm) and the maximum grain diameter (200 nm) at d=4.5 cm for I_d =20 mA and I_d =60 mA. The average grain diameter for using gold target is greater than the average grain diameter for using silver target.

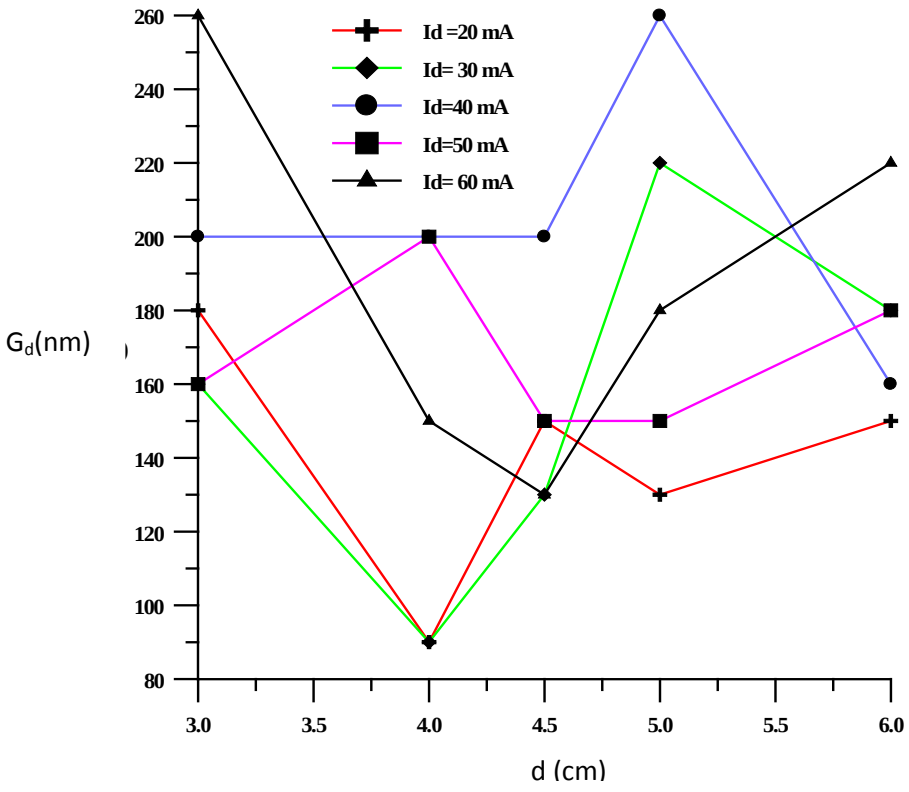

-a-

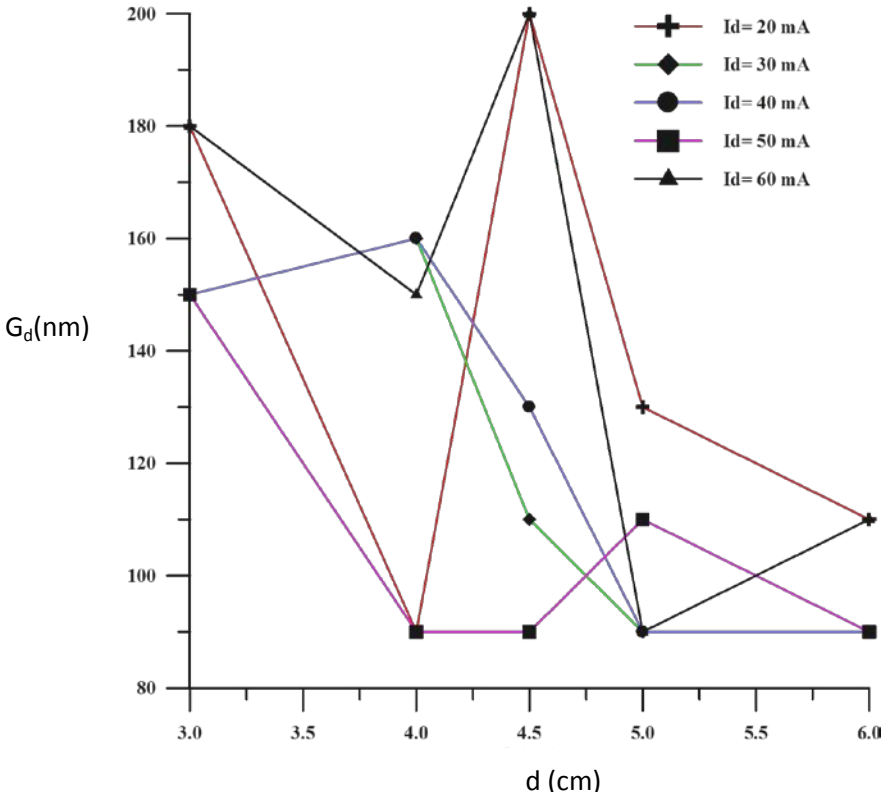

-b-

Figure(4-29) Variation of particles grain diameter as a function of electrodes separation at different sputtering currents for using **a)** gold target **b)** silver target.

4-5-2 Grain height

Using data from (AFM) in figures(4-27-c-f-i-l-o) at a constant sputtering current for using gold target, the average grain height are studied for different electrodes separation. Table (4-5) shows the maximum and the minimum average values of grain height.

.

Table (4-5) Maximum and minimum grain height for gold target at I_d=30 mA.

G_h (nm)	percentage%	d(cm)	T_e (eV)	$n_i(m^{-3})$	$n_e(m^{-3})$
15	19.17	5	3.74	$4.1512x10^{16}$	$3.2000x10^{16}$
6	22.95	4	4.132	$3.8527x10^{16}$	$2.8180x10^{16}$

Also, from figures(4-28-c-f-i-l-o) for using silver target the same study for the average grain height with different electrodes separation. Table(4-6) explain the maximum and the minimum values of average grain height.

Table(4-6) Maximum and minimum grain height for silver target at I_d=40 mA.

G_h (nm)	percentage%	d(cm)	T_e (eV)	$n_i(m^{-3})$	n_e (m^{-3})
50	38.94	6	4	$4.3435x10^{16}$	$3.2913x10^{16}$
5.5	21.76	4	4.4	$3.7709x10^{16}$	$2.9582x10^{16}$

It is notice that from tables(4-3) and (4-5) for using gold target, the minimum grain diameter and grain height are obtaining at the same electrodes separation (d=4 cm). Additionally, the maximum grain diameter and grain height are obtaining at the same electrodes separation (d=5 cm). Also, from tables(4-4) and (4-6) for using silver target, the maximum grain diameter and the minimum grain height are obtaining at the same electrodes separation (d=4 cm). And the minimum grain diameter is obtaining at (d=5 cm and d=6 cm) while the maximum grain height is obtaining at electrodes separation (d=6 cm). The effect of changing target material on grain average height at different electrodes separation can show in figure(4-30).

From figure(4-30-a) the minimum grain height for using gold target at the electrodes separation (d=4 cm) for all sputtering current except I_d=50 mA which is the maximum grain height. The minimum grain height for using silver figure(4-30-b) at electrodes separation (d=4 cm) for different sputtering currents and the maximum grain height at d=5 cm except I_d =40 mA .

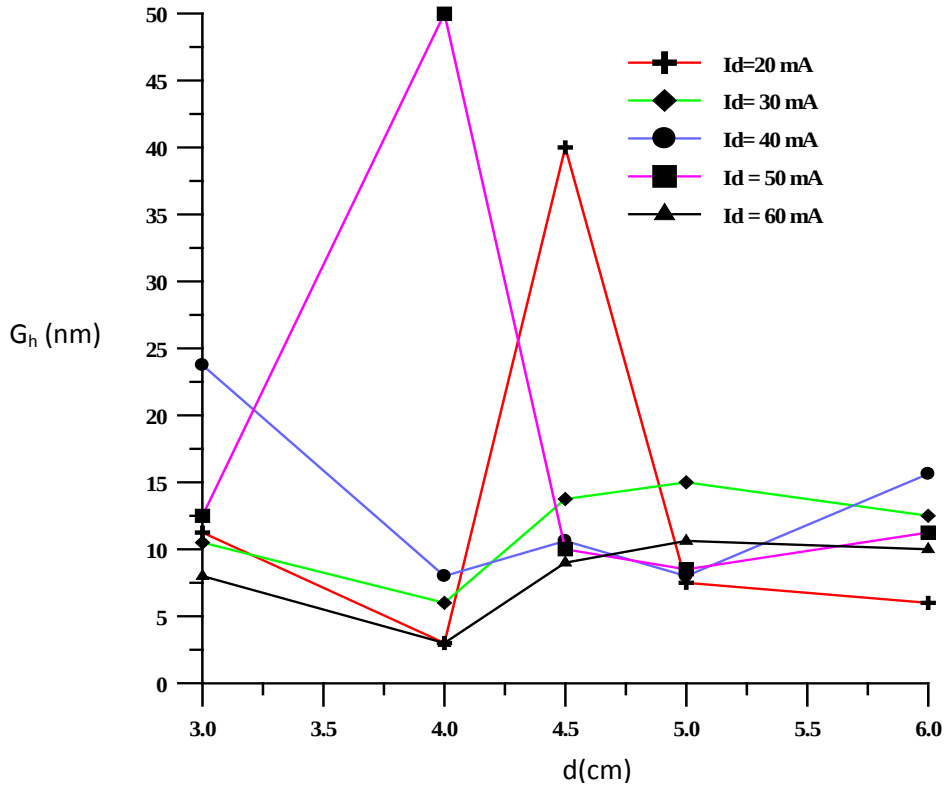

-a-

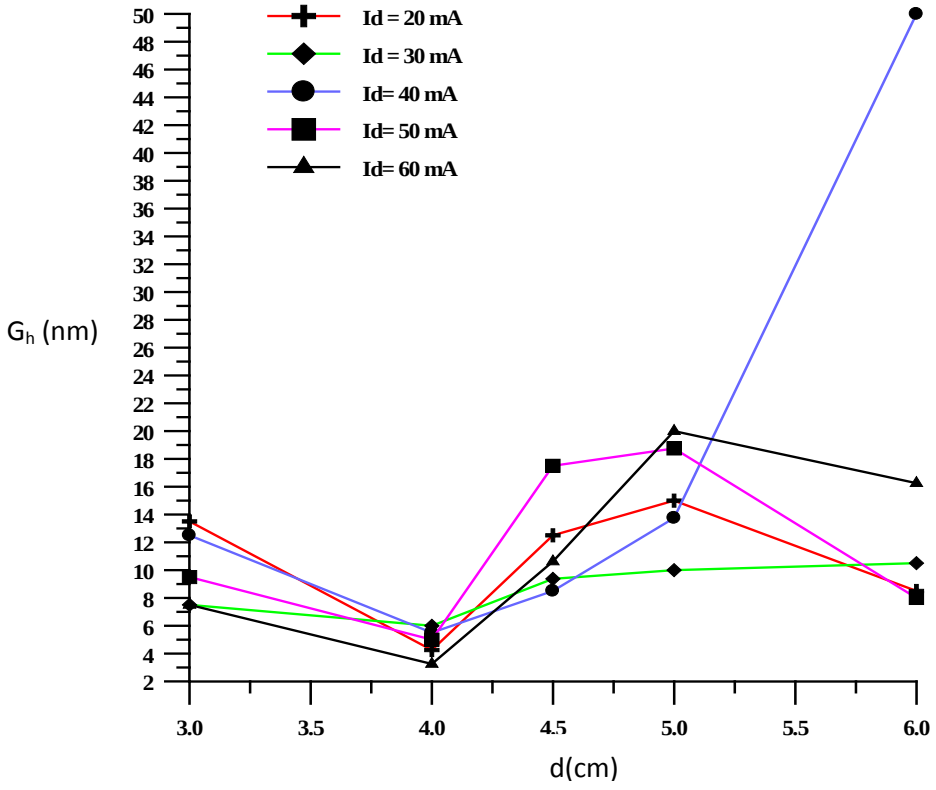

-b-

Figure(4-30)Variation of particles grain height as a function of electrodes separation at different sputtering currents for using
a) gold target **b)** silver target.

4-5-3 Sputtering yield

The sputtering yield Y(E) is calculated from equation (2-22), the energy of particles, E , is determined using the cathode voltage for different electrodes separation in figure(4-2) as a function of sputtering current for gold and silver as target materials are shown in figure(4-31).

Figure(4-31) indicated that the yield of sputtering as a function of discharge current at different electrodes separation for silver target is greater than the yield of sputtering for gold target.

4-5-4 Roughness average

From the figure(4-32) roughness average as a function of electrodes separation for using gold and silver targets which obtaining from the results of AFM. Nonlinear relation between roughness average and electrodes separation. The minimum roughness by using gold target for all sputtering current at d=4 cm except for I_d =50 mA as shown in figure(4-32-a). Also, by using silver target minimum roughness is obtaining also at the same electrodes separation d=4 cm for all sputtering currents except for I_d =30 mA is at d=4.5 cm as shown in figure(4-32-b).

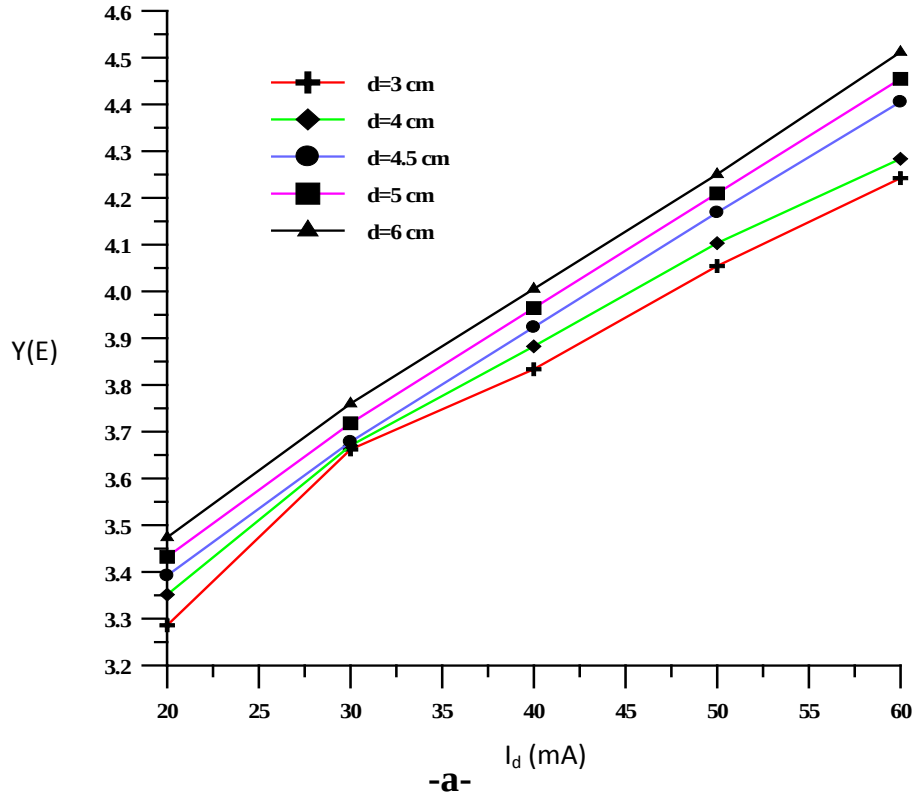

-a-

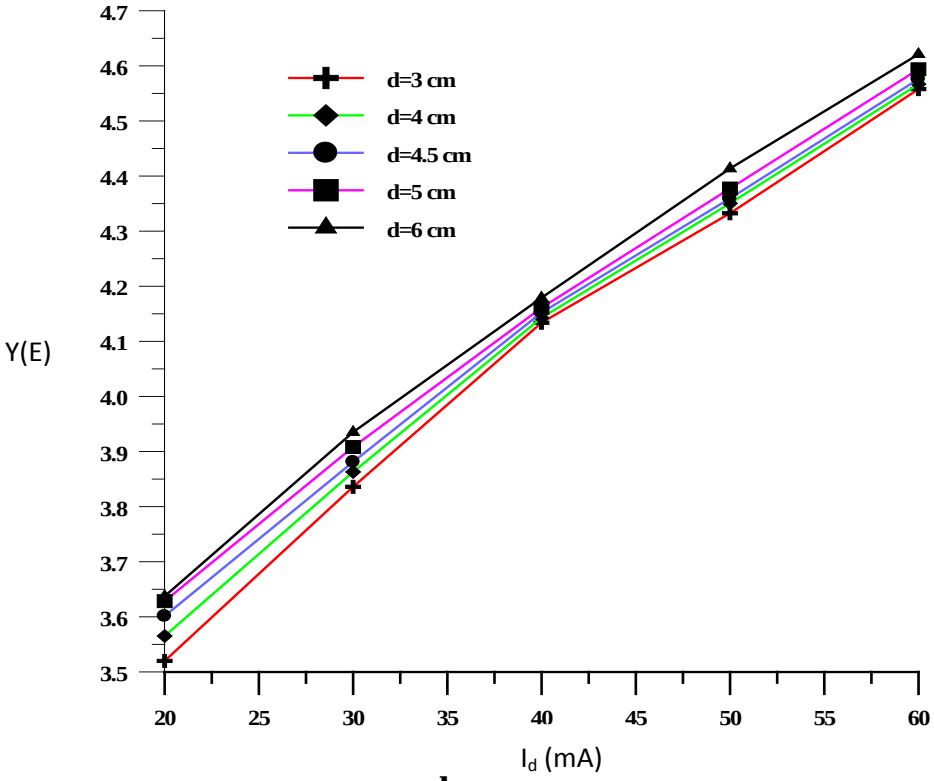

-b-

Figure(4-31) Variation of the rate sputtering as a function of sputtering current at different electrodes separation for using
a) gold target **b)** silver target.

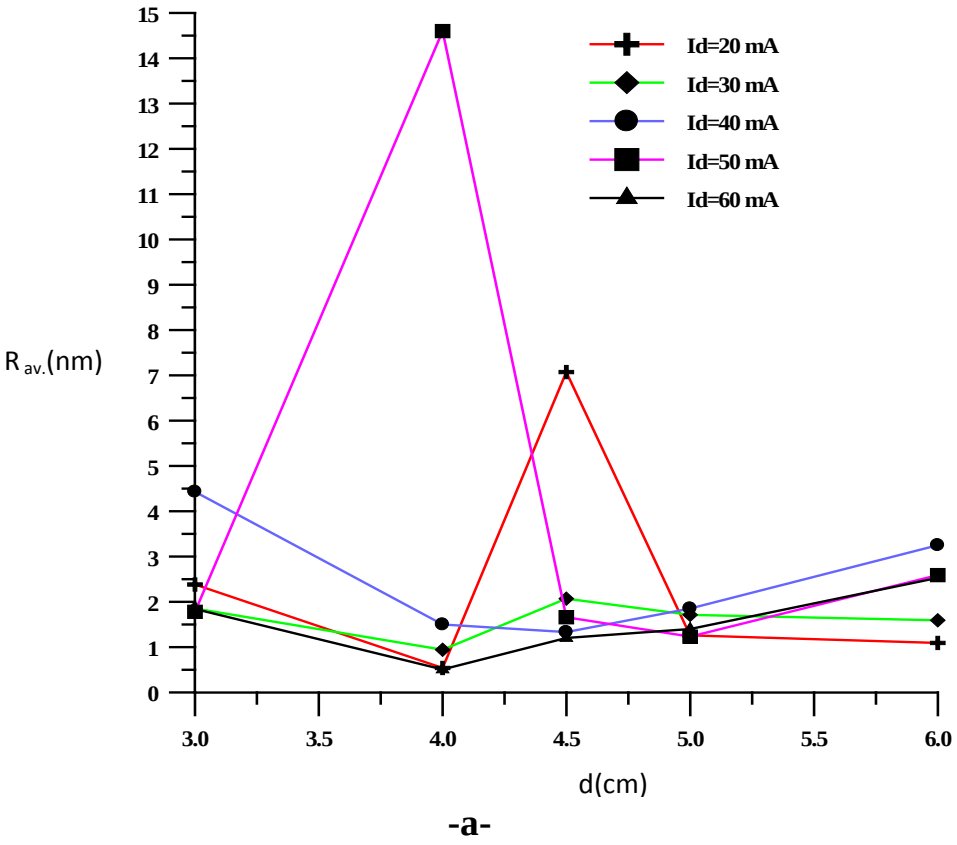

-a-

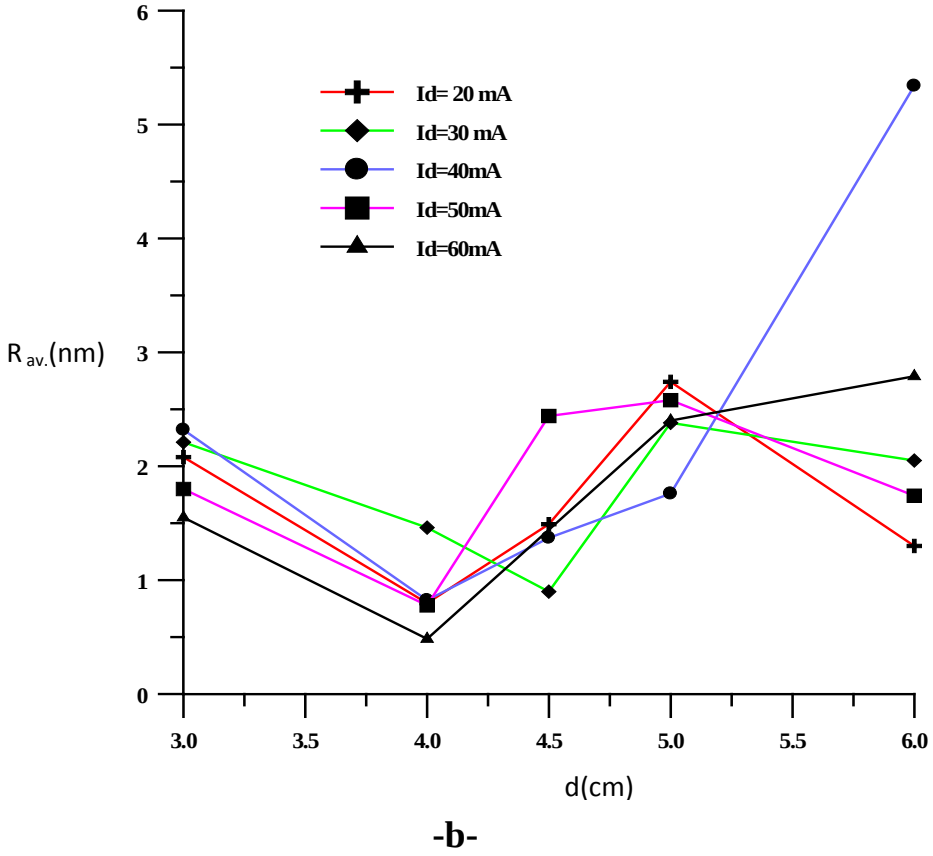

-b-

Figure (4-32) Roughness average as a function of electrodes separation for using **a)**gold target **b)**sliver target**.**

Chapter Five

Conclusions and Future Works

5-1 Conclusions

The results of experimental research in the present work, illustrate the importance of electrodes separation and target material on the coated samples using DC discharge low voltage plasma sputtering system. The following conclusion can be observed from these results:

1-The required discharge voltage for using gold as a target is greater than silver target.

2-The variation of electrodes separation and target material have been found effective and sensitive parameters on the values of electron temperature and ion density which are lead to change the surface morphology of the sample.

3-The effects of magnetic flux density is clear on the value of ion density which are slightly greater than electron density for both targets with a ratio of increasing (1.2%) for gold and (1.3%) for silver target.

4-The values of electron temperature for silver is greater than for gold target.

5-The relation of grain diameter, grain height and roughness, with different electrodes separation and target material is nonlinear.

6-Minimum values of grain diameter for silver target is (90 nm) at different sputtering current for electrodes separation

7-The sputtering yield for using silver target is greater than gold target.

5-2 Future Works

One can suggest the following subjects as a future works for our research:

1- Using another diagnostics method such as, microwave interferometry and Laser induced florescence.

2- Using RF magnetron sputtering system.

References

References

[1] A. Bogaerts,"The glow discharge :An exciting plasma ", J .Anal. At Spectrom, **14**,1375,1999.

[2] R.B.Heimann,"Plasma-spray coating principles and applications", VCH,Germany,1996.

[3] F.F.Chen,"Industrial applications of low-temperature plasma physics",Phys.Plasma, **2**,2164,1995.

[4] P.J.Kelly and R.D.Arnell,"Magnetron sputtering a review of recent development and applications", Vacuum , **56**,159,2000.

[5] S.M.Borah, A.R.Pal,H.Bailung and J.Chutia,"Effect of **E**x**B** electron drift and plasma discharge in dc magnetron sputtering plasma",Chin.Phys.B, **20**,014701,2011.

[6] N.Inagaki,"Plasma surface modification and plasma polymerization", Technomic Pub.Co.Inc. Lancaster, PA,1996.

[7]M.I. Boulos, P. Fauchais, and E. Pfender ,"Thermal plasmas fundamentals and applications", **1**, Springer science ,New York, 1994.

[8] R.J.Goldston and P.H.Rutherford, " Introduction to plasma physics", IOP Ltd 1995.

[9] B.Raul and A.Baragiola ,"Sputtering : Survey of observations and derived principles", Phil.Trans.R.Soc.Lond A, **29**,362,2004.

[10] A.Rockett,"The materials science of semiconductors", Springer,USA,2008.

[11] K.Wasa and S.Hayakawa,"Handbook of sputter deposition technology principle ,technology and applications", Noyes publications , New Jersey ,USA,1992.

[12] D.Bohm , E.H.S.Burhop and H.S.W.Massey,"The characteristics of electrical discharge in magnetic field", Ed. by A.Guthrie and R.K.Wakerling , M.Graw-Hill,New York,1949.

[13] E. Mahan, “Physical vapor deposition of thin film”, New York, Johan Wiley and Sons. Inc.,2000.

[14] S.C. Brown, “Introduction to electrical discharge in gases”, New York wiley,1966.

[15] L.I. Maissel and R. Glang, “Handbook of thin film technology”, New York, McGraw.Hill,1970.

[16] J. L. Vossen,“Thin Film Processes”, Academic Press , INC. , New York ,1978.

[17] R.K.Marcus, “Glow discharge spectroscopies”, Springer ,LLC, New York,1993.

[18] S.Maniv and W.D.Westwood,“Effect of H_2 on an argon discharge for planar magnetron sputter”, J.Vac.Sci.Technol., **17** ,403,1980.

[19] A.G.Spancer, C.A.Bishop and R.P.Howson,“The design and performance of planar magnetron sputtering cathodes”,Vacuum,**37**,363,1987.

[20] D.Czekaj,B.Gorncher ,E.K.Hollmann,V.A.Volpyas and A.G.Zaytser, “Incident ion energy spectrum and target sputtering rate in dc planar magnetron”, Vacuum ,**42** ,43,1991.

[21] P.Spatenka , I.Leipner ,J.Vlcek and J.Musil,“A comparison of internal plasma parameters in a conventional planar magnetron and a magnetron with additional plasma confinement”, Plasma source sci.technol. **, 6,**590,1997.

[22] I.Stokroos ,D.Kalicharan,J.J.L.Van Der Want and W.L.Jongebloed, “A comparative study of thin coatings of Au/Pd ,Pt and Cr produced by magnetron sputtering for FE-SEM”, J. Microscopy, **189**,79,1998.

[23] B.Szikora,“Bohm criterion in magnetron plasma”, Vacuum,**61**,397,2001.

[24] P.J.Kelly,J.Hisek,Y.Zhou,R.D.Pilkington and R.D.Arnell, "Advanced coatings through pulsed magnetron sputtering", Surface engineering,**20**,157,2004.

[25] C.Costin , G.Popa and G.Gousset,"On the secondary electron emission in dc magnetron discharge", J.Optoelectronics and advanced materials",**7**,2465,2005.

[26] W.Sum,T.Wen,L.Guo,H.Ping,C.Bao,H.Wang,S.Zeng,X.Gav and Y.Luo, "Characteristics of atmospheric-pressure radio-frequency glow discharges operated with argon added ethanol",J.Appl.Phy., **101**,123302,2007.

[27] O.Barannor ,M.Romanor,M.Wolter,S.Kumar and X.Zhong, "Low-pressure planar magnetron discharge for surface deposition and nanofabrication", Phys.plasma,**17**,053509,2010.

[28] Z.Xin,S.Xiao-Hui and Z.Dian-Lin, "Thickness dependence of grain size and surface roughness for dc magnetron sputtered Au films",Chin.phys.B,**19**,086802,2010.

[29] P.Asanithi ,S.Chaiyakun and P.Limsuwan,"Growth of silver nanoparticles by dc magnetron sputtering", J.Nanomaterials,**1**,ID963609,2012.

[30] A.Rauch and A.Anders,"Estimating electron drift velocities in magnetron discharges", Vacuum,**89**,53,2013.

[31] B.B.Sahu,J.G.Han, H.R.Kim,k.Ishikawa and M.Hori, "Experimental evidence of warm electron populations in magnetron sputtering plasma", J.Appl.Phys.,**117**,033301,2015.

[32] F. F. Chen, "Introduction to plasma physics", plenum press ,New York and London, 1974.

[33] M. A. Lieberman and A. J. Lichtenberg, "Principle of plasma discharges and materials processing ", Wiely, New York,2005.

[34] N. St . J. Braithwaite,"Introduction to gas discharge", Plasma Source Sci. Technol , **9** ,517,2000.

[35] F. F. Chen,"Introduction to plasma physics and controlled fusion", Plenum Press, New York, 1984.

[36] A. Fridman, A. Ghirokov and A. Gutsol, "Non-thermal atmospheric pressure discharge", J. Phys. D., Appl. Phys.,**38,** 1-24,2005.

[37] M. Konuma,"Film deposition by plasma techniques" , Springer-Verlag, NewYourk,1992.

[38] F. F. Chen and J. P. Chang, "Lecture notes on principles of plasma processing", Springer US,2003.

[39] R. Shishoo,"Plasma technologies for textiles",Boea Rahn Bosfon,New York,Washinton,p.7,2007.

[40] H. Andrei, V. V Covlea and E. Barna,"The smoothing and the digital processing of Langmuir probe characteristics" ,Romanian Rep. in phys.,**2,**55,51,2003.

[41] L. B. Loeb, "Basic process of gaseous electronics", U.C.P.,**2**,361,1960.

[42] M. Y. Naz , A. Ghaffar , N. U. Rehman , S. Naseer and M. Zakaullah ,"Double and triple Langmuir probes measurements in inductively coupled nitrogen plasma",Prog. Electromagnetic Research , **114** , 113,2011.

[43] F. F. Chen, "Use of electrostatic probes in plasma physics", P. Phy. Lab., Princeton, N,J, Paper No.4-2,Pp:150-154,1961.

[44] R. H. Huddleston, and S. L. Leonard, "Plasma diagnostic techniques" , Academic Press, Inc., New York,1965.

[45] K. A. Aadim, "Design and construction of DC planner magnetron sputtering to prepared Se thin film", Phd. Thesis, college of science, Baghdad university,2010.

[46] F. F. Chen, “Langmuir probe diagnostics” , Los Angeles,2003.

[47] R. L. Merlino, “Understanding Langmuir probe current –voltage characteristics”, Iowa, **75**,12,1078,2007.

[48] P. Sigmund,“Sputtering by ion bombardment :Theoretical concepts”, Sputtering by particle Bombardment , pp.9-71, Behrish , R.,Springer-Verlag,Berlin,1981.

[49] Y. Kudriavtsev , A. Villegas , A. Godines , R. Asomoza, “Calculation of the surface binding energy for ion sputtering particls”, Applied Surface Science **239** ,273,2005.

[50] G. Kaupp, “Atomic force microscopy ,scanning near field optical microscopy and nano scratching”, Spr.Sci.+Business Media,Germanny,2006.

[51] R. Bernardes-Filo ,O. Benedito Garrido de Assis,“Development of an algorithm for tip-related artifacts identification in AFM biological film imaging” ,Braz. arch. boil. technol.,**48**, Curitiba,2005.

[52] M. M. Pattison Mair , M. A. and Charles Slater,“Elementary chemistry”, M. A. M.B. Combirdg at university press**,**PP 314, 1887.

[53] F. Dean Toste, “Gold catalysis: An homogeneous Au approach”, series editor Graham J. Hutchings, London ,**14**,2014.

[54] A. R. Galaly,“The magnetized plasma effect on cathode fall thickness for helium gas discharge” ,Phy.Sci.Int.J.,**4**,1088,2014.

[55] M. N. Stankov,“Measurements and models of transient and stationary regimes of glow discharge in argon” ,J.phy.;**565,**012016,2014.

[56] E. F. Kotp and A. A. Al-Ojeery, “Studies the effect of magnetic field on argon plasma characteristics”,Aust. J. of Basic and Applied Science,**6**,817,2012.

الخلاصة

تتكون منظومة الترذيذ البلازمي من حجرة تفريغ اسطوانية مصنوعة من مادة (Bolosilicate) وتحتوي على قطبين دائرين من .st .st يحمل الكاثود، مادة الهدف وكذلك المغناطيس الثابت اما قطب الانود فيحمل النماذج الزجاجية التي سوف يتم طلاءها .في هذا البحث استخدمت مادتي الذهب والفضة كمادة لهدف.

الهدف من هذه الدراسة، هو دراسة تأثير عوامل التشغيل مثل، المسافة بين القطبين ونوع مادة الهدف على خصائص أشكال سطح زجاجي مطلي بوجود المجال المغناطيسي والتي تمت دراستها باستخدام مجهر القوة الذرية (AFM). وايضاً تم تحديد درجه حرارة الإلكترون و كثافة الايونات والالكترونات واعلومات البلازما الاخرى بواسطة مجس لانكمور المنفرد عند ضغط ثابت (0.2 mbar).

أظهرت نتائج هذه الدراسة بينت وجود زيادة خطية في كثافة الالكترونات والايونات وانخفاض أسي في درجة حرارة الالكترونات عند تغير المسافة بين القطبين ولخمسة قيم و (3,4,4.5,5 and 6)cm لمادتي الذهب والفضة وأيضا تبين ان فولتيات التفريغ باستخدام الذهب كهدف هي أكبر منها في حالة الفضة. كذلك، وجد انه بزيادة المسافة بين القطبين فان درجة حرارة الالكترونات تقل لمادتي الذهب والفضة وكثافة الايون تزداد مسببة زيادة في قطر وارتفاع الحبيبة لتيار الترذيذ(I_d=30 mA) باستخدام الذهب بينما يقل قطر الحبيبة ويزداد ارتفاعها باستخدام الفضة لتيار الترذيذ(I_d=40 mA).

من ناحيه اخرى، أن قيم درجة حرارة الالكترون باستخدام الفضة هي اكبر من القيم باستخدام الذهب وان علاقة قطر الحبيبة، وارتفاعها وخشونة السطح كدالة للمسافة بين القطبين هي ليست خطية. اصغر قيمة لمعدل قطر الحبيبة وارتفاعهاحصلنا عليه هو(90 nm) و(٦nm) على التوالي لمادتي الذهب عند تبار الترذيذ (I_d=30 mA) و(d=4 cm) .

وللفضة نفس قيمة قطر الحبيبة باستخدام الذهب عند(d=5 cm) لكن بارتفاع (5.5 nm) عند (d=4 cm) ولتيار الترذيذ (I_d=40 mA).

واصغر معدل ارتفاع للحبيبة لكل تيارات التفريغ (20,30,40,50 and 60 mA) عند نفس المسافة بين القطبين (d=4 cm) باستخدام الفضة والذهب ولكل تيارات التفريغ ماعدا(I_d=50 mA) والذي يمثل اكبر معدل ارتفاع للحبيبة فيه باستخدام الذهب.

واخيرا، ناتج عملية الترذيذ باستخدام الفضة اكبر مما عليه باستخدام الذهب.

جمهورية العراق
وزارة التعليم العالي والبحث العلمي
جامعة النهرين
كلية العلوم
قسم الفيزياء

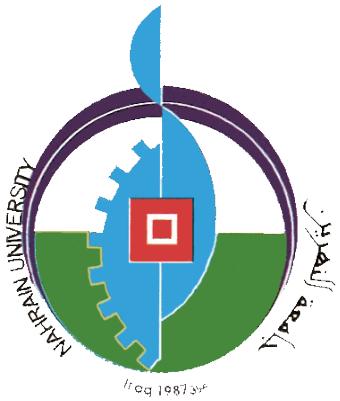

تأثير المسافة بين الاقطاب ومادة الهدف باستخدام الترذيذ المغناطيسي ذو التيار المستمر

رسالة

مقدمة إلى مجلس كلية العلوم / جامعة النهرين

كجزء من متطلبات نيل درجة الماجستير في علوم الفيزياء

من قبل

بان فيصل رشيد

بكالوريوس ١٩٩٦

إشراف

د. خالد عباس يحيى

أستاذ مساعد

شعبان ١٤٣٧ هجري

أيار ٢٠١٦ م